

THE NATURE OF THE BINDING  
IN HYDRIDE MOLECULES

By

IAN TERENCE KEAVENY, B.Sc.

A Thesis

Submitted to the Faculty of Graduate Studies  
in Partial Fulfilment of the Requirements

for the Degree  
Doctor of Philosophy

McMaster University

October, 1967

DOCTOR OF PHILOSOPHY (1967)  
(Chemistry)

McMASTER UNIVERSITY  
Hamilton, Ontario

TITLE: The Nature of the Binding in Hydride Molecules

AUTHOR: Ian Terence Keaveny , B. Sc. (Manchester  
University, England)

SUPERVISOR: Professor R. F. W. Bader

NUMBER OF PAGES: xiv, 233

SCOPE AND CONTENTS:

In Part I the one-electron charge distribution in the water molecule is obtained by demanding that this distribution balance the nuclear forces of repulsion and reproduce the observed dipole moment. Parameters contained in the molecular orbital description are then related to such concepts as hybridisation and bond polarities.

In Part II the electronic forces of attraction and the one-electron charge distribution, calculated from near Hartree-Fock wave functions, are used to interpret the binding in the first-row diatomic hydrides.



## PREFACE

The use of the one-electron charge distribution, and in particular its associated forces on the nuclei, to interpret the nature of the binding in molecules has not received the attention in the literature that it warrants. Not only are such calculations mathematically simple but also these properties being dependant on the real three-dimensional electron density, lend themselves to an easy physical interpretation.

The present research is an attempt to elucidate the forces operative in binding the nuclei. In Part I the "best" one-electron charge distribution for the water molecule, using only a limited set of basis functions, is obtained by demanding that this distribution produces a zero resultant force on the three nuclei. According to the Hellmann-Feynman theorem, the force on a nucleus in a molecule is the sum of the electronic force (which does not require the calculation of integrals involving the coordinates of more than one electron) and the classical forces of repulsion due to the other nuclei. This condition provides one with a number of constraints that any proposed density must fulfill and the successive steps leading to this equilibrium distribution of density contribute to an understanding of the principle of bond formation.

In Part II, on the other hand, the binding in the first-row diatomic hydrides, AH, whose charge distributions are known accurately, are examined by means of a detailed force

analysis complimented with measurements made on the one-electron charge distributions. The results of Part II have been submitted for publication in the Journal of Chemical Physics.

I wish to record my gratitude to the many people who have contributed to the completion of the present work. My interest in chemistry was first aroused by Mr. H. Worthington of De La Salle College, Salford, England. His encouragement and advice was gratefully appreciated. I would like to thank the Ontario Government and McMaster University for their financial assistance over the past four years and for making this visit to Canada possible.

I wish to extend my sincere thanks to my research supervisor, Professor R.F.W. Bader, for his willingness to discuss any and every problem. It was his originality and enthusiasm that have been both the source and mainstay of this work.

The co-operation of Professors R. Pitzer and J. Goodisman in furnishing numerical information required to check or perform certain calculations is appreciated. I would also like to extend my thanks to Dr. P. Cade in furnishing the wave functions for the first-row hydrides and his interpretation of the results obtained. The members of the computing centre at McMaster University, in particular Dr. Kenworthy, have provided valuable assistance in the computational work undertaken. Special thanks are due to Mr. H. Preston and Mr. W. Henneker for their general assistance through the course of this work. The use of the I.B.M. 7040 machine is gratefully acknowledged. I would like to thank Mr. P.

Curry for the careful drafting of the density contour maps and Mrs. H. Kennelly for the competent typing of this thesis.

I am most grateful to my parents both for their moral support and for making this all possible. Finally to my wife Sonja I dedicate this thesis with love and gratitude.

TABLE OF CONTENTS

	<u>Page</u>
PREFACE . . . . .	iii
LIST OF TABLES . . . . .	viii
LIST OF FIGURES . . . . .	x
GLOSSARY OF SYMBOLS EMPLOYED . . . . .	xiv
PART 1. THE NATURE OF THE BINDING IN THE WATER MOLECULE	
I. <u>INTRODUCTION</u> . . . . .	
(a) Historical . . . . .	1
(b) Theoretical . . . . .	7
II <u>DETERMINATION OF THE WAVE FUNCTION</u>	
(a) A description of the equivalent molecular orbitals. . . . .	27
(b) Method of calculation. . . . .	30
(c) Calculation of the parameters. . . . .	35
(d) Results. . . . .	43
III <u>DETERMINATION OF THE MOLECULAR PROPERTIES</u>	
(a) Diamagnetic susceptibility . . . . .	49
(b) Proton magnetic shielding constant . . . . .	54
(c) Electric field gradient. . . . .	57
(d) Electronic energy. . . . .	60
IV <u>DISCUSSION</u> . . . . .	71

	<u>Page</u>
PART II. THE NATURE OF THE BINDING IN THE FIRST- ROW HYDRIDES	
I. <u>INTRODUCTION</u> . . . . .	83
II <u>AN ANALYSIS OF THE BINDING IN TERMS OF THE CHARGE DISTRIBUTION</u>	
(a) Total molecular charge distribution . . . . .	97
(b) The density difference distribution . . . . .	106
III <u>AN ANALYSIS OF THE BINDING IN TERMS OF THE FORCES EXERTED ON THE NUCLEI.</u>	
(a) Introduction. . . . .	122
(b) The partial forces. . . . .	129
IV <u>A DISCUSSION OF THE BINDING IN THE AH MOLECULES</u>	
FIGURES AND TABLES . . . . .	155
APPENDIX . . . . .	189
BIBLIOGRAPHY . . . . .	229

LIST OF TABLES

<u>TABLE NO.</u>		<u>Page</u>
I	Individual orbital contributions to the forces for the water molecule at electrostatic equilibrium.	172
II	The effect of changing $\alpha$ on the individual orbital contributions to the forces.	173
III	The effect of changing $\delta$ on the individual orbital contributions to the forces.	174
IV	The effect of changing $\epsilon b$ on the individual contributions to the forces.	175
V	Parameters and computed $\Delta E$ for various density distributions in the water molecule.	176
VI	Atomic orbital coefficients in the lone pair and bonding orbitals $\phi_{\ell 1}^{\circ}$ , $\phi_{\ell 2}^{\circ}$ , $\phi_{b 1}^{\circ}$ and $\phi_{b 2}^{\circ}$ .	177
VII	Orbital parameters for the lone pair and bonding orbitals $\phi_{\ell 1}^{\circ}$ , $\phi_{\ell 2}^{\circ}$ , $\phi_{b 1}^{\circ}$ and $\phi_{b 2}^{\circ}$ .	178
VIII	Properties of the total density distributions for the diatomic AH hydrides.	179

<u>TABLE NO.</u>		<u>Page</u>
IX	Atomic and molecular electron populations in the bonding and non-bonding regions of the diatomic AH hydrides.	180
X	Total charge migration in the diatomic hydrides as determined by the density difference maps.	181
XI	Coefficients of the atomic orbitals on the A atom used to determine the $\Delta\rho_{UA}$ maps.	182
XII	Partial forces and their contributions for the $1\sigma$ density.	183
XIII	The energy of the atomic orbitals on the A atoms.	184
XIV	Partial forces and their contributions for the $2\sigma$ density.	185
XV	Partial forces and their contributions for the $3\sigma$ and $1\pi$ densities.	186
XVI	Total atomic, overlap and screening contributions for the AH hydrides.	187
XVII	Force contributions in LiH and LiF as determined by the density difference maps.	188

LIST OF FIGURES

<u>FIGURE NO.</u>		<u>Page</u>
I,II	The coordinate systems employed in the calculations. The bond length is R and the distance between the hydrogens is d	27
III	The relative directions of the lone pair and bonding orbitals in H <sub>2</sub> O	44
IV	Graphical representation of the variation of the forces $F_O$ , $F_{\parallel}$ , $F_{\perp}$ and DP with a change in the parameters $\delta, \alpha$ or $\epsilon b$	156
V	Definition of the in-and out-of-plane charge distributions	157
VI	Electron density contour map in a.u. for the water molecule. The bottom map is in a plane containing the three nuclei. The top map is in a plane perpendicular to the above passing through the oxygen nucleus	157
VII	Plot of $\Delta\rho_{SA}$ for H <sub>2</sub> O corresponding to an approximately sp <sup>3</sup> hybridisation of the oxygen atom. (a) the hydrogen nuclei are located at the ends of the two lines subtending the largest angle at the oxygen nucleus. The two inner lines are boundaries dividing the binding and antibinding regions. (b) plot of $\Delta\rho_{SA}$ in a perpendicular plane. The nearly	158



FIGURE NO.

Page

	horizontal line divides the binding region from the antibinding region.	
VIII	The in- and out-of-plane density difference maps (a) and (b) respectively for the water molecule.	159
IX	An electron density difference map between the LiF molecule and the Li and F atoms	160
X	Density difference maps for the stable first-row homonuclear diatomic molecules. The same scale of length applies to all the maps. The dotted line (shown in full for N <sub>2</sub> ) separate the binding from the antibinding regions.	161
XI	Total molecular charge density contours for the first-row diatomic hydrides in a.u. All maps are drawn to the same scale of length. The A nucleus is on the left in this and all succeeding figures. The innermost contours encircling the A nuclei have been omitted for the sake of clarity. The density at the A nucleus and at the proton is given in Table VIII .	162

<u>FIGURE NO.</u>		<u>Page</u>
XII	The definition of $r_A$ and $r_H$ . The outer line is to represent a typical 0.002 contour. The shaded areas indicate the non-bonded regions on A and H. The numerical integration used to obtain the non-bonded charges listed in Table IX was, however, extended beyond the 0.002 contour.	163
XIII	The binding and antibinding regions in the AH molecules with their respective electron populations.	164
XIV	Contour maps of the density differences $\Delta\rho_{SA}(\xi, \eta)$ (molecule-separated atoms) in a.u. for the first-row diatomic hydrides.	165
XV	Profiles of $\Delta\rho_{SA}(\xi, \eta)$ in a.u. along the internuclear axis. The abscissa (distance along the internuclear axis) is in a.u. with the A nucleus as origin.	166
XVI	The definitions of the A and B regions	163
XVII	Contour maps of the density differences $\Delta\rho_{SA}(\xi, \eta)$ (molecule-separated atoms) employing the spherically atomic A density.	167

<u>FIGURE NO.</u>		<u>Page</u>
XVIII	Contour maps of the density difference $\Delta\rho_{\text{UA}}(\xi,\eta)$ (molecule-united atom) in a.u. for the first-row diatomic hydrides.	168
XIX	Contour maps of the $1\sigma$ molecular orbital charge densities for LiH and HF.	169
XX	Contour maps of the $2\sigma$ molecular orbital charge densities for the first-row hydrides.	170
XXI	Contour maps of the $3\sigma$ molecular orbital charge densities for the first-row hydrides.	170
XXII	Contour maps of the $1\pi$ molecular orbital charge densities for the first-row hydrides.	171

GLOSSARY OF SYMBOLS EMPLOYED

$\alpha$ alpha	$\beta$ beta	$\gamma$ gamma	$\delta$ delta
$\epsilon$ epsilon	$\xi$ zeta	$\theta$ theta	$\lambda$ lambda
$\mu$ mu	$\pi$ pi	$\rho$ rho	$\sigma$ sigma
$\tau$ tau	$\nu$ upsilon	$\phi$ phi	$\chi$ chi
$\psi$ psi	$\omega$ omega		

$\psi$  - the single determinantal electronic wave function.

$\phi$  - molecular orbital.

$\chi_{\alpha}$  - an atomic orbital on nucleus  $\alpha$

$Z_{\alpha}$  - charge on nucleus  $\alpha$

$\rho$  - the single particle density arising from the electronic wave function.

$\alpha$  - the orbital exponent in the analytical expression for an atomic orbital.

1s - a 1s atomic orbital on oxygen =  $(\alpha^3/\pi)^{1/2} \exp(-\alpha r)$ .

h - a 1s atomic orbital for the hydrogen atom.

$S_0$  - the overlap between 1s and h.

$S_1$  - the overlap between two h orbitals.

2s - a 2s atomic orbital on oxygen =  $(\alpha^5/3\pi)^{1/2} r \exp(-\alpha r)$ .

$p_3, p_4$  - 2p atomic functions centred on hydrogens (1) and (2) respectively and pointing along the bond axis.

$p_x$  - a 2p<sub>x</sub> atomic orbital on oxygen =  $(\alpha^5/\pi)^{1/2} r \cos\theta \exp(-\alpha r)$

$p_y$  - a 2p<sub>y</sub> atomic orbital on oxygen =  $(\alpha^5/\pi)^{1/2} r \sin\theta \exp(-\alpha r)$  cos  $\phi$   
or  
sin  $\phi$

$S_2$  - the overlap between  $p_3$  and 1s.

NOTATION

The terminology conforms to that proposed by Mulliken as far as possible. The abbreviation L.C.A.O. is used to designate a linear combination of atomic orbitals, and an S.C.F. calculation refers to an energy variational calculation based on the self consistent field method.

PART I

THE NATURE OF THE BINDING IN  
THE WATER MOLECULE

## 1. INTRODUCTION

### (a) HISTORICAL

Molecules containing lone pairs of electrons have been of particular interest to chemists for a long time. The spatial distributions of such lone pairs and the part they play in determining the equilibrium configuration of the nuclei has received much attention in the literature.

The water molecule is probably the most discussed example in this class and consequently its historical treatment parallels the theoretical advances in wave mechanics.

The general conclusion that an electron pair bond is formed by the interaction of two unpaired electrons on each of two atoms was formally obtained by Heitler (1) and London (2) in 1927/1928. On this basis and because the two unpaired electrons on the oxygen atom are 2p, Pauling (3) suggested that the inter-bond angle in the water molecule was ideally  $90^\circ$ . The actual angle was, in fact, expected to be slightly larger due to the electrostatic interaction of the two hydrogen atoms.

It was first realized in 1930 (4) and then confirmed in 1932 (5) that three atoms in this molecule do form a triangle. The precise value of the H-O-H bond angle was then unknown but was believed to be between  $102^\circ$  and  $110^\circ$ .

Van Vleck and Cross (6) did a simple calculation that took the hydrogen repulsions, suggested by Pauling, into account. They showed that it would result in a bond opening of about  $10^\circ$  which was indeed very close to the experimental value.

In 1933 Bernal and Fowler (7), using Mulliken's (8) theory for the electronic structure of polyatomic molecules and Verwey (9) in 1941, again using qualitative arguments, predicted that the net electron density in the water molecule would resemble a tetrahedron with two corners of positive charge and two corners of negative charge. If we now assume that an isolated water molecule retains its essential features in the formation of ice, this result was in full agreement with the crystallographic work of Barnes (10). "The normal form of an ice crystal," he said, "is held together by hydrogen bonds in such a way that each molecule is surrounded by four others." Such a picture would also be consistent with the electrostatic theory of the hydrogen bond according to which the proton is attracted by a localised pair of electrons on another molecule.

Sidgwick and Powell (11), in 1940, collected experimental evidence on the stereochemistry of polyvalent atoms and attempted to relate it to the simplest explanation of their electronic structure, the size of their valency groups and the number of shared electrons they contain. It was concluded that both the lone and bonding pairs of electrons were equally important and that they were arranged symmetrically so as to minimize their mutual electrostatic repulsions. If this is the case then the geometrical configuration of these electron pairs depends only on their total number and not on their type. Thus, for example, molecules containing two, three or four valency pairs will be linear, trigonal and tetrahedral respec-

tively. Accordingly the water molecule with eight valence electrons was predicted to be tetrahedral with a bond angle of  $109^{\circ}28'$ .

Heath and Linnett (12) in 1948 suggested that if, in fact, the structure of the water molecule was nearly tetrahedral then it could be explained by means of a  $2s/2p$  hybridisation of the central oxygen atom<sup>a</sup>. The extent of this hybridisation is dependent on the bond angle and in the limit of complete mixing we will obtain four equivalent orbitals that point towards the four corners of a tetrahedron; two of these orbitals will be doubly occupied and two will be singly occupied and hence available for bond formation.

This description would give rise to a large concentration of negative charge behind the oxygen atom and two directed bond orbitals. The concentration of negative charge is commonly referred to as lone pair density, since it originates from atomic orbitals centred solely on one atom and consequently does not take part directly in the bonding.

Pople (14), allowing for the hybridisation suggested by Heath and Linnett, performed an equivalent molecular orbital calculation on the water molecule. He showed that a change in the bond angle will produce a change in the lone pairs and concluded that it was the electrostatic interaction of the lone and bonding pairs of electrons that is important in determining the

---

<sup>a</sup>The concept of hybrid orbitals was first suggested by Slater (13) in January 1931 and then by Pauling (3) in February of the same year.



equilibrium configuration, a result that Sidgwick and Powell obtained by purely qualitative arguments eleven years previous.

Sir Lennard-Jones (15) in 1952, argued that for an inert gas, like neon, in which all the orbitals are doubly occupied, then the electrons with  $\alpha$  spin are correlated amongst themselves and tend to take up a tetrahedral configuration. Similarly, electrons with  $\beta$  spin are correlated amongst themselves and tend likewise to take up a tetrahedral configuration, there being no correlation between the two tetrahedrae of different spins. With this in mind Pople(16) suggested that the electronic structure of certain hydride molecules can be discussed in terms of the basic neon structure by a successive removal of protons to their equilibrium bond length and angle. Consider, for example, the removal of two protons to form the water molecule. In the formation of these bonds there must be a correlation between the  $\alpha$  and  $\beta$  spin tetrahedra described previously and, once again, we have a picture that predicts a bond angle of  $109^{\circ}28'$  and a large concentration of negative charge behind the oxygen nucleus.

The actual bond angle is in fact  $104.45^{\circ}$  and a possible reason for this  $5^{\circ}$  shift has been suggested by Gillespie and Nyholm (17). The motion of the electrons in a bond, they said, is somewhat restricted by the electrostatic attraction of the protons. These electrons will tend to be more concentrated along the direction of the internuclear axis. Thus the electrons in the lone pair orbitals are best described as occupying

large and diffuse orbitals, whereas the electrons in the bonding orbitals are best described as being localised. As a consequence of both the Pauli and electrostatic forces there will be greater repulsions between the lone pairs than between the bonding pairs of electrons. Extensive use of this valence shell electron pair repulsion theorem, as it is known, by these workers has been instrumental in both predicting and explaining the structure of many molecules and in the case of  $H_2O$  would account for bond closing.

It has, however, been pointed out recently (18) that the Pauli repulsive forces were never operative in the lone pairs; it is rather a density shift into the binding region that causes the decrease in the bond angle.

This then is a brief discussion of the qualitative arguments pertaining to the water molecule. There is assumed some sort of relationship between the wave function and the molecular geometry; the bonding orbitals, for example, are made to point at the hydrogens. There is no prior reason for believing this to be the case and in fact it will be shown that such a description would lead, from a consideration of the forces acting on the nuclei, to an unstable molecule.

(b) THEORETICAL

In wave mechanics the stationary state of a molecular system containing  $N$  electrons is, in the Born-Oppenheimer approximation, given by the solution to the Schrödinger equation (19)

$$H \psi (1,2,\dots,N) = E \psi (1,2,\dots,N) \quad (1)$$

where  $H$  is the Hamiltonian operator corresponding to the classical energy of the system and  $\psi$  a wave function that involves both the spatial and spin coordinates of all the electrons.

As a consequence of writing the total wave function as an antisymmetrised product of orthonormal one-electron spin orbitals<sup>a</sup>

$$\psi = \frac{1}{\sqrt{N!}} \begin{vmatrix} \psi_1(1) & \dots & \psi_1(N) \\ \vdots & & \vdots \\ \psi_n(1) & \dots & \psi_n(N) \end{vmatrix}^b \quad (2)$$

Fock (20) in 1931 was able to devise a method, originally proposed in 1928 by Hartree (21), by which the  $3N$ -dimensional problem represented by equation (1) could be reduced to the solution of  $N$  three-dimensional Schrödinger equations of the type

$$H_{\text{eff}} \psi_i(1) = \epsilon_i \psi_i(1) \quad (3)$$

<sup>a</sup>Each spin orbital  $\psi_i$  is itself a product of a space function  $\phi_i$ , called a molecular orbital, and an  $\alpha$  or  $\beta$  spin function.

<sup>b</sup>In future a determinantal wave function of this form will be written as

$$\psi = \frac{1}{\sqrt{N!}} \left| \psi_1(1) \ \psi_2(2) \ \dots \ \psi_n(N) \right|$$

It was assumed that each electron  $i$  moved in an average potential field  $U_i$  provided by the remaining electrons and nuclei.  $H_{\text{eff}}$  is now the "Effective Hamiltonian" and is simply the sum of the kinetic energy of the electron and the above mentioned potential. If this field is chosen so as to be invariant under any of the symmetry operations of the point group to which the molecule belongs then the resultant molecular orbitals will be symmetry adapted. That is to say, they will span an irreducible representation of this point group.

The so-called Hartree-Fock method can thus be represented schematically as

$$\begin{array}{ccccccc} \psi_i & \text{-----} & U_i & \text{-----} & H_{\text{eff}} & \text{-----} & \psi_i \\ \uparrow & & & & & & \downarrow \end{array}$$


---

By assuming an initial set of eigenfunctions the field entering the Hamiltonian can be estimated and a new set of eigenfunctions can be calculated together with the corresponding electron density. From this data the field could be re-calculated; the procedure being repeated until self-consistency is reached.

A determinantal wave function as represented by equation (2) does not, in general, represent an exact solution of the Schrödinger equation; although electrons with parallel spins are kept apart, in accordance with the Pauli Principle. It is energetically unfavourable, because of coulombic repulsions, to put two electrons in the same orbital even though their spins are opposed and in an extended Hartree-Fock treatment,

all the electrons are represented by a different space function. A further improvement to the total wave function can be made by taking a linear combination of several determinantal wave functions, each formed from different spin orbitals; this being particularly necessary when we are dealing with open-shell configurations.

In the present calculations we are, however, concerned with the molecule in its ground state and as such, all the molecular orbitals will be doubly occupied. If this is the case then the total wave function can be adequately approximated by the singly determinantal form.

In principle, therefore, the Hartree-Fock equations can be solved by an iterative procedure in which one postulates an initial set of eigenfunctions. This is an extremely arduous task and it is found necessary to set further restrictions on each molecular orbital. It is generally assumed that these can be represented by some linear combination of atomic functions, called a basis set, centred on the constituent atoms.

$$\phi_i = \sum_j C_{ij} X_j \quad (40)$$

The methods of group theory have been particularly useful in this respect since it has been shown that the electron distributions in closed shell molecules have the same symmetry as the nuclear framework. Thus in the case of water molecular orbitals constructed in this way necessarily span the  $A_1$ ,  $A_2$ ,  $B_1$  or  $B_2$  irreducible representation of the  $C_{2v}$  point group. The electrons are thus depicted as being spread over the whole nuclear framework and are consequently as delocalised as possible.

Roothaan (22) was among the first to develop the mathematical consequences of this theory and the atomic orbital coefficients were obtained by invoking the minimum energy condition of the variation method. If the basis set is large enough then no error will be introduced by this approximation. However, if this is the case any attempt to interpret the chemical concepts of molecules and bonds in terms of the wave function are generally expressed as numerical coefficients and seem to bear very little relation to classical ideas (23). It is more rewarding from the chemical point of view to use a restricted basis set where accuracy is now sacrificed for insight. This consequently incurs an error and one might ask whether the electron density in molecules can be adequately described by a restricted set of basis functions which does not give a good energy - our criterion of accuracy lies in the agreement of calculated molecular properties.

Quantum mechanically every observable or observation can be represented by an operator. For a stationary state molecular system a series of density matrices can be defined which allow, in a more direct way, the average values of these operators to be calculated.

In atomic units for example the N-electron density matrix is defined as being

$$\rho_N = \psi(1,2,\dots,N) \psi^*(1,2,\dots,N) \quad (5)$$

where the asterisk signifies the complex conjugate. The majority of physical properties, and in particular those of interest to the chemist, depend only on the coordinates of one electron at a time. That is to say, they are indicative of the first order density matrix - this being readily obtained from equation (5) by integrating over the coordinates of all the electrons except those of electron number one.

Thus

$$\rho_1 = N \int \psi(1,2,\dots,N) \psi^*(1,2,\dots,N) d\tau_2 \dots d\tau_N$$

or by writing the wave function in its determinantal form

$$\rho_1 = \frac{N}{N!} \int |\psi_1(1) \psi_2(2) \dots \psi_n(N)| |\psi_1^*(1) \psi_2^*(2) \dots \psi_n^*(N)| d\tau_2 \dots d\tau_N$$

and since the electrons are indistinguishable, this will reduce to

$$\rho_1 = \frac{N(N-1)!}{N!} \sum_i \psi_i^*(1) \psi_i^*(1) = \sum_i \psi_i(1) \psi_i^*(1)$$

If we now represent the molecular orbitals by the symbol  $\phi_i$  then the one-electron density is simply given by

$$\sum_j n_j \phi_j(1) \phi_j^*(1)$$

where the summation is over all the occupied molecular orbitals  $j$ ,  $n_j$  being their respective occupation number.

The question one must now ask is whether the one-electron density as determined by an energy calculation, approximating to each molecular orbital by a limited set of basis functions, provides the best possible description of a molecule.

This is not necessarily the case since the Hamiltonian

operator being dependent on the simultaneous position of any two electrons will weight different regions in space than will another operator.<sup>a</sup> Mukherji and Karplus (24) have shown this to be true for hydrogen fluoride and they concluded that a better description of this molecule can be obtained by allowing the total energy to vary, subject to additional constraints. They required the resultant density distribution to give the correct dipole moment and quadrupole coupling constant as well as a reasonable, but not necessarily an absolute minimum, energy. In this way excellent agreement can be obtained for these one-electron properties without any serious impairment of the energy.

This would indicate that in a restricted basis set approximation, the one-electron properties associated with a molecule are important criteria when determining the form of the wave function.

Rather than use the energy to investigate the qualitative and quantitative aspects of the chemical binding, these phenomena are examined in terms of the electric fields at the nuclei and hence the forces exerted on the nuclei. The calculation of the forces is considerably simplified by the theorem derived independantly by Hellmann(25) and Feynman (25a). The electrostatic, or Hellmann-Feynman theorem, was

---

<sup>a</sup>It should be noted however that as the wave function becomes more apropos the energy, it will ultimately become good for other properties as well.



stated by Feynman as follows:

"The force on any nucleus (considered fixed) in a system of nuclei and electrons is just the classical electrostatic attraction exerted on the nucleus in question by the other nuclei and by the electron density distribution for all the electrons."

In equation (1), we have defined the normalized electronic wave function that satisfies the Schrodinger wave equation for the system. By multiplying both sides of this equation by  $\psi^*$ , the complex conjugate of  $\psi$ , and integrating over all space, the molecular energy of the system can be defined as

$$E = \frac{\int \psi^* H \psi d\tau}{\int \psi^* \psi d\tau} \quad (7)$$

The force on a given nucleus  $\alpha$  in the  $z$  direction, defined by  $F_{\alpha z}$  and equal to  $-dE/dz_{\alpha}$  will be from equation (7)

$$-\frac{dE}{dz_{\alpha}} = - \int \frac{d\psi^*}{dz_{\alpha}} \cdot H \cdot \psi d\tau - \int \psi^* \cdot \frac{dH}{dz_{\alpha}} \cdot \psi d\tau - \int \psi^* H \cdot \frac{d\psi}{dz_{\alpha}} \cdot d\tau$$

and since  $H$  is a real Hermitian operator

$$\int \psi^* H \frac{d\psi}{dz_{\alpha}} d\tau = \int \frac{d\psi^*}{dz_{\alpha}} \cdot H \psi d\tau$$

Furthermore, because  $\psi^*$  satisfies the Schrodinger equation

$H\psi^* = E\psi^*$  the force will reduce to

$$\begin{aligned}
F_{\alpha z} &= - \int \psi^* \cdot \frac{dH}{dz_{\alpha}} \psi d\tau - E \left[ \int \frac{d\psi^*}{dz_{\alpha}} \cdot \psi d\tau + \int \psi^* \cdot \frac{d\psi}{dz_{\alpha}} d\tau \right] \\
&= - \int \psi^* \cdot \frac{dH}{dz_{\alpha}} \cdot \psi d\tau - E \frac{d}{dz_{\alpha}} \int [\psi \psi^* d\tau] \\
&= - \int \psi^* \cdot \frac{dH}{dz_{\alpha}} \cdot \psi d\tau
\end{aligned}$$

However, since the kinetic energy of the electrons is independent of the nuclear displacement coordinates then

$$F_{\alpha z} = - \left\langle \frac{dV}{dz_{\alpha}} \right\rangle$$

In a system of nuclei ( $\alpha, \beta$ ) and electrons ( $i, j$ ) the potential energy can be expressed as

$$V = \sum_{\alpha \neq \beta} V_{\alpha\beta} + \sum_{\beta, i} V_{\beta i} + \sum_{i < j} V_{ij}$$

and since  $\sum_{i < j} V_{ij}$  is also independent of the nuclear coordinates

$$F_{\alpha z} = - \frac{d}{dz_{\alpha}} \sum_{\alpha \neq \beta} \frac{Z_{\alpha} Z_{\beta}}{r_{\alpha\beta}} \cdot e^2 + \sum_i e \int \psi Z_{\alpha} e \frac{d}{dz_{\alpha}} \frac{1}{r_{\alpha i}} \psi d\tau$$

or  $F_{\alpha z} = F_{\alpha z} \text{ (nuclear)} + F_{\alpha z} \text{ (electronic)}$

The nuclear contribution to the force is just the sum of the classical repulsive forces exerted by all the nuclei in the molecule. The electronic contribution is rather more complicated.

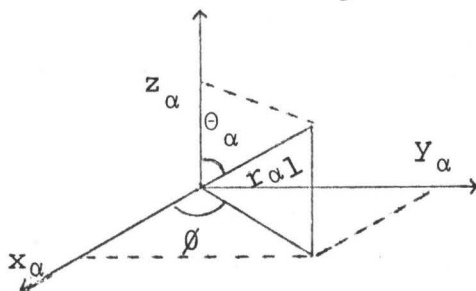
The electronic force operator  $Z_{\alpha} e \frac{d}{dz_{\alpha}} \frac{1}{r_{\alpha i}}$ , or simply  $\hat{O}(i)$ , depends only on the coordinates of one electron at a time and as such is determined by the first order density matrix. If the total wave function is written as a single

determinant of orthonormal molecular orbitals then

$$F_{\alpha z} \text{ (electronic)} = e \sum_j n_j \int \phi_j(1) \hat{O}(1) \phi_j^*(1) d\tau_1 \quad (8)$$

where the summation is over all the occupied molecular orbitals,  $n_j$  being their respective occupation numbers.

If we define the following coordinate system



then since  $r_{\alpha 1} = (x_{\alpha}^2 + y_{\alpha}^2 + z_{\alpha}^2)^{1/2}$ ;  $\frac{d}{dz_{\alpha}} \frac{1}{r_{\alpha 1}} = -\frac{\cos\theta_{\alpha}}{r_{\alpha 1}^2}$

the force operator  $O(1)$  reduces to

$$-\frac{Z_{\alpha} \cdot \cos\theta_{\alpha} e}{r_{\alpha 1}^2}$$

Thus we have that the force in atomic units<sup>a</sup> (a.u.) on any nucleus  $\alpha$  in the  $z$ -direction will be

$$+ \sum_{\alpha \neq \beta} \frac{Z_{\alpha} Z_{\beta}}{r_{\alpha\beta}^3} \bar{r}_{\alpha\beta} - Z_{\alpha} \sum_j n_j \int \phi_j(1) \cdot \frac{\cos\theta_{\alpha}}{r_{\alpha 1}^2} \cdot \phi_j^*(1) d\tau_1 \quad (9)$$

---

<sup>a</sup>One atomic unit of force is defined as  $\frac{e^2}{2a_0^2} = 8.2377 \times 10^{-3}$  dynes. The electronic charge is  $e$  and  $a_0$  is the Bohr radius.

NOTE - The sign convention in equation (9) and the ensuing work is such that a repulsive force on nucleus  $\alpha$  due to another nucleus is positive and an attractive force is negative.

In a more general form, applicable to polyatomic molecules equation (9) can be written

$$+ \sum_{\alpha \neq \beta} \frac{Z_{\alpha} Z_{\beta}}{r_{\alpha\beta}^3} \vec{r}_{\alpha\beta} - Z_{\alpha} \sum_j n_j \int \phi_j(1) \frac{\vec{r}_{\alpha 1}}{r_{\alpha 1}^3} \phi_j^*(1) d\tau_1 \quad (10)$$

Where now if we are considering a force along the bond

$$\vec{r}_{\alpha\beta} = r_{\alpha\beta} \cos \theta_{\alpha\beta} \quad \text{and} \quad \vec{r}_{\alpha 1} = r_{\alpha 1} \cos \theta_{\alpha 1}$$

and for a force perpendicular to the bond direction

$$\vec{r}_{\alpha\beta} = r_{\alpha\beta} \sin \theta_{\alpha\beta} \sin \phi \quad \text{and} \quad \vec{r}_{\alpha 1} = r_{\alpha 1} \sin \theta_{\alpha 1} \sin \phi$$

The Hellmann-Feynman theorem thus enables one to calculate the forces acting on a nucleus in a molecule if the electron density function is known. Alternatively we can calculate the equilibrium density from our knowledge of forces; the zero force requirement providing us with a number of constraints that any proposed density must fulfill.

Since each molecular orbital is approximated by a linear combination of atomic functions the different orbital contributions to the electronic force, defined by equation (10), can be broken down into three components:

ATOMIC FORCE<sup>a</sup>

$$Z_{\alpha} \langle \chi_{\alpha} | \frac{\vec{r}_{\alpha 1}}{r_{\alpha 1}^3} | \chi_{\alpha} \rangle^b \quad \text{OR} \quad A_{\alpha} (\chi_{\alpha} \chi_{\alpha})$$

This force arises from density centred on nucleus  $\alpha$  that is not centrosymmetric ( $\chi_{\alpha} \neq \chi_{\alpha}$ ). Small amounts of polarisation of this electron density will give rise to large atomic forces. This same density contributes an atomic dipole to the molecular dipole moment.

SCREENING FORCE

$$A_{\alpha} \langle \chi_{\beta} | \frac{\vec{r}_{\alpha 1}}{r_{\alpha 1}^3} | \chi_{\beta} \rangle \quad \text{OR} \quad P_{\alpha} (\chi_{\beta} \chi_{\beta})$$

This force on nucleus  $\alpha$  arises from density centred on nucleus  $\beta$ . The magnitude of the force depends on the depth of the penetration by nucleus  $\alpha$  into the atomic orbital charge clouds surrounding nucleus  $\beta$ . Such forces are important factors in determining the geometry of polyatomic molecules.

OVERLAP FORCES

$$Z_{\alpha} \langle \chi_{\alpha} | \frac{\vec{r}_{\alpha 1}}{r_{\alpha 1}^3} | \chi_{\beta} \rangle \quad \text{OR} \quad O_{\alpha} (\chi_{\alpha} \chi_{\beta})$$

---

<sup>a</sup>In these definitions all the forces will be considered on nucleus  $\alpha$  with a charge of  $Z_{\alpha}$ .  $\chi_{\alpha}$  refers to an atomic orbital on nucleus  $\alpha$  and  $\chi_{\beta}$  to one on nucleus  $\beta$ .

<sup>b</sup>For convenience an integration will be represented by the symbol  $\langle \dots \rangle$ .

This force on nucleus  $\alpha$  arises from an overlap charge distribution and its magnitude depends on the position of this charge density relative to the nuclei.

Berlin (26) in an imaginative treatment of the Hellmann-Feynman theorem has shown how bond formation can be understood in a classical framework. The space surrounding a molecule, he said, can be divided into binding and anti-binding regions dependent on whether charge situated in these regions exerts a net binding or antibinding force on all the nuclei.

The formation of a molecule from its constituent atoms must therefore result in a density shift into this binding region by an amount required to overcome the nuclear electrostatic forces of repulsion. This redistribution of electrons in bond formation can readily be examined by means of density difference maps, obtained by subtracting the atomic from the molecular density. If it is further remembered that the very existence of an electronic force is a direct result of bond formation then there will exist a fundamental and important relationship between the shift in density to the binding region accompanying molecular formation and the forces exerted by this density. In particular the three components of force will reflect a different aspect of the changes that take place in the atomic density distribution on bond formation. Such a relationship enables one to interpret the forces in the light of the density difference

maps and as a consequence will give one a greater insight as to the factors operative in both the formation and chemical nature of a molecule.

It is convenient at this time to turn our attention to the form of the molecular orbitals.

The symmetry adapted fully delocalised set as described previously are a particularly useful starting point when we are considering properties that depend on the molecule as a whole, such as the removal of an electron in the ionisation process. The wave functions obtained, however, seem to have very little connection with classical ideas. From the point of view of valency the chemist prefers to think of bond and lone pair orbitals as being localised.

Fock has shown that the single determinantal wave function as represented by equation (2), is invariant to unitary transformations among the molecular orbitals. Sir Lennard-Jones (27) using group theoretical arguments was able, by means of these unitary transformations, to convert the fully delocalised set into what are known as "Equivalent Molecular Orbitals" (E.M.O.) that could now readily be related to the bonding and lone pair ideas. These equivalent orbitals (E.O.) unlike the molecular orbitals, now form a basis for a reducible representation of the point

group to which the molecule belongs. Thus, for example, if  $\psi_1$  and  $\psi_2$  are two molecular orbitals belonging to the  $A_1$  irreducible representation, then two different orthogonal orbitals

$$(\sin\lambda\psi_1 + \cos\lambda\psi_2)$$

and

$$(-\sin\lambda\psi_2 + \cos\lambda\psi_1)$$

can be written which are formally just as correct and from the wave theory point of view equally as valid. The problem therefore reduces to one of selecting the appropriate value of  $\lambda$  by some convenient criteria of localisation.

Pople (14) has suggested that  $\lambda$  be chosen such that the 1s orbitals on hydrogen make no contribution to the lone pair density. By writing a set of orbitals that reflected his "ideal" case he examined the variation of the spatial distribution of the orbitals with a change in configuration. It was shown that the structure of the water molecule can be described by approximately two equivalent sets of orbitals that pointed towards the corner of a tetrahedron.



Peters (28), on the other hand, using a different method of localisation required that the hybrid bond orbitals pointed along the bond direction. In a recent publication he has discussed the form of the equivalent orbitals obtained in this way from reliable wave functions for a number of molecules. He was able to discuss quantitatively such terms as hybridisation and bond polarity. It was found that for the more complicated molecules, for reasons mentioned previously, it was not always possible to find an orthogonal transformation that would enable a description in terms of conventional lone pair and bonding pair ideas. When this was the case the imperfections were simply deleted at the expense of his orthogonality requirements. Some of the results were not as expected, and in the case of the O-H bond, the hybrid orbitals were in an opposite direction to that predicted.

Edminston and Ruedenberg (29), following the ideas proposed by Lennard-Jones and Pople (29a) developed a method of localisation without the use of symmetry arguments. They defined "localised molecular orbitals" or "Energy localised orbitals" as that set of molecular orbitals that minimised the orbital self-repulsion terms. Only in the presence of a symmetry group can they acquire properties which under certain circumstances make them equivalent. These workers were likewise able to define bonding and lone pair orbitals. However, they did not stipulate that the lone pairs had to be concentrated on one centre but rather allowed secondary contributions from neigh-

bonding atoms. It was suggested by them that the unusual direction of the hybrid orbitals, found by Peters, together with his non-orthogonality can in fact only be eliminated by an introduction of these secondary contributions.

Murrell and co-workers (30) have recently discussed the above and other methods of localisation. They concluded that a method based on Pople's, in which the E.O. are made as localised as possible, is probably the most useful and at the same time the least tedious approach.

These results indicate that the classical concepts of a chemical bond are indeed contained in a fully delocalised set of molecular orbitals, however, such ideas are in a concealed form requiring the use of unitary transformations. It would seem more logical therefore, if one's primary aim is to interpret the bonding in terms of the wave function, to approximate this total wave function by a set of molecular orbitals that were indicative of the bonding in the molecule. In the case of water this would lead to a description that involved two equivalent bonding orbitals, two equivalent lone pair orbitals and an inner shell orbital on the oxygen<sup>a</sup>. Bader and Jones (31) in such an approach, approximated to each of these orbitals by an appropriate linear combination of atomic functions. By requiring the resultant density distribution to give the correct forces they found that

---

<sup>a</sup>This implies a restricted basis set approximation since a separation into lone pair orbitals is only possible when the hydrogen nuclei are represented by a single atomic orbital.

equilibrium could only be reached when the orbitals are allowed to bend, each at an angle of  $22^\circ$ , from the corresponding bond angle (see also ref. 32).

It was decided in the present work to proceed along similar lines to those of Bader and Jones, however, several important and necessary refinements both in the form and calculation of the molecular orbitals have been made.

In the formation of the water molecule the 1s electrons on the oxygen are expected to be non-bonding, however, it is well known that in the presence of an electric field they will polarise to an extent necessary to overcome the force exerted by the field. This polarisation can be represented mathematically by mixing into this 1s function parametrically controlled amounts of 2s and 2p atomic functions. McWeeney and Ohno (38) have shown that the extent of the mixing can be greatly reduced when  $h_i^a$  / 1s orthogonality is taken into account. Even so, there will be a concentration of charge on one side of the oxygen nucleus and will consequently give rise to an atomic force of the type A(1s.2p). It has been shown (33) that these forces are very sensitive to the choice of the atomic orbitals representative of 2s and 2p. If, for example, Slater type functions are employed, as in the work of Bader and Jones, then this will lead to unusually large atomic forces. A more reliable value of this integral requires the use of accurate Hartree-Fock self-consistent field atomic functions to describe the 1s, 2s and 2p orbitals on the oxygen

---

<sup>a</sup>  $h_i$  represents the hydrogen's 1s atomic orbital

atom in its ground state. These have been determined by Clementi et al. (34) using a linear combination of six basic functions to describe the 1s and 2s atomic orbitals and a linear combination of four basic functions to describe the 2p atomic orbital. The values of the orbital coefficients and screening constants were obtained by the Hartree-Fock method described previously (see page 7). The use of these functions will, of course, greatly increase the mathematical computation but the criticism of Salem and Alexander will now be taken into account.

Hurley (35) has also criticised the use of the Hellmann-Feynman theorem in a molecular orbital calculation. He pointed out the sensitivity of the force operators, containing the term  $1/r^2$ , to small changes in electron density near the atomic centres. In an effort to overcome this, we have stipulated the dipole moment as an added requirement that our density distribution must simultaneously satisfy. This property is governed by density in the outermost regions of the molecule.

Once the wave function for a molecule has been calculated then before it can be meaningfully interpreted, we must be certain that our calculation is indeed accurate. This is most readily done by comparing the expectation values of certain operators with their experimental counterparts.

We decided to use the proton shielding constant, quadrupole coupling constant and diamagnetic susceptibility as

our yardstick. These depend on the average values of  $1/r_H$ ,  $1/r_O^3$  and  $r_O^2$ , respectively, and as a consequence will indicate the accuracy of our density distribution close to the proton, close to the oxygen nucleus and in regions removed from both nuclei.

A more critical appraisal of this distribution would be, however, an energy calculation which depends simultaneously on the coordinates of two electrons. Such a calculation can readily be performed by the use of the so-called Integral Hellmann-Feynman theorem, originally proposed by Parr (37).

Suppose the water molecule is in a static configuration X represented by a wave function  $\psi_X$  and another molecule is in a static configuration Y represented by a wave function  $\psi_Y$  then the difference in energy between the two systems is, in the Born-Oppenheimer approximation, given by

$$E_X - E_Y = \Delta E = \frac{\int \psi_X \Delta H \psi_Y d\tau}{\int \psi_X \psi_Y d\tau} \quad \text{a}$$

where  $\Delta H = H_X - H_Y$

By a suitable choice of Y, isoelectronic neon, all the two electron operators in  $\Delta H$  will vanish and since both  $\psi_Y$  and  $E_Y$  are known accurately, the energy  $E_X$  associated with our wave function  $\psi_X$  can most readily be determined.

Richardson and Pack (36) have looked at the usefulness and applicability of this theorem. They compared values of

---

<sup>a</sup>Since this equation does not satisfy a variational theorem, it cannot be used to obtain the wave function.

the computed bond dissociation energies for different trial wave functions. The values they obtained were not, in the main, in good agreement with their experimental values. They did find though, that the more accurate wave functions did give the closer agreement. For this reason it was thought that although the absolute value of our energy was not to be relied upon, it would give us valuable information when we were comparing different proposed trial functions.

Thus, in summary, the purpose of the present research has been to calculate the best one-electron density distribution for the water molecule using only a limited set of basic functions. By requiring this distribution to give both the correct dipole moment and zero resultant force on the nuclei, the values of the parameters contained in the basis set can be obtained. The accuracy of our description will then be assessed by comparing the expectation values of several observables with their experimental counterparts. An attempt will then be given to explain the nature of the bonding in terms of the wave function and the conclusions that have been reached.

## II DETERMINATION OF THE WAVE FUNCTION

### (a) A description of the Equivalent Molecular Orbitals

#### Coordinate system

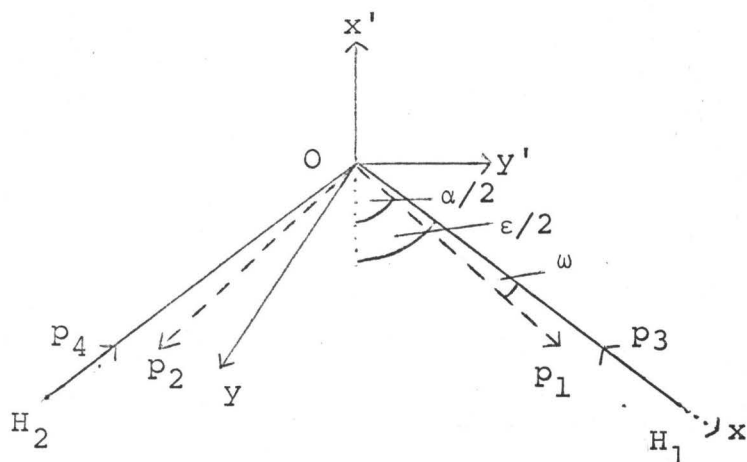


Figure I

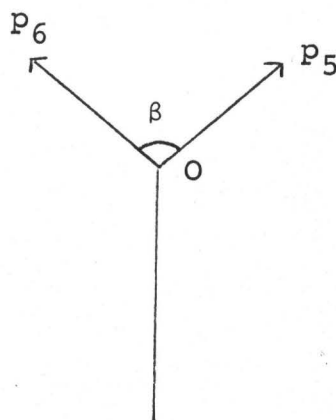


Figure II

#### Points to Note

1)  $1s$ ,  $2s$ ,  $p_0^a$ ,  $p_1$ ,  $p_2$ ,  $p_5$  and  $p_6$  are all atomic functions centred on the oxygen atom. These p functions can be expressed in terms of the  $xy$  or  $x'y'$  coordinate system as follows

$$p_0 = -px \cos(\epsilon/2) - py \sin(\epsilon/2)$$

$$p_1 = px \cos\omega + py \sin\omega$$

$$p_2 = px \cos t^b + py \sin t$$

$$p_5 = px \cos(\alpha/2) \cos(\beta/2) - py \sin(\alpha/2) \cos(\beta/2)$$

$$p_6 = -px \cos(\alpha/2) \cos(\beta/2) - py \sin(\alpha/2) \cos(\beta/2)$$

---

<sup>a</sup>For simplicity all 2p atomic functions will be written as  $p_i$

<sup>b</sup> $t = \alpha + \omega$

$$p_0 = px'$$

$$p_1 = -px' \cos(\alpha/2) + py' \sin(\alpha/2)$$

$$p_2 = px' \cos(\alpha/2) - py' \sin(\alpha/2)$$

$$p_5 = px' \cos(\beta/2) + pz \sin(\beta/2)$$

$$p_6 = px' \cos(\beta/2) - pz \sin(\beta/2)$$

2)  $h_1$  and  $h_2$  are atomic 1s functions centred on hydrogens one ( $H_1$ ) and two ( $H_2$ ) respectively.

3)  $p_3$  and  $p_4$  are atomic p functions centred on hydrogens one and two respectively and pointing along the bond direction.

The most general set of orbitals that can be written, using our limited set of basis functions, to represent the bonding lone pair and inner shell orbitals will be

#### BONDING ORBITALS

$$\phi_{b1} = \lambda(\cos\epsilon b \cdot 2s + \sin\epsilon b \cdot p_1 + C_3 \cdot 1s) + \mu(h_1^0 - \delta h_2^0)$$

$$\phi_{b2} = \lambda(\cos\epsilon b \cdot 2s + \sin\epsilon b \cdot p_2 + C_3 \cdot 1s) + \mu(h_2^0 - \delta h_1^0)$$

The superscript zero in  $h_1^0$  and  $h_2^0$  denotes that these functions are made orthogonal to the 1s atomic function on the oxygen and are thus given by

$$h_i^0 (i=1,2) = \frac{1}{(1 - S^2(h_i 1s))^{1/2}} (h_i - S(h_i 1s) \cdot 1s) = N_o (h_i - S_o 1s)$$

$$\text{Where } N_o = (1 - S_o^2)^{-1/2}$$

---

<sup>a</sup> An overlap integral of the type  $\langle x_i x_j \rangle$  will be given the symbol  $S(x_i x_j)$  and since  $S(h_i 1s)$ ,  $S(h_1 h_2)$  and  $S(p_3 1s)$  will be used extensively they are given the symbols  $S_o S_1$  and  $S_2$  respectively.



LONE PAIR ORBITALS

$$\phi_{\ell 1} = \cos \epsilon_1 \cdot 2s + \sin \epsilon_1 \cdot p_5$$

$$\phi_{\ell 2} = \cos \epsilon_1 \cdot 2s + \sin \epsilon_1 \cdot p_6$$

It is found, however, more convenient to write these orbitals in the form

$$\phi'_{\ell 1} = \cos \epsilon_1' 2s + \sin \epsilon_1' p_0$$

$$\phi'_{\ell 2} = p_z$$

which are obtained from  $\phi_{\ell 1}$  and  $\phi_{\ell 2}$  by correct unitary transformations. The parameters  $\epsilon_1$  and  $\epsilon_1'$  can now be shown to be related by the following three equations

$$\cos \epsilon_1 = \frac{1}{\sqrt{2} \cos \epsilon_1'} \quad \sin \epsilon_1 = \frac{\sin \epsilon_1'}{\sqrt{2} \cos (\beta/2)} = \cos^{-1}(-\cot^2 \epsilon_1)$$

INNER SHELL ORBITAL

$$\phi_0 = C_0 1s + C_1 2s + C_2 p_0$$

(b) Method of Calculation

These five orbitals can be seen to embody ten parameters

$\epsilon_b$  and  $\epsilon_l$  are the hybridisation parameters of the bonding and lone pair orbitals

$\lambda/\mu$  the polarity factor for the bonding orbitals.

$\alpha$ , the angle between the  $p_1$  and  $p_2$  functions. It is termed the orbital angle and when  $\alpha \neq \epsilon$  the bonds are "bent".

$\delta$  a parameter that determines the extent of delocalisation of the equivalent orbitals.

$C_0$ ,  $C_1$  and  $C_2$  determine the amount of ls polarisation.

$C_3$  determines the amount of ls in the bonding orbital.

In order that the total one-electron density can be written in the form

$$\rho = 2(\phi_{b1}^2 + \phi_{b2}^2 + \phi_{\ell1}^2 + \phi_{\ell2}^2 + \phi_o^2)$$

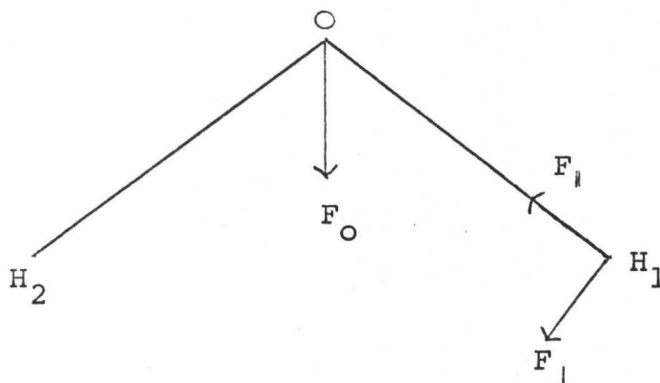
the equivalent molecular orbitals are both normalised and mutually orthogonal. That is to say

$$\begin{aligned} \langle \phi_{b1} \phi_{b1} \rangle &= 1 & \langle \phi_{b1} \phi_{b2} \rangle &= 0 & \langle \phi_{b1} \phi_{\ell1}' \rangle &= 0 \\ \langle \phi_o \phi_o \rangle &= 1 & \langle \phi_{b1} \phi_o \rangle &= 0 & \langle \phi_o \phi_{\ell1}' \rangle &= 0 \end{aligned}$$

These conditions enable six of the ten parameters to be determined and the requirement that the resultant density distribution give the correct zero force and dipole moment may be used to fix the remaining four.

FORCE REQUIREMENTS

In the water molecule all the forces can be broken down into three components  $F_{\text{O}}$ ,  $F_{\parallel}$  and  $F_{\perp}$ ; the remaining components giving trivial conditions being zero by symmetry alone.



$F_{\text{O}}$  - This is the force on the oxygen along the symmetry axis in the direction shown.

$F_{\parallel}$  and  $F_{\perp}$  - These are the forces on the hydrogen nucleus in a direction parallel and perpendicular to the bond axis.

NOTE: In all calculations of  $F_{\parallel}$  and  $F_{\perp}$  hydrogen one,  $H_1$ , will only be considered.

At equilibrium the nuclear forces of repulsion must equal the electrostatic forces of attraction. The nuclear forces of repulsion,  $F_{\text{i}}^{\text{N}}$ , can readily be shown to be

$$\begin{aligned} F_{\text{O}}^{\text{N}} &= 2 \times \frac{8}{R^2} \times \cos(\epsilon/2) \\ &= 8 \times 0.3739 \text{ a.u.} \end{aligned}$$

$$\begin{aligned} F_{\perp}^{\text{N}} &= \frac{1}{d^2} \times \cos(\epsilon/2) \\ &= 0.0748 \text{ a.u.} \end{aligned}$$

$$F_{\parallel}^N = \frac{8}{R^2} + \frac{1}{d^2} \times \sin(\epsilon/2)$$

$$= 2.5383 \text{ a.u.}$$

If we now represent  $F_i(\phi_j^2)$  as being the force exerted by the electron density contained in the  $j^{\text{th}}$  molecular orbital in the  $i^{\text{th}}$  direction, then at equilibrium we have

$$F_{\perp}(\phi_{b1}^2) + F_{\perp}(\phi_{b2}^2) + 2F_{\perp}(\phi_{\ell}^2) + F_{\perp}(\phi_O^2) = \frac{1}{d^2} \cos(\epsilon/2) \quad (11)$$

Where no distinction is made between the forces exerted by  $\phi_{b1}$  and  $\phi_{b2}$  or  $\phi_{\ell 1}$  and  $\phi_{\ell 2}$  then the two forces are equal.

$$F_{\parallel}(\phi_{b1}^2) + F_{\parallel}(\phi_{b2}^2) + 2F_{\parallel}(\phi_{\ell}^2) + F_{\parallel}(\phi_O^2) = \frac{8}{R^2} + \frac{1}{d^2} \sin(\epsilon/2) \quad (12)$$

$$2F_O(\phi_b^2) + 2F_O(\phi_{\ell}^2) + F_O(\phi_O^2) = \frac{2}{R^2} \cos(\epsilon/2)^a \quad (13)$$

#### DIPOLE MOMENT REQUIREMENT

For a molecule to possess a permanent dipole moment then there must be a separation of the centroids of positive and negative charge (39). If the centroids of these charges are taken to lie along the symmetry axis then the nuclear contribution to the dipole moment will be

$$DP_N = 2 \times 1.81 \times \cos(\epsilon/2) = 2.2179 \text{ a.u.}$$

and since the dipole moment is a one-electron property the centroid of negative charge, along this same direction is given by

$$\int \rho_1(\vec{r}) \vec{r} \, d\tau_1$$

where  $\vec{r}$  is a vector equal to  $r \cos\theta$ ,  $\theta$  being the angle between

---

<sup>a</sup>a common factor of eight, the nuclear charge on the oxygen atom, has been removed from the nuclear and electronic forces

the one electron density at the point  $\vec{r}$  and the symmetry axis. The total dipole moment, equal to 0.7240 from experiment, will be the sum of the nuclear and electronic contributions

$$DP = DP_N - DP_E = 0.7240 \text{ a.u.}$$

The electronic contribution can again be broken up into a sum of separate orbital components and thus we have as our fourth equation, that the density distribution must satisfy

$$DP_N - DP_E (\phi_O^2) + 2DP_E (\phi_{bl}^2) + 2DP_E (\phi_\ell^2) = 0.7240 \text{ a.u.} \quad (14)$$

The force and dipole moment equations together with the six orthonormal requirements enable one to calculate the ten parameters appearing in the equivalent molecular orbitals. The solutions to these ten equations are, however, not easy to find by conventional methods because of their complicated mathematical form - see appendix (1). For this reason we have found it necessary to proceed as follows:

An initial choice of four parameters was made such that by means of the orthonormalisation requirements the remaining six could be determined. Using these ten parameters the values of the three forces and dipole moment were compared with their true results, the two only agreeing when the numerical values of our original choice was correct. This process could then be repeated, varying the initial four parameters, until a solution was obtained.

For convenience  $\delta, \alpha, \epsilon b$  and  $C_3$  were chosen and using the

orthogonality of the bonding and lone pair orbitals  $\epsilon l'$  could be determined from the equation

$$\tan \epsilon l' = \frac{[\lambda/\mu \cos \epsilon b + S(h_1^0 2s) - \delta S(h_2^0 2s)]}{[-\sin \epsilon b S(p_1 p_0) + S(h_1^0 p_0) - S(h_2^0 p_0)]}$$

Orthogonality of the two bonding orbitals now allows  $\lambda/\mu$  the polarity factor, to be found the absolute values of  $\lambda$  and  $\mu$  being obtained from the normalisation of these same orbitals.

$$\begin{aligned} \left(\frac{\lambda}{\mu}\right)^2 \{C_0^2 + \cos^2 \epsilon b + \sin^2 \epsilon b S(p_1 p_2)\} + \left(\frac{\lambda}{\mu}\right) \{2(\cos \epsilon b S(h_1^0 2s) + \\ \sin \epsilon b S(h_1^0 p_2)) = \delta(\cos \epsilon b S(h_1^0 2s) + \sin \epsilon b S(h_1 p_2))\} + \\ S(h_1^0 h_2^0) (1 + \delta^2) - 2\delta = 0 \end{aligned}$$

and

$$\begin{aligned} \frac{1}{\mu^2} = \left(\frac{\lambda}{\mu}\right)^2 (1 + C_3^2) + \frac{2\lambda}{\mu} \{\cos \epsilon b S(h_1^0 2s) + \sin \epsilon b S(h_1 p_1)\} \\ - \delta(\cos \epsilon b S(h_2^0 2s) + \sin \epsilon b S(h_2 p_1))\} + (1 + \delta^2 - 2 S(h_1^0 h_2^0)). \end{aligned}$$

By invoking (i)  $\langle \phi_o \phi_o \rangle = 1$  (ii)  $\langle \phi_o \phi_\ell \rangle = 0$  and (iii)  $\langle \phi_o \phi_b \rangle = 0$  the three remaining parameters,  $C_0$ ,  $C_1$  and  $C_2$ , that determine the extent of inner shell polarisation, can readily be shown to be given by

$$\begin{aligned} C_2 &= \left[ \frac{1}{\left(\frac{D-BE}{A}\right)^2 + E^2 + 1} \right]^{1/2} \\ C_1 &= -EC_2 \\ C_0 &= -\frac{(BC_1 + DC_2)}{A} \end{aligned}$$

where

$$A = \lambda/\mu C_3$$

$$B = \lambda/\mu \cos \epsilon b + S(h_1^0 2s) + \delta S(h_2^0 2s)$$

$$D = \lambda/\mu \sin \epsilon b S(p_0 p_1) + S(h_1^0 p_0) - \delta S(h_2^0 p_0)$$

$$E = \tan \epsilon$$

The problem is thus one of finding the values of  $\delta, \alpha, \epsilon b$  and  $C_3$  such that equations (11), (12), (13) and (14) are satisfied. This is most conveniently achieved by defining a function  $R(\delta, \alpha, \epsilon b, C_3)$  such that it represents the squares of the differences of  $F_0, F_{\parallel}, F_{\perp}$  and DP from their true values. That is to say

$$R(\delta, \alpha, \epsilon b, C_3) = (F_0 - 0.3739)^2 + (F_{\parallel} - 2.5383)^2 + (DP - 0.7240)^2 + (F_{\perp} - 0.0748)^2 \quad (15)$$

thus requiring us to find a solution that

$$R(\delta, \alpha, \epsilon b, C_3) = 0$$

#### MINIMISATION OF R

For simplicity of explanation, it will be assumed that R is a function of two variables, X and Y. In order that we might distinguish between the different approximations to these variables they will be given the subscript I where now  $X(I)$  and  $Y(I)$  represent the  $I^{\text{th}}$  approximation to their true values.

By an initial arbitrary choice of  $X(I)$ ,  $Y(I)$  the value of  $R(X(I), Y(I))$  can be determined and the slope at this point is given by

$$\frac{dR}{dX(I)} = \frac{R(X(I) + h, Y(I)) - R(X(I) - h, Y(I))}{2h}$$

$$\frac{dR}{dY(I)} = \frac{R(X(I), Y(I) + h) - R(X(I), Y(I) - h)}{2h}$$

where  $h$  is a small increment dependant initially on the values of  $X(I)$  and  $Y(I)$ . A new point  $X(2)$ ,  $Y(2)$  is now picked such that it reflects the magnitude and sign of the calculated slopes each coordinate  $X(2)$ ,  $Y(2)$  being weighted individually. A function  $VAL(2)$  is then defined

$$VAL(2) = R(X(2), Y(2)) - R(X(I), Y(I))$$

Or more generally

$$VAL(I) = R(X(I), Y(I)) - R(X(I-1), Y(I-1))$$

such that an examination of its sign would indicate whether we are in fact moving towards the correct point —  $R$  equals zero.

With two variables the problem is three-dimensional. With four variables the problem is thus five-dimensional and consequently becomes very much more complicated. Points of reflection, minima that do not cross the planes containing  $R = 0$  and other geometrical hazards cause this method to fail



or at least run into difficulties. The situation must somehow be simplified. The most logical way would be to reduce the number of parameters and hence the number of conditions that our density distribution must satisfy.

It is known from previous experience (31) that  $F_O$ , the force on the oxygen nucleus, is almost totally determined by an inner polarisation of the oxygen 1s atomic orbital. If we thus assume  $C_O = 1, C_1 = C_2 = 0$ , and consequently  $C_3 = 0$ , and no longer have  $F_O$  as a requisite that our density distribution must satisfy then the problem reduces to one in four dimensions  $R$  now being defined as

$$R(\delta, \alpha, \epsilon, \beta) = (F_{\perp} - 0.0748)^2 + (F_{\parallel} - 2.5383)^2 + (DP - 0.7240)^2 \quad (16)$$

It was not, however, possible to find a solution to this simplified equation. In order that we attain the force perpendicular and dipole moment requirement density has to be concentrated in the region defined by the H-O-H bonds and if possible close to the symmetry axis. This is achieved by both bending the bonding orbitals,  $\alpha \neq \epsilon$ , and increasing the angle  $\beta$  between the lone pair orbitals. Such a removal of density both from the top of the molecule and from the bond direction causes the force parallel to fall well below its true value. One way in which we might expect to overcome this situation is by redefining  $R$  as being

$$R(\delta, \alpha, \epsilon, \beta) = (F_O - 0.3739)^2 + (F_{\perp} - 0.0748)^2 + (DP - 0.7240)^2 \quad (17)$$

where now a density shift into this previously defined region will help all the three forces. Again, no balance point could be reached and this time an examination of the analytical expressions contained in  $F_O$ ,  $F_I$  and DP gave us the reason. Such an examination revealed the importance of the atomic force integral

$$\langle ls_A p_A \cos \theta_A / r_A^2 \rangle = A \text{ (lsp)}$$

which in the case of A equal to oxygen<sup>a</sup> had the impressive value of 2.8673 a.u. This importance can best be exemplified by comparing the two centre overlap force integrals on the oxygen due to the overlap density ( $h_1^o p$ ) and ( $h_1 p$ ) defined as being 0 ( $h_1^o p$ ) and 0 ( $h_1 p$ ) respectively where

$$h_1^o = (1 - S_O^2)^{-1/2} (h_1 - S_O \text{ ls}) = 1.0018(h_1 - 0.0560 \text{ ls})$$

These integrals have the following values

$$0 (h_1^o px)^b = 1.0018(0 (h_1 px) - S_O A (\text{lsp}_x)) = 0.1875 \text{ a.u.}$$

$$0 (h_1 px) = 0.3480 \text{ a.u.}$$

and

$$0 (h_1^o py) = 1.0018(0 (h_1 py) - S_O A (\text{lsp}_y)) = 0.0912 \text{ a.u.}$$

$$0 (h_1 py) = 0.2517$$

---

<sup>a</sup> The atomic orbitals on the oxygen are given in appendix (3).

<sup>b</sup> The method of solving these integrals is given in appendix (2); their analytical forms together with their numerical answers are given in appendix (4).

That is to say by introducing  $S_o = 0.0560$ , or in other words by making the hydrogen 1s orbital orthogonal to the 1s orbital on the oxygen, we decrease  $0(h_{1px}^o)$  from 0.3480 a.u. to 0.1875 a.u. and  $0(h_{1py}^o)$  from 0.2517 a.u. to 0.0912 a.u., this decrease being due to the large atomic force term - underlined in both expressions. It is for this reason that a balance point could not be reached. The introduction of  $S_o$  is in fact admitting the importance of the 1s atomic orbital on the oxygen and we felt that before this could be done it must be represented more accurately by allowing for inner shell polarisation. This 1s polarisation, as stated previously, is almost totally responsible for  $F_o$  reaching its true value of 0.3740 a.u. and can be made to compensate the decrease in the overlap forces due to the introduction of  $S_o$ . It was thus assumed, for the moment, that  $S_o = 0.0$  and consequently  $h_i^o = h_i$ . This being the case then a solution to equation (17) such that  $R(\delta, \alpha, \epsilon b) = 0$  was most readily obtained and the values of  $\delta, \alpha$ , and  $\epsilon b$  are

$\delta$	$\alpha$	$\epsilon b$
0.3882	73.1652 <sup>o</sup>	123.2862 <sup>o</sup>

A value of 1.32 has been used for the screening coefficient of the hydrogen 1s atomic orbital. This figure was obtained by using an empirical rule discussed by Bader (41) which relates the screening in the separated atom (1.0) to that in the united atom. By this rule  $\xi = Z_s - \Delta Z e^{-R}$  where  $\Delta Z = Z_s - Z_u$ . The  $Z_s$  and  $Z_u$  refer to the effective nuclear charges calculated

by Slater's rules (including the factor  $1/n$  where  $n$  is the principal quantum number) for the electron in the separated and united atom respectively. What effect the value of this screening coefficient had on the equilibrium position is best exemplified by determining a new balance point using a value of 1.2

$\delta$	$\alpha$	$\epsilon b$
0.4166	82 2745	134.9600

Although there is a slight change in these parameters it is not serious and one can safely conclude that a slight variation around the chosen value of 1.32 will not drastically affect the final result.

Introduction of  $S_0$  equal to its correct value now, as predicted, caused the force on the oxygen nucleus to drop by 0.18 a.u. leaving the dipole moment and force perpendicular unchanged. By allowing for inner polarisation  $F_0$  could be increased to 0.3740 but now, because of the added parameter we must also require that our density distribution give the correct force parallel. The results of such a calculation are given below

$C_0$	$C_1$	$C_2$	$C_3$	$\delta$	$\alpha$	$\epsilon b$
0.9951	-0.0439	-0.0880	-0.0850	0.3882	73.1652	123.2862
		$F_0$	$F_{\perp}$	DP	$F_{\parallel}$	
		0.3686	0.0750	0.7210	2.4103	
TRUE						
VALUE	_____	0.3739	0.0748	0.7240	2.5383	

Although excellent agreement is obtained for  $F_O$ ,  $F_{\perp}$  and DP, the force parallel fell 5% below its true value. One way in which we might expect to improve this value is to add a 2p function on the hydrogen atoms, with a coefficient of  $C_4$ , in the hope that an atomic polarisation similar to that on the oxygen atom would cause a density shift of sufficient magnitude to raise the force parallel by the required 0.12 a.u. If this is the case then the bonding orbitals can now be written<sup>a</sup>

$$\phi_{b1} = (\cos\epsilon b2s + \sin\epsilon b p_1 + C_3 1s) + \mu(C_4 p_3^0 + (h_1 - \delta h_2^0))$$

$$\phi_{b2} = (\cos\epsilon b2s + \sin\epsilon b p_2 + C_3 1s) + \mu(C_4 p_4^0 + (h_2 - \delta h_1^0))$$

The superscript zero again signifies that they have been made orthogonal to the oxygen 1s atomic orbital and hence

$$p_i^0 = (1 - S(p_i 1s)^2)^{-1/2} (p_i - S(p_i 1s) 1s) = N_1 (1 - S_2 1s)$$

$$\text{where } N_1 = (1 - S_2^2)^{-1/2} \text{ and } S_2 = \langle p_i 1s \rangle$$

The orthonormality requirements together with the force and dipole moment equations must now be re-defined. Assuming  $C_4$  to be  $0.03^b$  and taking the screening coefficient of the 2p function to be 0.66, half that of the hydrogen 1s, a new

<sup>a</sup>These orbitals are no longer the most general set of orbitals that can be written.

<sup>b</sup>Nesbet (42) in a calculation on LiH found the 2p function on the hydrogen to have a coefficient between 0.01 and 0.02. Using this as a yardstick, the value of 0.03 was estimated.

balance point produced the following results

$F_{\text{O}}$	$F_{\perp}$	DP	$F_{\parallel}$
0.3661	0.0747	0.7220	2.4052

Not only have we given an upper limit to  $C_4$ , but we have also given the 2p functions their maximum directional character, in an attempt to increase the  $F_{\parallel}$ , by pointing them along the bond. Even so,  $F_{\parallel}$  has hardly changed. The atomic force integral,  $A(1sp_3)$ , which we hoped would be important contributes only 0.1825 a.u. to  $F_{\parallel}$ . This low value is a consequence of the diffuse density around the hydrogen, explicable in terms of the low 1s and 2p screening coefficients, when compared to that around the heavier oxygen nucleus. An increase in this coefficient from 0.66 to 1.00, although doubling  $A(1sp_3)$  was found to increase the force parallel by only 0.01 a.u. It was thus concluded that for all intents and purposes, no loss in accuracy would result in our description of the water molecule if  $C_4$  is assumed to be zero in the equivalent molecular orbital scheme. Using a screening coefficient of 1.32 for the hydrogen 1s atomic orbital and assuming  $C_4 = 0.0$ , then the parameters obtained together with the resultant orbitals representative of the bonding, lone pair and inner shell electrons are given as

$\delta$	= 0.3882	$\lambda$	= 0.7978	$C_2$	= -0.0880
$\alpha$	= 73.1652 <sup>o</sup>	$\mu$	= 0.4599	$C_3$	= -0.0850
$\epsilon_b$	= 123.2862 <sup>o</sup>	$C_{\text{O}}$	= 0.9951	$C_4$	= 0.0000
$\epsilon_{l'}$	= 26.5336 <sup>o</sup>	$C_1$	= -0.0439		

(d) RESULTS

$$\phi_{b1} = -0.4379(2s) + 0.6668(p_1) - 0.0678(1s) + 0.4599(h_1^0) \\ - 0.1785(h_2^0)$$

$$\phi_{b2} = -0.4379(2s) + 0.6668(p_2) - 0.0678(1s) + 0.4599(h_1^0) \\ - 0.1785(h_2^0)$$

$$\phi_{\ell 1}' = 0.8946(2s) - 0.4469(p_0)$$

$$\phi_{\ell 2}' = Pz$$

$$\phi_0 = 0.9951(1s) = 0.0439(2s) - 0.0880(p_0)$$

If we now define a coordinate system according to figures (I) and (II) and write the lone pair orbitals as

$$\phi_{\ell 1} = \cos\epsilon_1(2s) + \sin\epsilon_1(p_5)$$

$$\phi_{\ell 2} = \cos\epsilon_1(2s) + \sin\epsilon_1(p_6)$$

then

$$P_5 = \cos(\beta/2)(px') + \sin(\beta/2)(pz)$$

$$P_6 = \cos(\beta/2)(px') - \sin(\beta/2)(pz)$$

Thus we get by substitution

$$\phi_{\ell 1} = \cos\epsilon_1(2s) + \sin\epsilon_1\cos(\beta/2)(px') + \sin\epsilon_1\sin(\beta/2)(pz)$$

$$\phi_{\ell 2} = \cos\epsilon_1(2s) + \sin\epsilon_1\cos(\beta/2)(px') - \sin\epsilon_1\sin(\beta/2)(pz)$$

If on the other hand we took linear combinations of  $\phi_{\ell 1}'$  and

$\phi_{\ell 2}'$  remembering that  $p_0 \equiv px'$ , then

$$\phi_{\ell 1} = 1/\sqrt{2}(\cos\epsilon_1'(2s) + \sin\epsilon_1'(px') + pz)$$

$$\phi_{\ell 2} = 1/\sqrt{2}(\cos\epsilon_1'(2s) + \sin\epsilon_1'(px') - pz)$$

which leads on inspection to the following relationships

$$(A) \cos \epsilon l = (1/\sqrt{2}) \cos \epsilon l'$$

$$(B) \cos (\beta/2) = \frac{\sin \epsilon l'}{\sqrt{2} \sin \epsilon l}$$

$$(C) \sin (\beta/2) = \frac{1}{\sqrt{2} \sin \epsilon l}$$

From our force calculation  $\epsilon l'$  was determined to be  $-26.53^\circ$  and from equation (A), since  $\cos(X) = \cos(-X)$ ,  $\epsilon l$  will be  $\pm 50.76^\circ$ . However, we know that since  $\epsilon l'$  is negative,  $-\sin(X) = \sin(-X)$ , then  $\beta$ , the angle between the lone pairs, will be greater than  $180^\circ$ , therefore  $\cos(\beta/2)$  will be negative. For the coefficient preceding the  $p_x'$  atomic function in  $\phi_{\ell 1}$  and  $\phi_{\ell 2}$  to be negative  $\sin(\epsilon l)$  must be positive and hence  $\epsilon l$  will be  $+ 50.76^\circ$ . From equation (C),  $\beta/2$  can be shown to be  $114.06^\circ$  and hence  $\beta$  will be  $228.12^\circ$ .

Figure III represents the relative directions of the bonding and lone pair orbitals in the water molecule

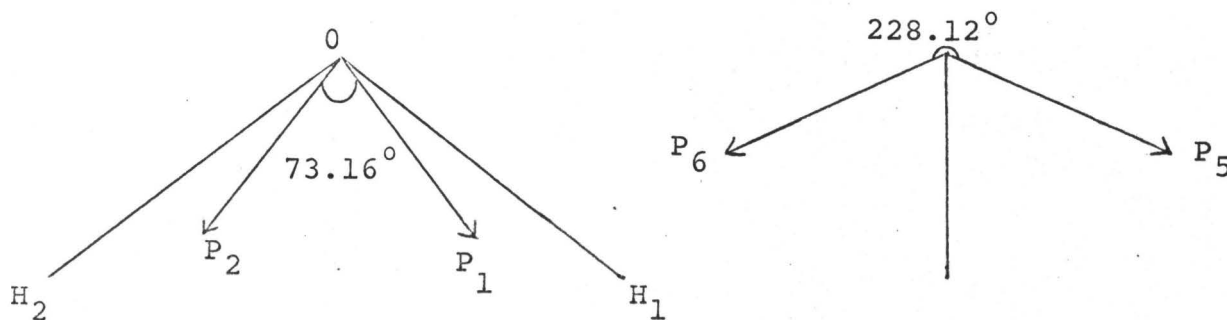


Figure III



The features of these equivalent molecular orbitals strongly resemble those found by Bader and Jones. The lone pair orbitals are, however, at a much greater angle with a hybridisation determined<sup>a</sup> to be  $sp^{1.5}$  compared to  $sp$ . The bonding orbitals are slightly more polar having a  $\lambda/\mu$  ratio of 1.735 compared with 1.563. These orbitals also contain a larger amount of 2s but again with a negative coefficient. The orbital angle  $\alpha$  of  $73.16^\circ$  corresponds to an angle,  $\omega$ , between the bond and orbital direction of  $15.64^\circ$  compared with  $22^\circ$  as determined by Bader and Jones.

A fuller discussion of these results and the conclusions drawn from them will be left until later, however, it is informative at the present time to take a closer look at the contributions that the different orbital densities make to the forces and dipole moment and examine what effect, if any, results from varying  $\delta$ ,  $\alpha$ , and  $\epsilon b$ , the three parameters for which  $R(\delta, \alpha, \epsilon b) = 0$ , about their accepted values.

Table I lists the force and dipole moment contributions for this equilibrium position.

As a consequence of  $\beta$  being greater than  $180^\circ$ , the lone pairs have a large positive contribution to both the force on oxygen and the electronic contribution to the total dipole moment, this latter quantity being measured in the same direction as  $F_O$ . The lone pair density, because of its location can

---

<sup>a</sup>  $\phi_{\ell 1} = \cos\epsilon 12s + \sin\epsilon 1p_5 = 0.6326.2s + 0.7745p_5 = 40\% 2s + 60\% 2p$

also be seen responsible for roughly one half of the force parallel. If we now turn our attention to the bonding orbitals then the force on the oxygen nucleus due to this density is in an unexpected direction. Because of the negative 1s and 2s coefficients appearing in these orbitals integrals of the type  $A(1sp)$  and  $A(2sp)$  account for over  $-0.50$  a.u. of the total  $-0.57$  a.u. contribution. It is for this reason that both inner shell polarisation and, to a large extent, re-orientation of the lone pair density is necessary. In the determination of  $DP_E$  atomic integrals are not nearly as important; this being indicated by both the value and sign of  $DP_E(\phi_b^2)$  and  $DP_E(\phi_o^2)$ .

Table II shows the effect of varying  $\alpha$  about  $73^\circ$  keeping  $\delta$  and  $\epsilon b$  fixed. As  $\alpha$  is decreased then  $\beta$ , the angle between the equivalent lone pairs is decreased. This causes a shift in density to the top of the molecule and as such, one expects the contribution of these orbitals to  $F_o$ ,  $F_{\parallel}$ ,  $F_{\perp}$  and DP to drop. An increase in  $\alpha$  causes the bonding orbitals, on the other hand, to concentrate more density in the region of the O-H bond. As a consequence of this there will be an increased contribution by these orbitals to both  $F_{\perp}$  and DP but a decreased contribution to  $F_{\parallel}$ .

Table III shows the effect of changing  $\delta$  while  $\alpha$  and  $\epsilon b$  are fixed. As  $\delta$  is increased, then  $\beta$  also increases. This has the effect of placing density, contained in the lone pair orbitals, into the binding region below the oxygen nucleus and by definition, such density will increase all the force

contributions: since  $\delta$  determines the amount of delocalisation of the two bonding orbitals, an increase in  $\delta$  will cause a decrease in the overlap of the two hydrogens

$$S(h_1^0 h_2^0)(1 + \delta^2) - 2\delta \quad \text{to} \quad S(h_1^0 h_2^0)(1 + \delta'^2) - 2\delta'$$

Electron density contained in these orbitals will thus be removed from the vicinity of the symmetry axis and placed closer to the O-H bonds. This will lead to an increase in  $F_{\parallel}$  and a decrease in both  $F_{\perp}$  and  $DP_E$ .

Finally, Table IV shows the effect of varying  $\epsilon b$ , keeping  $\alpha$  and  $\delta$  constant. As  $\epsilon b$  increases then  $\beta$  increases and for reasons described previously, all the force components due to the lone pair density will increase;  $\epsilon b$  determines the hybridisation of the bonding orbitals. As  $\epsilon b$  is increased, then since the 2s atomic function in the bond has a coefficient of  $\cos(\epsilon b)$  and the  $p_{\perp}$  atomic function a coefficient of  $\sin(\epsilon b)$ , such a bond will progressively lose its directional<sup>a</sup> character; caused by a decrease in the 2p coefficient and an increase in the 2s coefficient. The results of this "transformation" are reflected in the contributions that  $\phi_{b1}^2$  and  $\phi_{b2}^2$  make to the forces.

If we now turn our attention to the total forces  $F_O$ ,  $F_{\parallel}$ , and  $F_{\perp}$  and DP then their variation with  $\delta$ ,  $\alpha$ , and  $\epsilon b$  can best be represented graphically. (See Figure IV).

The similarity in effect of  $\alpha$  and  $\delta$  is immediately obvious being reflected in the slopes of their graphs. An increase in

<sup>a</sup> This is assuming  $180^{\circ} > b > 90^{\circ}$

either of these parameters will not only cause a similar bond density shift, see previously, but also result in  $\beta$ , the lone pair angle, increasing in the same direction and by roughly the same amount. This equivalence in action causes the force components, due to the lone and bonding pair density, and consequently the total force to react in a similar way with a change in  $\alpha$  or  $\delta$ .

If on the other hand, we increase  $\epsilon b$ , then although  $\beta$  is increased; the density shift due to the bonding orbitals will be in an opposite direction - an increase in  $\epsilon b$  causes the bonding orbitals to be less directional and density is removed from a region close to the O-H bond. The slopes of the lines obtained by varying  $\epsilon b$  now depends on the relative magnitude of the bonding and lone pair components and will not necessarily be in the same direction as those obtained for  $\alpha$  and  $\delta$ .

In the light of this, it can now be understood why it was impossible to find a solution that would simultaneously give the correct dipole moment, force parallel and force perpendicular. An increase in either  $\alpha$  or  $\delta$  or both is required to meet  $F_{\parallel}$ . Such an increase in these parameters will seriously affect the dipole moment causing it to rise rapidly. This increase in the dipole moment can only be counter balanced by an increase in  $\epsilon b$ , however, this would cause  $F_{\parallel}$  to drop and by roughly the same amount that  $\alpha$  or  $\delta$  increased it.

### III DETERMINATION OF THE MOLECULAR PROPERTIES

Before we can meaningfully interpret our results, we must be certain that the calculated density is a physically reasonable one. Many of the observable properties of a molecule are determined by the simple three-dimensional one-electron density. Three such properties, the diamagnetic susceptibility, the diamagnetic contribution to the nuclear screening constant and the electric field gradient at the oxygen nucleus will provide us with a means of estimating this accuracy.

#### (a) Diamagnetic Susceptibility

Van Vleck (43) has pointed out that the total magnetic susceptibility of a molecule not having a resultant spin is composed of two terms

$$\chi = \chi_d + \chi_{HF}$$

$\chi_d$ , the diamagnetic term, has the form

$$\chi_d = - \frac{e^2}{6mc^2} \times 2 \times \sum_{i=1}^5 \int \phi_i |r_A^2| \phi_i d\tau \quad (18)$$

where each  $\phi_i$ , representative of our equivalent molecular orbitals, is averaged over the operator  $r_A^2$ ,  $r_A$  being the distance of the one-electron density from the point A.  $\chi_{HF}$  is a term that arises in all molecules and is the temperature independent paramagnetic contribution often being referred to as the "high frequency" term or the Van Vleck paramagnetism. This high frequency term can be calculated knowing the rotational magnetic moment of a molecule since the magnetic

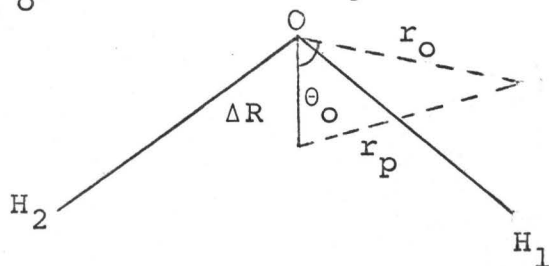
moment arising from this rotational motion is determined entirely by the induced paramagnetism. Weltner (44), using the centre of mass as his origin of coordinates, obtained for  $\chi_{HF}$  in the case of  $H_2O$ ,  $1.46 \times 10^{-6}$  e.m.u./mole. If the total magnetic susceptibility for liquid water is taken as  $-13.0 \times 10^{-6}$  (45), and assuming this to be fairly independent of phase, then a value of  $\chi_d$  for water vapour equal to  $-14.46 \times 10^{-6}$  e.m.u./mole is to be expected.

From quantum mechanics, if the wave function for a molecular system is known, then the expectation value of the diamagnetic susceptibility, from equation (18) is given by

$$\langle \chi_d \rangle = - \frac{Ne^2}{6mc^2} 2 (\chi(\phi_O^2) + \chi(\phi_{b1}^2) + \chi(\phi_{b2}^2) + \chi(\phi_{\ell1}^2) + \chi(\phi_{\ell2}^2))$$

$$\text{where } \chi(\phi_i^2) = \langle \phi_i | r_O^2 | \phi_i \rangle$$

taking the oxygen atom as the centre of coordinates. Although the total magnetic susceptibility is independent of our choice of origin, the values of  $\chi_d$  and  $\chi_{HF}$  are not, and since  $\chi_{HF}$  has been measured relative to the centre of mass, then so must  $\chi_d$ . This means that the total wave function should be averaged over  $r_p^2$  and not  $r_O^2$ , these two being related by



$$\Delta R = 0.1232$$

$$r_p^2 = r_O^2 + \Delta R^2 - 2r_O \cos \theta_O \Delta R \quad (19)$$

The average value of  $r_O^2$  has been calculated, using the previously determined wave function, to be 19.1733 a.u. (see appendix (5)), and since the last term in equation (19),  $r_O \cos \theta_O$ , is just the electronic contribution to the dipole moment  $\chi_d$  is given by

$$\chi_d = 19.1733 + 10\Delta R^2 - 2\Delta R(2.181 \cos(\epsilon/2) - 0.7240)$$

$$\chi_d = -14.9318 \times 10^{-6} \text{ e.m.u./mole}$$

Because of the nature of the operator, the diamagnetic susceptibility is largely determined by the density in the outermost regions of the molecule. The bond polarity and orbital exponent on the hydrogen 1s atomic orbital play an important role in determining its magnitude. The bond polarity because its ratio  $\lambda/\mu$  when small will weight the regions remote from the oxygen nucleus and the orbital exponent because it determines how diffuse or otherwise the electron density surrounding the hydrogen will be. A low value of this screening coefficient will lead to a more diffuse density in the outer regions of the molecule and thus cause an increase in the absolute value of  $\chi_d$ .

In a recent publication, Hake and Baynyard (46), have quoted the diamagnetic susceptibility for the water molecule obtained by different approximations to the wave function. If to this list we add the results obtained by Bader and Jones and our present calculation then

METHOD	$\chi_d \times 10^{-6}$
<sup>a</sup> extended O.C.E. <sup>A</sup>	-15.56
<sup>b</sup> minimal M.C.E. <sup>B</sup>	-15.20
<sup>c</sup> united atom	-12.59
<sup>d</sup> E.M.O.	-12.19
<sup>e</sup> present work	<u>-14.93</u>
<sup>f</sup> experimental	-14.46

a) Moccia (47)    b) Ellison and Schull (48)    c) this value was fixed from experiment    d) Bader and Jones    f) Weltner (44)  
 A) one centre expansion                      B) multicentre expansion

The discrepancies in the two central field treatments, a and c, is probably due to the difficulty in getting a reasonable electron density distribution far from the expansion centre, this fact being further emphasized by their expectation values for the dipole moment. The diamagnetic susceptibility, as determined by Ellison and Schull is too big and it has been suggested by Bader and Jones that this is due to both the low polarity of their O-H bond and the small value of their orbital exponent (1.0) for the hydrogen 1s atomic function. By taking a value of 1.32 these workers were able to get much closer agreement between the calculated and experimental values. They do point out, however, that this value of 1.32 is probably too high overestimating the 1s contraction and causing their calculated  $\chi_d$  to be too low. This is not found to be the case in our result. In the light of this perhaps a more reasonable



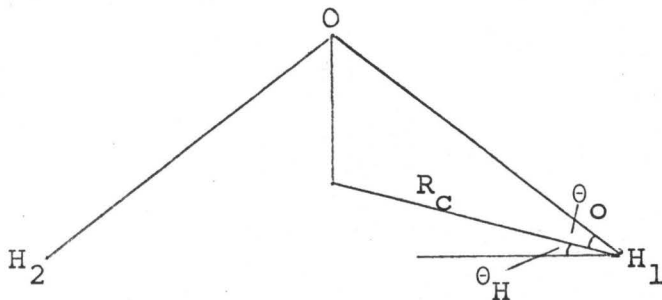
explanation would be the inadequacy of Slater-type functions, used in their basis set, causing the density to be slightly compressed around the oxygen nucleus.

Our value of  $\chi_d$  equal to  $-14.93 \times 10^{-6}$  e.m.u./mole, yields a total magnetic susceptibility of  $-13.47 \times 10^{-6}$  e.m.u./mole as compared to the experimental value of  $-13.0 \times 10^{-6}$  e.m.u./mole. Part of this discrepancy can be attributed, according to Venkatachalam and Kabadi (49), to hydrogen bond formation in the liquid phase for which the experimental value was obtained.

(b) Proton Magnetic Shielding Constant

The contribution to the total proton magnetic shielding constant can be divided into two parts, a diamagnetic contribution,  $\sigma_d$ , and a paramagnetic contribution,  $\sigma_p$ . The paramagnetic contribution can itself be divided into ground state,  $\sigma_p(G)$ , and excited state,  $\sigma_p(E)$ , terms.

Unfortunately there is no experimental determination of the spin rotational constant for water vapour and consequently no available measure of  $\sigma_p$ . However, Chan and Das (50) have shown that by a suitable choice of origin,  $\sigma_p$  can be estimated for a molecule with a known dipole moment. By taking this origin as the electronic centroid,  $\sigma_p(E)$ , the excited state contribution to  $\sigma_p$ , can be made to disappear. The ground state contribution,  $\sigma_p(G)$ , is now proportional to the electric field at the proton along the line joining it to the electronic centroid, this field being equal and opposite to that produced by the nuclei. Thus in the case of water, defining the co-ordinate system



it can be shown that

$$\sigma_p(G) = -\frac{\alpha^2}{3}R_C \left[ \frac{\cos\theta_H}{R_H} + \frac{8\cos\theta_O}{R} \right]$$

where  $R_c$  is the distance of the proton from the electronic centroid and the angles  $\theta_H$  and  $\theta_O$  are measured relative to the proton. For water  $\sigma_p(G) = -7.76 \times 10^{-5}$

Thus

$$\sigma = (\sigma_d - 7.76 \times 10^{-5})$$

where  $\sigma_d$  is the diamagnetic contribution to the proton shielding constant. This diamagnetic part measures what the shielding would be if the whole electronic structure was free to rotate about the nucleus without interference from the other nuclei. Since it is a measure of the potential energy of the nucleus in the electric field of the electrons,  $\langle 1/r_H \rangle$ , it can be evaluated from the ground state wave function of the molecule (51), (see appendix (6))

$$\sigma_d = - \frac{e^2}{3mc^2} \sum_{i=1}^5 \langle \phi_i | 1/r_H | \phi_i \rangle$$

That is to say, the one-electron density is averaged over the operator  $1/r_H$ . This operator by its very nature will weight the density distribution in a region close to the proton.

In the table below are listed the results obtained in the present calculation

	$\phi_o$	$\phi_{\ell 1}$	$\phi_{\ell 2}$	$\phi_{b1}$	$\phi_{b2}$
A <sup>a</sup>	1.1070	0.9810	1.2600	1.3654	0.8008
B	1.1060	0.9808	1.2998	1.1946	0.8848
C	1.1070	0.9809	1.2582	1.3780	0.8050
D	1.1070	0.9808	1.2576	1.3916	0.8050
	$-\frac{e^2}{3mc^2} \times d$		SG on	SC on	$10^5 \sigma$
		hi	pi		
A <sup>a</sup>	515140	1.32	/	2.03	
B	5.4662	1.20	/	1.94	
C	5.5294	1.32	.66	2.05	
D	5.5422	1.32	1.00	2.08	

<sup>a</sup> The molecular parameters in A, B, C, and D were obtained by

- A) Here the hydrogens have been represented by a 1s atomic function with a screening coefficient (S.C.) of 1.32
- B) The hydrogens are again represented by a 1s atomic function but now with a S.C. of 1.2
- C) The hydrogens are represented by a linear combination of a 1s (S.C. 1.32) and a 2p (S.C. 0.66) atomic functions
- D) Finally, the hydrogens are represented by a linear combination of a 1s (S.C. 1.32) and a 2p (S.C. 1.0) atomic functions

The experimental value is  $2.97 \times 10^{-5}$  according to Das and Ghose (52) obtained from measurements of Gutowsky and Hoffman (53) on the chemical shift of hydride molecules relative to methane. This estimate is based on a value of  $2.66 \times 10^{-5}$  for the shielding constant of the proton in the hydrogen molecule.

The foregoing table of results does show that the one-electron density as determined from force considerations, can give a reasonable measure of the proton magnetic shielding constant. Perhaps a more accurate determination of  $\sigma_p$  will remove some of the discrepancy.

(c) Electric Field Gradient

Unfortunately the quadrupole coupling constant of the oxygen atom in the water molecule has not been determined experimentally. However, by calculating the electric field gradient ( $q$ ) at the position of the oxygen nucleus and using the nuclear quadrupole moment ( $Q$ ) for  $O^{17}$ , then a value can be predicted through the relationship

$$\text{quadrupole coupling constant} = e Q q$$

The nuclear quadrupole moment measures the departure of the nuclear charge distribution from a spherical shape. Elongated nuclei have a positive  $Q$  and flattened nuclei have a negative  $Q$ ;  $q$  is the field gradient at the position of the oxygen nucleus. If this field gradient changes rapidly with angle then the various orientations of the non-spherical nucleus with respect to a chosen axis will give different energies. In order to estimate  $q$ , we have only to calculate the mean value of  $\frac{d^2V}{dz^2}$  where  $z$  is taken to lie along the principle axis of symmetry and  $V$  is the electrostatic potential in the molecule.  $V$  can be broken down into two components,  $V_n$  and  $V_e$ , a nuclear and electronic potential respectively. As a consequence of this,  $q$  can be written

$$q = q_n + q_e$$

where  $q_n$  and  $q_e$  represent the electric field gradients due to the protons and all the electrons in the molecule

$$q_n = \frac{d^2V_n}{dz^2} = \frac{d^2(e/R)}{dz^2} = \frac{d^2}{dz^2} \left( \frac{e}{x^2+y^2+z^2} \right) = e \left( \frac{3\cos^2(\epsilon/2)-1}{R} \right) = 0.0211 \text{ a.u.}$$

and since there are two protons

$$q_n = 0.0422 \text{ a.u.}$$

Using similar arguments for  $q_e$

$$q_e = -e \int \psi \left( \frac{3\cos^2\theta - 1}{r_o^2} \right) \psi d\tau$$

$r_o$  is the length of the radius vector drawn from the oxygen nucleus to the electron that is inclined at an angle  $\theta$  to the symmetry axis.

Using  $\chi$  equal to the calculated wave function for the water molecule then

$$q_e = -2e \sum_i q_i$$

where each  $q_i$  represents the different contributions to the electric field gradient due to density contained in  $\phi_o, \phi_{\ell 1}, \phi_{\ell 2}, \phi_{b1}$  and  $\phi_{b2}$ . These have been calculated to be (see appendix (7))

$q_o$	$q_{\ell 1} = q_{\ell 2}$	$q_{b1} = q_{b2}$	$q_T$
0.0218	-0.7140	0.8536	0.3010

therefore

$$q_e = -2eq_T = -0.6020 \text{ a.u.}$$

The magnitude of  $q_e$  is largely determined by the amount of 2p character along the  $q$  direction, in this case the symmetry axis, relative to the amount at right angles to this axis. The contribution from a  $p_z$  orbital is (-2) times that for  $p_x$  or  $p_y$  orbital. Townes and Dailey (54), considering only the contributions from p orbitals, have attempted to predict the nature of the bonds in many molecules. The qualitative basis

for their arguments is based on the incorrect assumption that bonds largely p in character must correspond to an orbital angle of  $90^\circ$  or greater. Their approach, in the case of ammonia, has been criticized by Bader and Jones (55) and the arguments they have used also apply to the water molecule.

From a knowledge of the electric quadrupole hyperfine constant for the  $^{17}\text{O}$  nucleus  $Q$ , the nuclear electric quadrupole moment, can be determined (56). However, such a calculation requires an accurate description of the electric field gradient at the position of this nucleus. Bessis, Lefebvre-Brion and Moser (57), using an approximation to the extended Hartree-Fock (58) function for the  $^3\text{P}_2$  and  $^3\text{P}_1$  states of the oxygen atom, determined this field gradient and predicted a value of  $Q$  equal to  $-0.024$  barns. The small magnitude indicates the odd neutron in  $^{17}\text{O}$  produces a very small distortion of the closed shell eight protons and eight neutrons. Using this value and the previously calculated  $q$ , a value of  $2.09 \times 10^{-20}$  e.s.u. for the quadrupole coupling constant of  $^{17}\text{O}$  in  $\text{H}_2\text{O}$  is predicted.

(d) Electronic Energy

The majority of available molecular wave functions have been obtained by the minimum energy condition of the variational method (59) . The resultant approximate wave function, which is the best in terms of total energy, does not necessarily yield the best charge distribution which governs other molecular properties. Karplus and Mukherji (24) have found this to be the case, in the framework of a limited basis set approximation, for HF. It was concluded that a better overall picture of this molecule can be obtained by making a small sacrifice in the energy subject to additional one-electron constraints. The advantage of their method lies in the fact that a relatively simple basis set can now give a reasonable description of a molecule. The question we must now ask is whether a wave function obtained by satisfying one-electron properties can accurately predict two-electron properties. In particular, as the density in the water molecule becomes more apropos the forces will the energy also improve. Such an energy calculation is quite complicated since it involves the two-electron operator  $1/r_{ij}$ . A mathematically simpler and more elegant method would be to use the so-called Integral Hellmann-Feynman theorem originally proposed by Parr (37). According to this theorem, the difference in energy,  $\Delta E$ , between two systems X and Y represented by the wave functions  $\psi_X$  and  $\psi_Y$  respectively is, in the Born-Oppenheimer approximation, given by



$$\Delta E = \frac{\int \psi_X \Delta H \psi_Y d\tau}{\int \psi_X \psi_Y d\tau} \quad (20)$$

where

$$\Delta H = H_X - H_Y$$

Equation (20) is exact for exact wave functions, however, since it does not satisfy a variational theorem it cannot be used to determine the wave function directly.

Richardson and Pack (36) have recently examined the usefulness and applicability of this theorem. They compared for a number of molecules the computed values for the bond dissociation energy with their experimental counterparts. In this case,  $\psi_X$  would represent the proposed ground state wave function for system X and  $\psi_Y$  the wave function representative of the dissociated atoms also in their ground state. By using a constant approximation to  $\psi_Y$ , accurate Hartree-Fock functions, they compared  $\Delta E$  (experimental) with  $\Delta E$  (calculated) for different proposed trial wave functions. Although the agreement of these two quantities was, in the main not good they did show that the more accurate description of the molecule did give the better result. The reason for this discrepancy has been pointed out by Musher (60). For approximate wave functions  $\psi_X$  and  $\psi_Y$  which are accurate to certain orders in smallness parameters  $n_X$  and  $n_Y$  respectively then the computed value of  $\Delta E$  will be accurate to this same order in  $n_X$  and  $n_Y$ . This suggests that the Integral Hellmann-Feynman theorem has little utility, for calculations involving approximate systems, in determining the absolute value of the system's energy.

By taking  $\psi_Y$  to represent the proposed wave function for the water molecule and  $\psi_X$  to represent the accurate Hartree-Fock function for the iso-electronic neon atom, then all the two-electron operators appearing in  $\Delta H$  will vanish.  $\Delta E$  is now given by  $(E_{Ne} - E_{H_2O})$  and since  $E_{Ne}$  is known,  $E_{H_2O}$  can be calculated. Following the arguments of Musher, the absolute value of either the energy or energy difference calculated in this way is not to be relied upon. The computed values can however, according to the results of Richardson and Pack, still be used to discuss the relative merits of different proposed trial functions.

The proof of the relationship given by equation (20) is elementary. The two Schrodinger equations for system X and Y are of the form

$$H_X \psi_X = E_X \psi_X \quad (21)$$

$$H_Y \psi_Y = E_Y \psi_Y \quad (22)$$

By multiplying equation (21) by  $\psi_Y$  integrating over all space and applying the Hermitian property

$$E_X = S^{-1} \int \psi_X H_X \psi_Y \, d\tau \quad (23)$$

where

$$S = \int \psi_X \psi_Y \, d\tau$$

Similarly for equation (22)

$$E_Y = S^{-1} \int \psi_X H_Y \psi_Y \, d\tau \quad (24)$$

On subtracting equations (23) and (24), then the required result is obtained.

$$\Delta E = E_X - E_Y = S^{-1} \int \psi_X \Delta H \psi_Y d\tau \quad (25)$$

$\Delta H$ , the difference in the Hamiltonian operators for the two systems, is defined as being

$$\Delta H = H_X - H_Y = \Delta V_{nn} + \Delta V_{ee} + \sum_i H'(i)$$

where

$$H'(i) = V_{ne}^X(i) - V_{ne}^Y(i)$$

Now, since the systems X and Y are chosen so as to be iso-electronic, then  $\Delta V_{ee}$ , the difference in the electron-electron repulsion energy, will vanish and the equation representative of  $\Delta H$  will contain only  $\Delta V_{nn}$  and  $\Delta V_{ne}(i)$ .  $\Delta V_{nn}$  is the difference in the nuclear-nuclear repulsion energy and  $\Delta V_{ne}(i)$  is the difference in the nuclear-electron attraction energy. Since  $\Delta V_{nn}$  is dependent only on the coordinates of the nuclei and we are assuming the Born-Oppenheimer approximation, then  $\Delta E$ , the difference in energy, depends only on the coordinates of the  $i^{\text{th}}$  electron. By remembering that all the electrons are equivalent, equation (25) can be further simplified to give

$$\begin{aligned} \Delta E &= \Delta V_{nn} + S^{-1} \int \psi_X \left[ \sum_i H'(i) \right] \psi_Y d\tau \\ &= \Delta V_{nn} + \frac{N}{S} \langle \psi_X H'(1) \psi_Y \rangle \\ &= \Delta V_{nn} + \langle \rho_{XY} H'(1) \rangle \end{aligned}$$

Here  $\rho_{XY}$  is the one-electron normalized transition or rearrangement density and  $N$  is the total number of electrons contained in the system  $X$  (and  $Y$ ).

If  $\psi_Y$  represents the calculated wave function for the water molecule and  $\psi_X$  the wave function for isoelectronic neon, then  $\rho_{XY}(1)$  is defined as being

$$\rho_{XY}(1) = \frac{N}{S} \int \psi_X(1,2,\dots,N) \psi_Y(1,2,\dots,N) d\tau_2 \dots d\tau_N$$

where  $N(=10)$  is the total number of electrons and

$$S = \int \psi_X(1,2,\dots,N) \psi_Y(1,2,\dots,N) d\tau_1 d\tau_2 \dots d\tau_N$$

$\psi_Y$  was approximated by a single Slater determinant of one-electron equivalent molecular orbitals.

$$\psi_Y = \frac{1}{\sqrt{10!}} |\phi_1(1)\alpha(1)\phi_1(2)\beta(2)\dots\phi_5(10)\beta(10)|$$

If we further take the best possible single-determinant approximation to  $\psi_X$ , namely the Hartree-Fock self-consistent field wave function

$$\psi_X = \frac{1}{\sqrt{10!}} |\phi_6(1)\alpha(1)\phi_6(2)\beta(2)\dots\phi_{10}(10)\beta(10)|$$

then, according to Kim and Parr(61), the working formula for

the Integral Hellmann-Feynman theorem will be

$$\Delta E = \Delta V_{nn} = 2 \sum_{\substack{\ell=1 \\ (\ell=\ell+5)}}^{N/2} \frac{\langle \phi_{\ell} | H' | \phi_{\ell} \rangle}{D_{XY}} D_{XY}(\ell | \ell') + 2 \sum_{\substack{\ell=1 \\ m' = m+5}}^{N/2} \frac{\langle \phi_{\ell} | H' | \phi_{m'} \rangle}{D_{XY}} D_{XY}(\ell | m') \quad (26)$$

where

$$D_{XY} = \langle \psi_X | \psi_Y \rangle = \det^a (\langle \phi_{\ell} | \phi_{m'} \rangle)$$

and

$$D_{XY}(\ell | m') = \text{cofactor of the } \ell, m' \text{ element in } D_{XY}.$$

On replacing  $\langle \phi_{\ell} | H' | \phi_{m'} \rangle$  by the symbol  $H'_{\ell m'}$ , and  $D_{XY}(\ell | m')$  by the symbol  $\det(S_{\ell m'})$  equation (26) can be rewritten as

$$\Delta E = \Delta V_{nn} + \frac{2}{\det(S_{\ell m'})} \sum_{\substack{\ell=1 \\ \ell' = \ell+5}}^{N/2} (H'_{\ell \ell}, \det(S_{\ell \ell'})) + \sum_{\substack{m=1 \\ m' = m+5}}^{N/2} H'_{\ell m}, \det(S_{\ell m'}) \quad (27)$$

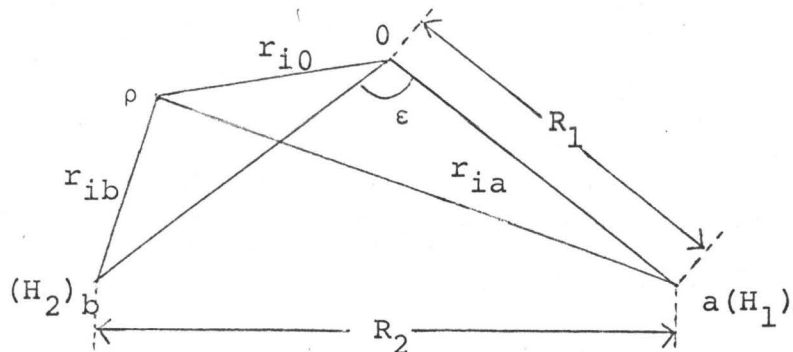
Let us now turn our attention to the form of the operator  $H'$ . This is defined as being the difference in the Hamiltonian for the water molecule and the neon atom

$$H' = H_{\text{Ne}} - H_{\text{H}_2\text{O}}$$

---

<sup>a</sup>det. is taken to represent determinant.

$H_{H_2O}$  according to the coordinate system below



will be

$$H_{H_2O} = \frac{1}{2} \sum_i \nabla_i^2 - Z_O \sum_i \frac{1}{r_{iO}} + \sum_{i < j} \frac{1}{r_{ij}} + Z_O \sum_{\alpha=a,b} \frac{1}{r_{\alpha O}} + 1/R_2$$

where  $Z_O$  is the nuclear charge on the oxygen atom and  $\alpha$  defines the hydrogens a and b. Similarly

$$H_{Ne} = \frac{1}{2} \sum_i \nabla_i^2 - Z_{Ne} \sum_i \frac{1}{r_{iNe}} + \sum_{i < j} \frac{1}{r_{ij}}$$

By making the oxygen and neon nuclei lie at the origin of the coordinate system, then since  $r_{iO} = r_{iNe}$

$$H' = \Delta H - 2 \sum_i \frac{1}{r_{iO}} + \sum_i (1/r_{ia} + 1/r_{ib}) + \Delta V_{nn}$$

where

$$\Delta V_{nn} = - \frac{2Z_O}{R_1} - \frac{1}{R_2} = K$$

All the electrons are, however, equivalent in which case the one-electron integral

$$\int \psi_X^{H'}(i) \psi_Y d\tau$$

requires only a knowledge of the transition density,  $\rho_{XY}$ , averaged over the operator  $H'(1)$

$$H'(1) = \left( - \frac{2}{r_{10}} + \frac{1}{r_{1a}} + \frac{1}{r_{1b}} \right) + K \quad (28)$$

where  $r_a$  and  $r_b$  are the distances of electron (1) from the hydrogens (1) and (2) respectively.

Equation (27), which determines the difference in energy between the water molecule and the neon atom, thus depends on two distinct types of integrals. There is the conventional overlap integral  $S_{ij}$  and an integral that involves the operator  $H'$ ,  $H'_{ij}$ . In a form more applicable to the present calculation, this equation can be written

$$\Delta E = \frac{2}{\text{TOT}} (H'_{16}\text{SUM}(1) + H'_{17}\text{SUM}(2) + \dots + H'_{510}\text{SUM}(25)) + K$$

Here TOT replaces  $\det(S_{1m})$  and corresponds to the expansion of a 5 x 5 determinant of overlap integrals (see appendix (8)). Associated with every  $H'_{ij}$  term appearing in the expression for  $\Delta E$ , there will be a determinant of overlap integrals, given the symbol SUM(I). Each SUM(I) is defined as being the cofactor of the  $i,j$  element in the 5 x 5 determinant TOT and will consequently be of dimension 4 x 4 containing 4! or 24 terms (see appendix (9)).

The  $H'_{ij}$ 's are obtained by averaging the appropriate transition density  $\phi_i\phi_j$  over the operator  $H'$ . Because of the nature of  $H'$ , equation (28), there will arise three distinct types of one-electron integrals

$$(i) \langle \phi_i \frac{1}{r_o} \phi_j \rangle \quad (ii) \langle \phi_i \frac{1}{r_a} \phi_j \rangle \quad (iii) \langle \phi_i \frac{1}{r_b} \phi_j \rangle$$

where  $i = 1, 2, 3, 4$ , and 5 refers to the five occupied molecular orbitals and  $j = 6, 7, 8, 9$ , and 10 refers to the occupied atomic

orbitals on neon. By defining the  $\phi_i$ 's and  $\phi_j$ 's as being

$$\begin{array}{ll}
 \phi_1 = \phi_0 & \phi_6 = 1s \\
 \phi_2 = \phi_{b1} & \phi_7 = 2s \\
 \phi_3 = \phi_{b2} & \phi_8 = 2px = r \cos \theta e^{-\alpha r} \alpha^{5/2} / \sqrt{\pi} \\
 \phi_4 = \phi_{\ell 1} & \phi_9 = 2py = r \cos \theta \sin \phi e^{-\alpha r} \alpha^{5/2} / \sqrt{\pi} \\
 \phi_5 = \phi_{\ell 2} & \phi_{10} = 2pz = r \cos \theta \cos \phi e^{-\alpha r} \alpha^{5/2} / \sqrt{\pi}
 \end{array}$$

then the analytical forms of the integrals represented by equations (i), (ii), (iii) and the overlap integrals  $\langle \phi_i \phi_j \rangle$ , together with their numerical values are given in appendix (10).

Although the calculation of  $\Delta E$  requires only the knowledge of relatively simple one-electron integrals, the form of the equations involved can be seen to be quite complicated. In order to substantiate the present approach it was thought advisable to duplicate a result obtained by Richardson and Pack. In a similar calculation on LiH they took the wave function for this molecule, obtained by Kahalas and Nesbit (62), to represent  $\psi_Y$  and using  $\psi_X$  to represent the wave function for the iso-electronic beryllium atom calculated  $\Delta E$ . This is only a four-electron problem, as compared to the present ten-electron problem, and as such is much simpler. If  $\phi_1$  and  $\phi_2$  represent the two occupied molecular orbitals on LiH and  $\phi_3$  and  $\phi_4$  the two occupied atomic orbitals on beryllium, then according to the previous arguments and symbolism

$$\Delta E = \frac{2}{\text{TOT}} (H_{13} \text{SUM}(1) + H_{14} \text{SUM}(2) + H_{23} \text{SUM}(3) + H_{24} \text{SUM}(4)) + K$$



where now

$$\text{TOT} = (S_{13}S_{24} - S_{14}S_{23})$$

$$\text{SUM}(1) = S_{24}$$

$$\text{SUM}(2) = -S_{23}$$

$$\text{SUM}(3) = -S_{14}$$

$$\text{SUM}(4) = S_{13}$$

$$K = Z_{\text{Li}}/R$$

The operator  $H'$ , appearing in the integrals  $H_{ij}$ , is now equal to  $(1/r_b - 1/r_a)$  with  $a$  and  $b$  referring to the Li and H nuclei respectively. In this way, the result of Richardson and Pack was duplicated.

For the present calculation on the water molecule  $\Delta E = (E_{\text{Ne}} - E_{\text{H}_2\text{O}})$  and since from experiment,  $E_{\text{Ne}}$  and  $E_{\text{H}_2\text{O}}$  are known to be  $-128.55$  and  $-76.46^a$ , respectively, a value of  $\Delta E$  equal to  $-52.09$  should be obtained. The results obtained are summarized in Table V. Each  $\Delta E$  calculation is representative of a different approximation to the forces. The orbital parameters were obtained by a minimisation of the previously defined function  $R$  in the usual way, however, it was only stipulated that the resultant density distribution give the correct dipole moment. This, of course, is not sufficient to characterize completely the parameters appearing in our basis set and consequently there are a very large number of possible solutions that meet this requisite. Of the few listed in Table V, numbers 1, 2 and 3 were obtained for  $S_0 = 0.056$  and 4 and 5

---

<sup>a</sup> All the energies are expressed in a.u.

were obtained for  $S_0 = 0.0$ . The orbital parameters for calculation number 1 approximate very closely those expected from an  $sp^3$  hybridisation scheme and hence a tetrahedral electronic configuration. According to the results of earlier workers (7,9,14,17) this was assumed to be the case in the water molecule where  $\alpha$ , the orbital angle, was taken to equal  $\epsilon$ , the bond angle. Table V shows, however, that the computed value of the energy for this point is the poorest of all the cases considered here. It can also be seen that from an examination of the forces acting on the nuclei an unstable molecule would result for such a description. Only by orbital bending, which essentially increases the p-character in the bonding orbitals and the s-character in the lone pairs, can electrostatic equilibrium be attained. Although it is very difficult to relate the form of the  $\Delta E$  equation with the orbital parameters, one point is clear, as the density distribution becomes more apropos the forces then the energy also improves. The best value for the energy difference was in fact obtained using the orbital parameters that gave the best forces. The absolute value of  $\Delta E$  was not, however, in good agreement with the predicted value of -52.09 but for reasons described previously, this is not surprising. The fact that  $\Delta E$  improves as the forces improve is very encouraging and adds weight to the supposition that a wave function as determined by satisfying a one-electron property does not necessarily predict inaccurate two-electron properties.

#### IV DISCUSSION

Once the wave function for a molecule is known, then the problem reduces to one of interpreting it. From a chemical viewpoint the binding in a molecule is of primary concern and such ideas as ionicity, covalency and partial ionic character have received widespread use in this context. The water molecule is particularly useful from this point of view and in many instances has been used as a prototype for a series of molecules containing lone pairs of electrons.

The general approach has been to assume a direct relationship between the orbital form of the wave functions and the geometry of the molecule. In particular, the bonding orbitals are made to point directly along the bond axis. Following the simple qualitative arguments given previously, this would lead to a description for the water molecule that involved two bonding and two lone pair orbitals in a near tetrahedral and consequently  $sp^3$  configuration.

The results of the present calculation have not found this to be the case. Not only are the bonding orbitals at an angle  $\omega$  to the bond direction but they are also associated with negative hybrids. This has the effect of removing bonding electrons from the internuclear region, and further, they put these electrons into that region of space previously occupied by the lone pairs. Meanwhile, the lone pairs, being at an

angle  $\beta$  greater than  $180^\circ$ , cause this previously vacated density to be replaced.

Such a description would seem to have little, if any, connection with the more conventional picture. However, if one remembers the arguments of Edminston and Ruedenberg, then perhaps the unusual direction of our bond hybrids can be removed by the introduction of secondary contributions into the lone pair orbitals from neighboring atoms. According to the results of these authors, the secondary contributions invariably appear with a negative coefficient and seem to lie within the range  $-0.1$  to  $-0.2$ .

The problem is thus to produce a new set of orbitals such that now the  $1s$  atomic functions centred on the hydrogens (1) and (2) are introduced into the lone pair description. This is most readily achieved, from our previous definitions of  $\phi_{\ell 1}$ ,  $\phi_{\ell 2}$ ,  $\phi_{b1}$ , and  $\phi_{b2}$ , by means of an orthonormal transformation such that now<sup>a</sup>

$$\phi_{\ell 1}^{\circ} = 1/(1 + g) ((\phi_{\ell 1} - g\phi_{\ell 2}) - g^{1/2}(\phi_{b1} + \phi_{b2}))$$

$$\phi_{\ell 2}^{\circ} = 1/(1 + g) ((\phi_{\ell 2} - g\phi_{\ell 1}) - g^{1/2}(\phi_{b1} + \phi_{b2}))$$

$$\phi_{b1}^{\circ} = 1/(1 + g) ((\phi_{b1} - g\phi_{b2}) - g^{1/2}(\phi_{\ell 1} + \phi_{\ell 2}))$$

$$\phi_{b2}^{\circ} = 1/(1 + g) ((\phi_{b2} - g\phi_{b1}) - g^{1/2}(\phi_{\ell 1} + \phi_{\ell 2}))$$

The parameter  $g$  can now be varied at will and with every new value, the form of the orbital will change. The total density distribution, and consequently its associated molecular proper-

<sup>a</sup> for their expanded forms see appendix (11)

ties, are however invariant, for a given set of orbital parameters, to such an orthonormal transformation. By a careful manipulation of  $g$ , both the bonding and lone pair orbitals can, in agreement with the predictions of Edminston and Ruedenberg, be made to point in the "correct" direction. This would correspond, according to the coordinate system of Fig. 1, to the following signs in the oxygen 2s and p atomic orbital coefficients

$$\phi_{\ell 1}^{\circ} \rightarrow (+ 2s + px' + pz)$$

$$\phi_{\ell 2}^{\circ} \rightarrow (+ 2s + px' - pz)$$

$$\phi_{b1}^{\circ} \rightarrow (+ 2s - px' + py')$$

$$\phi_{b2}^{\circ} \rightarrow (+ 2s - px' - py')$$

By expanding  $\phi_{\ell 1}^{\circ}$ ,  $\phi_{\ell 2}^{\circ}$ ,  $\phi_{b1}^{\circ}$ , and  $\phi_{b2}^{\circ}$ , the variation of the different atomic orbital coefficients with a change in  $g$  can be calculated and these are given, for a few sample points, in Table VI. A value of  $g$  greater than or equal to  $\sim 0.08$  satisfies the above requirements; however, it should be remembered that the lone pair orbitals no longer have their conventional meaning since they are not centred on one nucleus and can consequently take part directly in the bonding. The secondary contributions  $c^{\ell}(h_1^{\circ} + h_2^{\circ})$ , introduced into these orbitals is indeed both negative and within the predicted range.

By now writing the new lone pairs in the familiar form

$$\begin{aligned} \phi_{\ell 1}^{\circ} = & \lambda' (\cos \epsilon l (2s) + \sin \epsilon l \cos(\beta/2) (px') + \sin \epsilon l \sin(\beta/2) (pz)) \\ & + \mu' (h_1^{\circ} + h_2^{\circ}) \end{aligned}$$

$$\phi_{\ell 2}^0 = \lambda' (\cos \epsilon l (2s) + \sin \epsilon l \cos(\beta/2) (px') - \sin \epsilon l \sin(\beta/2) (pz) + \mu' (h_1^0 + h_2^0)$$

it can be seen that

$$\begin{aligned}\lambda' \cos \epsilon l &= c^{\ell} (2s)^a \\ \lambda' \sin \epsilon l \cos(\beta/2) &= c^{\ell} (px') \\ \lambda' \sin \epsilon l \sin(\beta/2) &= c^{\ell} (pz) \\ \mu' &= c^{\ell} (h_1 + h_2)\end{aligned}$$

and similarly for the bonding orbitals

$$\begin{aligned}\lambda \cos \epsilon b &= c^b (2s) \\ -\lambda \sin \epsilon b \cos(\alpha/2) &= c^b (px') \\ \lambda \sin \epsilon b \sin(\alpha/2) &= c^b (py') \\ \lambda c_3 &= c^b (1s) \\ \mu &= c^{b1} (h_1) \\ -\mu \delta &= c^{b1} (h_2)\end{aligned}$$

Using these relationships, Table VII can be constructed. As  $g$  changes then  $\lambda/\mu$  and  $\lambda'/\mu'$ , the bonding and lone pair polarity factors, change drastically as do the other important parameters  $\alpha$ ,  $\delta$ ,  $\epsilon b$ , and  $\epsilon l$ . These changes, brought about by our orthogonal transformation, will not alter the overall picture of the water molecule and in particular the total density and hence the resultant electrostatic forces will remain the same. The various orbital contributions to these forces will however be different.

The equivalent molecular orbitals obtained from calculation number 4, vaguely resembles the tetrahedral case and it <sup>a</sup> where no distinction is made between  $b1$  and  $b2$  or  $\ell 1$  and  $\ell 2$  then  $c^{b1} = c^{b2}$  and  $c^{\ell 1} = c^{\ell 2}$ .

is interesting to examine a force analysis for this data

FORCE	$\phi_{\ell 1}^2$	$\phi_{\ell 2}^2$	$\phi_{b1}^2$	$\phi_{b2}^2$	$\phi_o^2$	TOTAL
$F_o$	-0.5265	-0.5265	0.2112	0.2112	0.9988	0.3682
$F_{  }$	0.3833	0.3833	0.7208	0.3063	0.6127	2.4064
$F_{\perp}$	-0.0405	-0.0405	0.0569	0.0954	0.0030	0.0743
$DP_E$	-0.5218	-0.5218	1.2651	1.2651	0.0112	-1.4978

The charge distribution in the bonding orbitals is now such that it exerts a positive binding force on all the nuclei. The lone pair density similarly acts as predicted by the tetrahedral bonding scheme. One point to note about the lone pair orbitals is the large negative contributions that they now make to the electronic dipole moment; a point that has been used to reason the existence of both a large dipole, equal to  $(DP_N - DP_E)$ , and an  $sp^3$  hybridisation scheme. It should, however, be remembered that this state of affairs is only possible when the lone pair orbitals are no longer localised on one centre.

The results listed in Tables VI and VII, of course, represent only a few of an infinite number of possible hybrid schemes all producing the same net density distribution. The large variation of the parameters contained in the lone pair and bonding orbitals with a change in  $g$ , emphasizes the point at hand. Any description of the bonding in terms of the molecular orbitals, and in particular in terms of  $\lambda/\mu, \alpha, \delta, \epsilon_b,$  and  $\epsilon_l$ , is not unique and as such not very useful. To talk of a particular bond or lone pair hybridisation is meaningless.

A more realistic approach to the problem would be one that is independent of the form of the orbitals. Such a property is the one-electron density distribution. This can be represented pictorially by a contour map obtained by mapping the function

$$\begin{aligned} \rho(\vec{r}) &= \frac{N}{N!} \int |\psi_1(1)\psi_2(2)\dots\psi_N(N)| |\psi_1(1)\psi_2(2)\dots\psi_N(N)| d\tau_2\dots d\tau_N \\ &= 2 \sum_{i=1}^5 \phi_i(1)\phi_i(1) \end{aligned}$$

for different values of  $\vec{r}$  and connecting points of equal density<sup>a</sup>.

The in- and out-of-plane contour maps, defined by Fig. V below

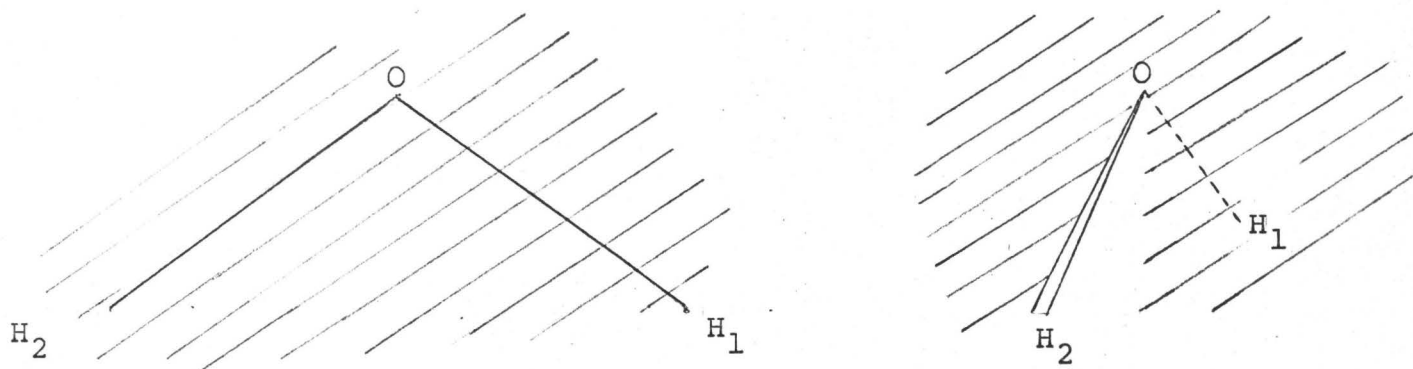


Fig. V

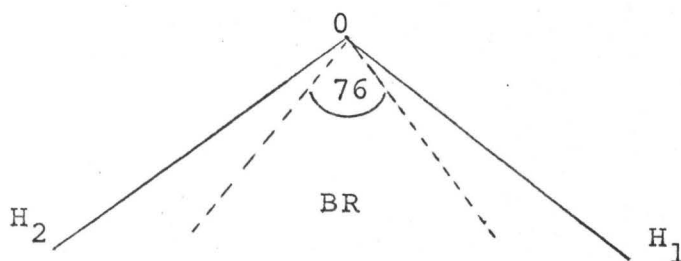
and given in Fig. VI, adequately point out the lack in prominence of the lone pair density. If the hybridisation had been  $sp^3$ , or better if the electron density distribution had been tetrahedral,

<sup>a</sup>because of the extensive use of these contour maps in the second part of this thesis, a fuller discussion of their calculation will be left until later (see appendix (12)). It is sufficient to know at the moment that each line represents an equidense surface whose magnitude is indicated in atomic units.



a large concentration of charge above the oxygen nucleus would have been expected. The contours around this nucleus are in fact very nearly spherical with if anything a slight inward polarisation necessary to overcome the nuclear force of repulsion on this nucleus.

According to the arguments of Berlin (26), a molecule can be divided into binding and anti-binding regions. Electron density placed in these regions will respectively, either exert forces on the nuclei pulling them together or alternately exert unequal forces on the nuclei and lead to a separation of the molecule into atoms. The binding region (BR) for a heteronuclear diatomic molecule AB in which  $Z_A > Z_B$  consists of two boundary surfaces. One surface, through B, curls back onto itself to form an enclosed region, while the boundary surface through the nucleus of greater charge opens up and approaches a straight line perpendicular to the bond axis (see Figure XVI). The binding region for the water molecule can be constructed by superimposing two such O-H diagrams inclined at the bond angle with a common oxygen nucleus. Since the antibinding regions in the vicinities of the protons (including those generated by the diatomic H-H group) lie outside the binding region, this will give



The position of the boundary curves, dashed lines, clearly

answers the question where density must be concentrated in order to get a state of electrostatic equilibrium on molecular formation. How much charge must be placed in this region is best answered by picking some standard density that is known to be insufficient from this point of view. If, for example, the molecule is taken to lie in the XY plane with the z-axis coincident with the axis of quantisation, the standard density could be chosen such that it places the nuclei ( $H_1, H_2$  and O) at their equilibrium positions each with its original atomic density. One particular description of the oxygen atom would be to take the  $M_L = 0$  component of the  $^3P$  ground state. This would correspond to circular contours of density in the molecular plane and a doubly occupied " $p_\pi$ " orbital. Since the density on the oxygen atom is centro-symmetric, it will exert no atomic force on this nucleus. In addition, at the equilibrium bond length and angle the hydrogen nuclei will penetrate the shell containing the oxygen density. According to Gauss's law, this density will now shield less than eight units of positive nuclear charge and consequently there will be a net force of repulsion on the hydrogen nuclei. Following similar arguments, each hydrogen nucleus is shielded by less than one unit of negative charge and there will be a net force of repulsion of the hydrogen nuclei due to a mutual penetration of the others charge cloud. There are, of course, many equivalent descriptions for  $\rho_O(\vec{r})$ , each leading to an unstable molecule. One alternative, for example, would be to sphericallise the

charge density on the oxygen nucleus by placing 4/3 electrons in each of  $p_x$ ,  $p_y$  and  $p_z$ . This, however, places less density in  $p_x(p_y)$  than the chosen valence description and therefore will shield the hydrogen nuclei even less.

The difference between the one-electron molecular density ( $\rho(\vec{r})$ ) and the standard one-electron density ( $\rho_0(\vec{r})$ ) then tells us how the density is rearranged on molecular formation. This rearrangement can similarly be represented by a contour map obtained by plotting the function

$$\Delta\rho(\vec{r}) = \rho(\vec{r}) - \rho_0(\vec{r})$$

for different values of  $\vec{r}$  and joining together points of equal density. A full contour in these maps is taken to mean a buildup of charge density in that region on molecular formation whereas a dashed contour implies the removal of charge on molecular formation.

Bader (63) has recently examined the form of the  $\Delta\rho$  map for the frequently quoted tetrahedral description of the water molecule in which  $\alpha$ , the orbital angle, equals  $\epsilon$ , the bond angle. The plots he obtained are given in Fig. VII. Density is clearly removed from the binding region and placed above the oxygen nucleus. Remembering that the original atomic density was insufficient to balance the nuclear forces of repulsion, then there will be a net force on the oxygen nucleus in a direction that opposed bond formation. It was concluded that only by assuming  $\alpha \neq \epsilon$  could charge be accumulated

in the binding region. What effect does this orbital binding have on the form of the wave function? The  $p_1$  and  $p_2$  atomic functions appearing in the bonding orbitals  $\phi_{b1}$  and  $\phi_{b2}$ , respectively, can be written in terms of the  $X'Y'$  coordinated system as follows

$$p_1 = -px' \cos (\alpha/2) + py' \sin (\alpha/2)$$

$$p_2 = -px' \cos (\alpha/2) - py' \sin (\alpha/2)$$

Since  $\alpha/2$  is less than  $90^\circ$  then as  $\alpha$  is decreased,  $\sin(\alpha/2)$  will decrease but  $\cos(\alpha/2)$  will increase. That is to say orbital bending, and hence electrostatic equilibrium will convert  $py'$  into  $px'$ . Figure VIII representative of the  $\Delta\rho$  map obtained for the proposed wave function of the present work, reflects this transition. The dashed contours in the  $Y'$  direction are indicative of  $py'$  density removal and the full contours in the  $X'$  direction are indicative of a  $px'$  density build-up. Moreover, this transformation places density that was originally almost totally in the anti-binding region into a region above and below the oxygen nucleus. In particular, density is placed in the binding region between the three nuclei, a requirement that any proposed density must satisfy. Charge is also concentrated around the hydrogen atoms and the inner polarisation observed is consistent with the large nuclear force of repulsion  $F$ .

Since the density or density-difference maps are representative of the one-electron charge distribution, there

will exist a direct correlation between their form and any molecular property that depends on the first-order density matrix. The electrostatic forces of attraction are particularly important since their existence is a direct consequence of bond formation. By accumulating information contained in both the contour maps and relating this information to the forces, it should be possible to interpret the nature of a chemical bond.

However, before any general conclusions can be made it is necessary to know what characteristics are associated with a certain type of bond. This implies a detailed study into the form of the one-electron density distributions, with particular reference to the forces operative, for a series of molecules. Keeping this in mind, it is now convenient to introduce the second part of the thesis.

PART II

THE NATURE OF THE BINDING IN THE  
FIRST-ROW DIATOMIC HYDRIDES

## I. INTRODUCTION

The chemical nature of a bond is largely determined by the distribution of the valence electrons in the molecule and in particular whether these electrons are shared or localized. It is the way in which the original atomic charge distributions rearrange on molecular formation that determines what forces are operative in binding the nuclei and consequently the physical and chemical properties of the molecule.

The purpose of the present work is to interpret the nature of the binding in the first-row diatomic AH hydrides in terms of the molecular charge distribution and the forces that this charge density exerts on the nuclei. Furthermore a break-down of the electronic forces into those exerted by the individual molecular orbital charge densities enables each molecular orbital to be classified as binding, antibinding or nonbinding. Such a description will provide a quantitative assessment of their relative binding ability; for a given molecule or through the complete series of molecules.

While any chemical bond accumulates charge in the binding region, to an extent sufficient to balance the nuclear force of repulsion, there are two extreme ways in which electrostatic equilibrium and hence a stable chemical bond can be attained. In an ionic bond, for example, valence charge is

transferred from one atom to another and it is the charge density localized on one atom which exerts the net binding force on both nuclei. In a covalent bond on the other hand it is the migration of charge from both nuclei into the binding region and the mutual attraction of both nuclei by this density that is the identifying feature. Taking the lithium fluoride molecule to be representative of the ionic bond and a series of homonuclear diatomics ( $A_2$ ) to be representative of the covalent bond, ionic and covalent binding have recently been given new definitions based on the disposition of the charge density in a molecule (65,66).

The majority of molecules however fall into a category that is intermediate between these two limiting cases having partial ionic or partial covalent character. Here charge is neither transferred completely nor shared equally. From this point of view the first-row diatomic hydrides LiH, BeH, BH, CH, NH, OH and HF form an interesting and important homologous series. It is of considerable interest to determine whether or not the binding in this series of molecules can be usefully classified according to the definitions previously proposed and found to hold for the extreme bindings found in LiF and the homonuclear diatomics.

In the formation of an ionic bond  $A^+B^-$  an electron is completely transferred from nucleus A, with a charge of  $Z_A$ , to nucleus B, with a charge of  $Z_B$ . Nucleus A then has only  $(Z_A-1)$  electrons associated with it while nucleus B has



$(Z_B + 1)$  electrons. According to Gauss's law the field external to the spherical charge distributions surrounding A and B can be considered as originating on the centres A and B respectively. Nucleus B thus experiences a net force of attraction whereas nucleus A experiences a net force of repulsion. For a stable molecule to be formed in this way the charge density surrounding A and B must be polarized by an extent necessary to overcome these net attractive and repulsive forces. If on the other hand an electron is only partially transferred from A to B dependent on the extent of this transfer atomic polarizations may or may not result. When this is the case the bond is said to have partial ionic character. Pauling (67) has suggested two ways in which this quantity can be estimated. One is based on the ratio of the observed dipole moment to the value  $eR_e$ , where  $R_e$  is the equilibrium bond length, and another is based on the difference in the electronegativities of the two atoms forming the bond. From a more theoretical point of view the binding can be studied in terms of the wave function . If this wave function can be written in the form

$$\psi = \lambda_I \psi_I + \lambda_C \psi_C$$

where  $\psi_I$  and  $\psi_C$  refer to the ionic and covalent part of  $\psi$  then the partial ionic character of the bond, which is universally represented as being some function of the coefficients  $\lambda_I$  and  $\lambda_C$ , can be estimated assuming  $\langle \psi_I \psi_C \rangle = 0$ . Although

this overlap term might be zero when averaged over all space it is not necessarily zero at every point in space. When discussing the spatial distribution of electrons it must not be neglected because it is, after all, the basic issue in ionic character. Löwdin and Shull (68) in their interpretation of the bond character preferred to use natural spin orbitals obtained from  $\psi$  by diagonalising the first-order density matrix. It was shown by them that crude approximations to these natural spin orbitals  $\chi_i$  using different proposed wave functions share many of their invariant properties and most important to a bond analysis the invariance of the occupation numbers. Such a method is however unsophisticated and requires new definitions since now the  $\chi_i$ 's no longer represent or can readily be related to the covalent and ionic parts of the wave function. It is as yet not clear to what extent these new definitions will reproduce the concept that the chemist has of partial ionic character (69).

As an increasing number of Hartree-Fock wave functions become available for molecules then it is obvious that a simpler and more direct method of interpreting the chemical bond is needed. The very complexity of these functions seriously handicaps a discussion in terms of hybridization, polarities, ionic character, etc. An alternative approach, and one proposed by Bader and Henneker (65), would be to examine the explicit characteristics of the molecular one-electron charge distribution; especially since a Hartree-Fock wave function

yields a one-electron density correct to the second order. By taking some standard atomic density ( $\rho_0$ ) which is known to be insufficient to balance the nuclear forces of repulsion the molecular ( $\rho$ ) minus atomic density

$$\Delta\rho(\vec{r}) = \rho(\vec{r}) - \rho_0(\vec{r})$$

can be plotted for different values of  $\vec{r}$ ;  $\rho_0$  could, for example, be the separated atoms in their ground state in which case  $\Delta\rho$  is given the symbol  $\Delta\rho_{SA}$ . The resultant density difference contour map would now show the regions in the molecule where charge had migrated in order to reach a state of electrostatic equilibrium and hence a stable chemical bond.

The lithium fluoride molecule has a dipole moment of 6.284D (70). Since the separation of equal and opposite charges at the observed lithium fluoride bond length gives a dipole moment of 7.51D it is obvious that this molecule is strongly ionic by any previous definition. In fact the discrepancy between the observed and theoretical dipole moment is to be expected because of the back polarization of the density remaining on the Li and F nuclei which must accompany an electron transfer. The  $\Delta\rho_{SA}$  plot obtained by Bader and Henneker (Fig. IX) clearly shows that density has been transferred from the lithium atom to the fluorine atom. Both the charge increase around the fluorine atom, as indicated by the large diameter of the zero contour, and the direction of the atomic polarizations at the Li and F nuclei are consistent with an electron transfer and hence an  $\text{Li}^+\text{F}^-$  description.

In this way the ionic bond can be given a new definition based on the characteristic features of the LiF  $\Delta\rho_{SA}$  map, these are (i) a transfer of charge from one atom to another, the charge increase being localized on one atom as indicated by the fact that the contours are approximately centred on one of the nuclei and the region of increase is bounded by a zero contour which encompasses only a single nucleus (ii) a polarization of the density increase localized on the anion and of the density remaining on the cation in a direction counter to the direction of charge transfer.

Using a similar approach Bader, Henneker and Cade (66) have recently studied the rearrangement of charge on molecular formation for a series of homonuclear diatomic molecules  $A_2$ . The  $\Delta\rho_{SA}$  maps they obtained are shown in Fig. X. In every case there is an increase of the charge density in the binding region which is symmetrically placed between both the nuclei. Since this increase in the density is relative to a distribution which does not place sufficient density in the binding region to balance the forces of nuclear repulsion it is the force exerted by this shared density which binds the nuclei in these molecules. The direction of the atomic polarizations now accompanying bond formation could conceivably be in any direction. They are, in fact, found to be opposite of those noted above as being a necessary consequence of ionic binding.

While it is the primary purpose of this work to examine the nature of the binding in the first-row hydrides

there are several other questions of interest concerning this series. Since the dipole moment of LiH is 5.882D (72) it is expected to be highly ionic in the sense  $\text{Li}^+\text{H}^-$ , HF on the other hand with a dipole moment of 1.942D (73) is expected to be polarized in the opposite direction,  $\text{H}^+\text{F}^-$ . The fact that the hydrogen forms the negative pole in LiH and the positive pole in HF is suggestive that there is a change in the binding type as one goes along the series  $\text{LiH} \rightarrow \text{HF}$ . Fajans (74) has recently predicted that this change occurs between BH and CH. His arguments are based on the quanticule theory originally proposed with Berlin (75). Here the electrons are classified according to whether they are quantized with respect to the field of both nuclei or to the field of a single nucleus. Blinder (76) using quite different considerations based on the linear combination of atomic orbitals-molecular orbital theory (LCAO-MO) suggested that the change in bonding type occurs between BeH and BH. Another question of interest concerns repeatedly proposed models for the diatomic hydrides based on the penetration of the united atom (UA) by the proton. It has been known for some time, from spectroscopic observation (77), that the properties and electronic transitions of the diatomic hydrides AH are closely related to the appropriate united atom. If  $\Delta\rho_{\text{UA}}$  represents the molecular minus united atom density, where the united atom is centred on the heavy nucleus A, then bond formation can now be identified with the removal of a proton from the united atom to the

equilibrium bond length. Thus dependant on the nature and magnitude of the density shifts observed in these  $\Delta\rho_{UA}$  maps it should be possible to estimate the applicability of such models.

Whether or not the density in the hydride series can still be classified as shared or localized, where the change-over from one mechanism to the other occurs and if they resemble the united atom approximation are however questions of secondary importance in this study. It is the relationship between the redistribution of charge on molecular formation to the nature of the binding that is our primary aim.

The physical picture provided by the one-electron charge distribution may be carried even further through the use of the Hellmann-Feynman theorem. This theorem relates the forces acting on a nucleus to the one-electron density. These forces of attraction are rigourously determined by classical electrostatics and hence provide an added basis for the discussion of a chemical bond. Just as the formation of a molecule AB can be likened to the redistribution of atomic A and B charge density so can the forces of attraction holding the molecule together be compared with those experienced by the separated atoms. At large internuclear AB separations the total density of the system  $\rho$  is simply the sum of the atomic densities

$$\rho = \rho_A + \rho_B$$

where  $\rho_A$  and  $\rho_B$  refer to some atomic density centred on the A and B nuclei respectively. In a similar way the forces of attraction can be broken down into those due to charge centred on A and those due to charge centred on B. Since these atomic densities are centrosymmetric the only forces of attraction on the A and B nuclei will be of the screening type due to density centred on the B and A nuclei respectively. Furthermore since the A nucleus does not penetrate the charge contained on the B nucleus and since this charge, according to Gauss's law, can be considered as centred on B the net force on the A nucleus simply reduces to

$$F_A(R \rightarrow \infty) = \frac{Z_A Z_B}{R^2} - \frac{Z_A Q_B}{R^2} = \frac{Z_A}{R^2} (Z_B - Q_B)$$

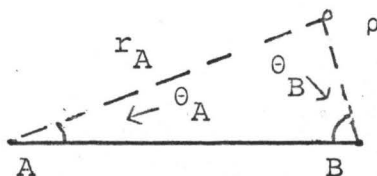
The first term in this expression represents the nuclear force of repulsion and the second term represents the electronic force of attraction. At these distances  $Q_B$  will be the the number of electronic charges on B and since  $F_A(R \rightarrow \infty) = 0$ ,  $Z_B$  must equal  $Q_B$ . Similarly for the net force on the B nucleus to be zero  $Z_A = Q_A$ , where  $Q_A$  is the number of electronic charges on A.

At the equilibrium bond length  $R_e$  the atomic densities are rearranged in a manner that is characteristic of the nature of the binding. The total molecular density can now be written in the form

$$\rho = \rho_A + \rho_{AB} + \rho_B$$

As before  $\rho_A$  and  $\rho_B$  are the atomic densities centred on the A and B nuclei respectively, however there now appears in this expression for  $\rho$  a central overlap term due to density that is centred on both the A and B nuclei. The electronic forces in a molecule can be broken down into three separate components; an atomic force, a screening force and an overlap force. Whereas in the separated atoms it was the screening contribution due to the charge on the A and B nuclei that was responsible for electrostatic equilibrium, molecular formation and the accompanying density shift will now cause the nature of the binding to change. At the equilibrium bond length the density around each of the nuclei is allowed to relax and rearrange itself in such a way that once again  $F_A(R_e) = F_B(R_e) = 0$ .

The nature of this density shift  $\Delta\rho_{SA}$  will be reflected in the values of the atomic, overlap and screening force contributions to  $F_A$  and  $F_B$  relative to their values at large internuclear separation. Consider, for example, the forces on nucleus A due to the molecular charge density. If the atomic density on A,  $\rho_A$  is not centrosymmetric there will result an atomic force on this nucleus equal to  $Z_A \langle \rho_A O_A \rangle$ . Because of the nature of the operator,  $O_A = \cos \theta_A / r_A^2$ , where





the magnitude and direction of this force is determined by the magnitude and direction of the density shift, accompanying molecular formation, near to the A nucleus. In a similar way the overlap or shared density  $\rho_{AB}$  has associated with it an overlap force,  $Z_A \langle \rho_{AB} \ 0_A \rangle$ . The magnitude of this force is dependant on the magnitude of the density shift into the overlap region and equally important the location of this charge increase with respect to both the A nucleus and the bond axis. Finally there is a screening force on A due to density that is completely localized on B,  $Z_A \langle \rho_{AB} \ 0_A \rangle$ . In the case of the separated atoms it was this screening force that was totally responsible for electrostatic equilibrium. The amount by which the A and B nuclei have been descreened on molecular formation and where this descreened density is transferred will, of course, be important factors when considering the nature of the binding.

The net force on the A nucleus can now be written as

$$F_A(R_e) = \frac{Z_A}{R_e^2} (Z_B - Q_B')$$

The three components of  $Q_B'$  atomic, overlap and screening represent the number of virtual charges which when placed on the B nucleus exerts the same field at the A nucleus as does the component of the density being considered  $\rho_A$ ,  $\rho_{AB}$  or  $\rho_B$ . Since at large internuclear separations the atomic and overlap charge contributions are zero and the screening charge contribution was simply  $Z_B$  their molecular values will be of

prime importance.

Consider, for example, the case of a complete electron transfer from A to B. In an idealized ionic bond there is no overlap or shared density and hence no corresponding force contribution. The complete transfer of an electron will increase the screening of the anion by unity and decrease the screening of the cation by unity. The increased screening of the anionic nucleus exerts a net force of attraction on the cation and there must result a negative atomic force due to a back polarization of the density on the cation. The net force of repulsion acting on the anionic nucleus because of the charge transfer is in turn balanced by a positive atomic force term. Thus in an ionic bond the cationic nucleus is bound by the charge transferred to the anion and the anionic nucleus is bound by the force arising from an inwards polarization of the same density. In a similar way the identifying features of a covalent bond can be summarized in terms of the forces acting on the nuclei. In this case it is the migration of charge to the internuclear region that is responsible for bond formation. This migration should be reflected in a decreased screening contribution for both nuclei to the total electronic force on A and B relative to their separated atomic values. Such a descreening will result in a net force of repulsion which is balanced by an overlap contribution.

Using a similar approach Bader and Henneker (78) have

also given an interpretative discussion of the binding in the molecules LiH and HF. These workers used extended LCAO-MO-SCF wave functions which are only slightly less accurate than those employed here. It is their general method that will be extended and applied to all of the first-row hydrides. By accumulating the information contained in the charge distributions and a force analysis the binding in these molecules will be examined on the basis of classifications previously employed. Whether or not density can be classified as shared or localized in the intermediate cases of the hydrides and where, if at all, the alleged discontinuity occurs are questions that will also be dealt with.

The molecular charge distributions, or charge density differences, are based on wave functions given by Cade and Huo (79) which are alleged to be very close approximations to the Hartree-Fock wave functions. The results presented are for  $\text{LiH}(X^1\Sigma^+)$ ,  $\text{BeH}(X^2\Sigma^+)$ ,  $\text{BH}(X^1\Sigma^+)$ ,  $\text{CH}(X^2\Pi_r)$ ,  $\text{NH}(X^3\Sigma^-)$ ,  $\text{OH}(X^2\Pi_r)$  and  $\text{HF}(X^1\Sigma^+)$  states at  $R_e$  (Exptl.). The calculated  $R_e$  value is usually very close to  $R_e$  (Exptl.) so that no significant misrepresentation is likely from the use of  $R_e$  (Exptl.) instead of  $R_e$  (Calcd.).

Each wave function is approximated by a single Slater determinant of one-electron spin orbitals. The individual orbitals span an irreducible representation of the  $C_{\infty h}$  point group to which the molecules belong and can therefore have

either  $\sigma$  or  $\pi$  symmetry. A molecular orbital of  $\sigma$  symmetry is represented by a linear combination of 16 basis functions; 12 centred on A and 4 centred on H. The  $\pi$  molecular orbitals on the other hand are approximated by a linear combination of 8 basis functions; 6 centred on A and 2 centred on H. That is

$$\sigma^a = (1s_A + 1s'_A + 2s_A + 2s'_A + 3s_A + 2p_A + 2p'_A + 2p''_A + 2p'''_A + 3d_A + 3d'_A + 4f_A + 1s_H + 1s'_H + 2s_H + 2p_H)$$

$$\pi = (\pi 2p_A + \pi 2p'_A + \pi 2p''_A + \pi 2p'''_A + \pi 3d_A + \pi 4f_A + \pi 2p_H + \pi 3d_H)$$

---

<sup>a</sup>The wave function for LiH is an exception in that one of the  $2p_A$  functions is substituted by  $3p_A$ .

## II AN ANALYSIS OF THE BINDING IN TERMS OF THE CHARGE DISTRIBUTIONS

### a) TOTAL MOLECULAR CHARGE DISTRIBUTIONS

The three-dimensional one-electron charge distribution is obtained by plotting the function

$$\rho(\vec{r}) = \sum_i n_i \phi_i^2$$

for different values of  $r$ . Here the summation is over all the occupied molecular orbitals  $\phi_i$ , each with an occupation number  $n_i$  equal to 1 or 2. By joining together points of equal charge density the contour maps shown in Fig. XI were obtained<sup>a</sup>.

These represent the total charge distribution in a plane passing through the A and H nuclei where the outer contour in each molecule is 0.002 a.u. which encloses over 95% of the total charge.

The length of the molecule  $L$  is defined as being the distance between the points where the 0.002 a.u. contour crosses the internuclear axis. If  $r_A$  and  $r_H$  are taken to represent the distances of the A and H nuclei out to the 0.002 a.u. contour respectively (see Fig. XII), then these together with  $L$  have been measured and are listed in Table VIII. The length  $L$  determines the molecular size. This is a very useful concept since several of the latter numbers of the series (NH and CH) have been trapped as impurities in rare gas and other molecular crystals.<sup>(80)</sup> A knowledge of the specific sizes can

<sup>a</sup> see Appendix (12)

be used to predict, for example, the substitution of CH or NH for a neon atom in solid neon and the distortions one might expect.

The length  $L$  takes on its lowest value for the HF molecule and increases regularly with increasing bond length through the series up to LiH where there is a sudden drop. The distance of the A atom to the 0.002 contour,  $r_A$ , parallels the behaviour of  $L$  there being an almost constant increase of 0.3 a.u. going from HF to BeH with again a sudden drop for  $r_{Li}$ .

The size of the non-bonded region on the hydrogen nucleus on the other hand increases regularly, as indicated by  $r_H$ , through the series from a value of 1.9 in HF to a value of 2.9 in LiH. In fact the ratio of the molecular length to the bond length,  $L/R_e$ , which is related to the rate at which density falls off on the non-bonded side of the nucleus, takes on an almost constant value. LiH is however exceptional, due to its anomalous length  $L$ , where here the ratio  $L/R_e$  drops significantly from 3.7 to 2.6.

While the actual changes in the atomic density distribution of the separated atoms and the appropriate united atom relative to the molecular density distribution will be considered in detail later, it is useful to obtain an idea of the relationship of the "size" of the molecule relative to the size of the separated atoms A and H. For this reason the radius of the appropriate separated atom is also given

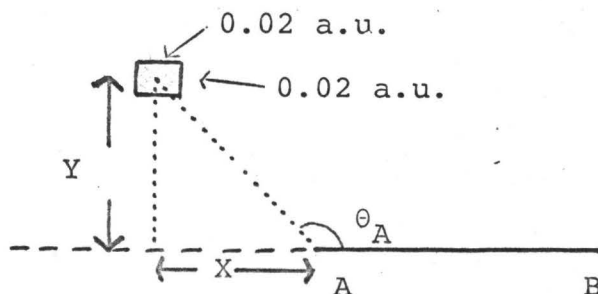
in Table VIII. In HF  $r_F$  is slightly less than its atomic value of 2.8 whereas  $r_{Be}$  in BeH is slightly greater than its atomic value of 3.6 with  $r_A$  for the intermediate members consistent with this gradual change. Once again LiH is exceptional where now the molecular  $r_{Li}$  value of 1.7 is almost one-half the atomic value of 3.2 and very nearly equal to the radius of the  $Li^+$  ion (which is 1.8 bohr). This together with the unusual length of the LiH molecule is indicative of a charge removal from the non-bonded side of the lithium nucleus.

Since the radius of the 0.002 contour in an isolated hydrogen atom is  $\sim 2.5$  a.u. and keeping in mind the fact that  $r_H$  for  $H^-$  is expected to be greater than this then the anomalous short length of LiH seems to result from a transfer of charge from near the Li nucleus to around the proton. Moreover the major fraction of negative charge in LiH appears as monocentric contours which can be considered as density localized on the Li nucleus. This charge transfer appears counter to, but not inconsistent with, the behaviour of the remaining first-row hydrides. In this series HF to BeH density is rather transferred in the opposite direction that is to say from the proton to the A atom. The number of negative contours around the proton decreases and in HF such contours have almost disappeared the molecule now resembling a fluoride ion polarized by a proton.

This reversal in charge transfer is also borne out

by the direction of outer polarization as indicated by the dipole moment. The dipole moment is determined by averaging the charge distribution over the operator  $\vec{z} = r \cos \theta$  and consequently its magnitude and direction is governed by density in the outer regions of the molecule. Examination of the outer density contours in the total density maps indicates that there is a change in the direction of polarization between BeH and BH in accordance with the change in sign of the observed dipole moment  $\mu$  (Table VIII).

If the allocation of charge in these density maps is known then they can be used for a more quantitative discussion. One way to determine how much charge is transferred or remains in a particular region of the molecule can be obtained by integrating the charge density, which is elliptical coordinates<sup>a</sup> will be  $|\psi_{AH}(\xi, \eta, \phi)|^2$ . Integration over all space will just give the total number of electrons  $N$ . However, integration over certain restricted volumes will give the charge contained in these volumes. By taking a grid of 0.02 a.u. and assuming that the density contained in the volume element ( $.0008 \times \pi \times Y$ ) is constant, where for example



<sup>a</sup> see Appendix (2)



the amount of charge on the non-bonded side of A and H can be calculated. The size of the grid chosen in the numerical integration is important and obviously the smaller it is then the more accurate the result. Such calculations are however limited by the number of iterations necessary to span a particular volume and hence the computational time. A value of 0.02 a.u. was considered reasonable as shown by integrating the total molecular volume. In the case of LiH, for example, this led to a total of 3.99 electrons as compared to the expected value of 4. As further proof calculations were recorded using a 0.01 a.u. and 0.005 a.u. grid and the values obtained were invariant in the first two decimal places to those obtained using the 0.02 a.u. grid.

The non-bonded charge on A corresponds to the amount of negative charge contained within the volume bounded by a plane perpendicular to the bond axis and passing through the A nucleus (see Fig. XII.) Similarly defined is the non-bonded charge on the hydrogen nucleus.

The computed values of the atomic and molecular electron populations, as obtained by the numerical integration technique, are listed in Table IX. The atomic populations are defined by placing the A and H atoms in their ground state and at the equilibrium bond length  $R_e$  and integrating over the appropriate volume.

If the A or H nuclei did not penetrate the electronic charge

on the H and A atoms respectively then the total number of electrons in the three defined regions before molecular formation could be readily calculated. Thus for example the Be and H atoms with electronic configurations  $1s^2 2s^2$  and  $1s^1$  respectively would place  $1e^-$  in the non-bonded region of the Be atom,  $0.5e^-$  in the non-bonded region of the H atom and  $2.5e^-$  in the overlap region. The fact that  $0.56e^-$  are found in the non-bonded region of the hydrogen atom shows that this nucleus has penetrated the atomic charge cloud on the Be atom to the extent of  $0.06e^-$ .

The amount of non-bonded charge on the A nucleus before molecular formation approximates very closely the value expected for the free atom and even in HF the hydrogen atom contributes only  $0.04e^-$  to the non-bonded charge on F.

On molecular formation the electrons will redistribute themselves. In an ionic description of LiH the single  $2s$  valence electron in the Li atom will be transferred to the hydrogen atom. This leaves an inner-shell of two  $1s$  electrons on Li which, for reasons described previously, will polarize counter to the electron transfer. If this is the case then the number of electrons on the non-bonded side of the Li nucleus should be slightly greater than 1. A value of  $1.09e^-$  is obtained. Similarly the ionic model for BeH demands an occupation of  $1.5e^-$  in the non-bonded region of Be. The value of  $1.96e^-$  actually found indicates that the net amount of charge present in this region has not changed from the

atomic value. In the remaining members of the series, the formation of the molecule results in an average increase of  $0.23e^-$  over the atomic value of the population in the non-bonded density on A. Note that the presence of the  $F^-$  ion in HF would require an increase of  $0.5e^-$  over the atomic value in the non-bonded region, or  $0.25e^-$  more than is actually found. Turning now to the non-bonded charge on the hydrogen then again the series is clearly divided at BeH. The increase in the non-bonded charge on H in LiH is indicative that the charge lost by the Li atom in molecular formation is now on the H. For  $BH \rightarrow HF$  this charge migration is rather in an opposite direction from the H atom to the A atom, being the greatest for HF and the least for BH.

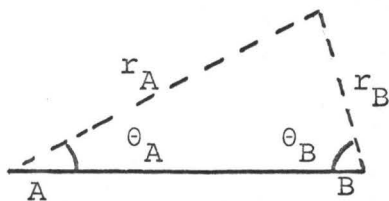
While the non-bonded charge population may be used as a necessary condition for the presence of ionic species in a molecule, it is not a sufficient one since it gives no information of how the charge is distributed on the bonded side of the nuclei. Nevertheless the variation in the number of non-bonded charges found in the hydrides is suggestive of an ionic description for LiH, an equal partitioning of the charge for BeH and an unequal sharing of the charge distribution in the remaining molecules.

Just as the total molecular density can be divided into bonding and non-bonding regions it can similarly be divided into binding and antibinding regions. According to the arguments of Berlin for a diatomic molecule AB with nuclear

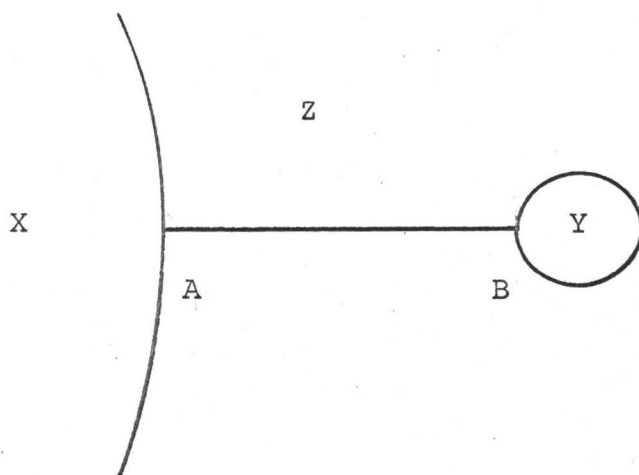
charges  $Z_A$  and  $Z_B$  then these regions are defined according to whether the quantity

$$\frac{Z_A \cos \theta_A}{r_A^2} + \frac{Z_B \cos \theta_B}{r_B^2}$$

where



is positive or negative respectively. For the case when  $Z_A > Z_B$ , as in the hydrides considered here, then the boundary surface through  $Z_B$  curls back into itself and forms an enclosed region (Y) while the other boundary surface through A extends in both directions (X).



As the difference between the nuclear charges  $Z_A$  and  $Z_B$  increases then the volume of the enclosed antibinding region Y

decreases and the surface defining the X region approaches a plane perpendicular to the bond axis. The number of electrons contained in the regions X, Y and Z, within the boundary curves  $F(\xi, \eta) = 0$  have been calculated in a manner similar to that described previously. These values together with the shapes of the binding and antibinding regions are given in Fig. XIII. While in every case more charge is placed in the binding region it is the magnitude of this charge and in particular its location with respect to the A and H nuclei that is important in determining the bond type. For the series HF to BeH there is an almost constant 54% of the total electronic charge contained in the binding region Z, BeH is intermediate with 57% and LiH contains 65%. This together with the anomalous distribution or partition of charge in LiH would suggest a different binding mechanism than in the remaining members of the series with BeH as intermediate between the two types.

While the analysis of the total charge distribution is suggestive of the kind and variation of the bonding in these molecules it does not allow for an unequivocal decision to be made for any of the species. The question as to whether the density is best described as shared or localized has not been answered. To answer this question one must be able to partition the total charge density in some unambiguous manner and this is impossible, particularly for the density in the region between the nuclei, if one considers the total density maps. However, the difficulty of partitioning and

describing the character of a total charge distribution may be overcome in an objective manner through the use of density difference maps.

(b) THE DENSITY DIFFERENCE DISTRIBUTION

The density difference distribution as represented by a contour map shows the net re-organization of charge density on molecular formation. By taking some standard atomic density  $\rho_0$  which is known to be insufficient to balance the nuclear forces of repulsion then the molecular minus atomic density maps show the regions to which charge is either removed or transferred to obtain a state of electrostatic equilibrium and hence a stable chemical bond. One can, for example, consider the hydride molecules AH as being formed from the separated atoms A and H. By placing the atoms A and H in their ground state and at the equilibrium AH bond length then the migration of charge density with bond formation can be related to the nature of the bond. An alternative description would be to consider the difference between the charge density distribution of the molecule AH and the charge density distribution of the united atom (UA) coincident with the A nucleus in AH. Here bond formation is identified with the removal of a proton from the united atom to the equilibrium bond length  $R_e$  and now the contour maps are given the symbol  $\Delta\rho_{UA}(\xi, \eta)$ .

Consider first the density difference distributions involving the separated atoms,  $\Delta\rho_{SA}(\xi, \eta)$ . These are given

for the first-row hydrides in projection in Fig. XIV and in profile in Fig. XV. The dashed contours denote that the value of the molecular density distribution is less than that obtained from the overlap of the atomic densities and hence that charge has migrated away from these regions in the formation of the molecule. The solid contours denote an increase in the molecular density over the combined atomic densities. To obtain the maximum amount of chemical information from such a density different plot the densities of the atoms are taken to be in a valence state. Each atom A, in its ground state, will be in an axial electric field. If this field and the Z-direction are made coincident then there will result a splitting of the  $m_\ell = \pm 1$  and  $m_\ell = 0$  components of the three-fold degenerate  $\ell = 1$  atomic orbital on A. The  $m_\ell = \pm 1$  components ( $\rightarrow P_\Pi$ ) although still degenerate are lowered in energy and the  $m_\ell = 0$  component ( $\rightarrow P_\sigma$ ) increases in energy. This would imply that the atomic density distribution should be derived from the  $M_L = 0$  component of the atomic ground state with the exception of CH and OH for which equal mixtures of  $M_L = \pm 1$  should be employed. Such a description preserves the very useful picture of a chemical bond formation given by the valence bond theory since a spherical average over the ground state configuration would neglect the preferred direction towards the other atom. Thus for elements with partial occupation of the p orbitals this procedure results in a valence state density with a single

vacancy in the  $2p\sigma$  orbital and in an averaging of the remaining  $P$  electrons in the  $2p\pi$  orbitals. Finally since in all the  $\Delta\rho$  maps calculated Hartree-Fock wave functions are employed both for the molecule and for the separated atoms, these giving the one-electron density distributions correct to the second order, it is expected that the main and characterizing features of the  $\Delta\rho_{SA}$  and  $\Delta\rho_{UA}$  contour maps are correctly represented.

Turning to Fig. XIV and the  $\Delta\rho_{SA}$  diagrams for the hydride series the most striking feature is the large removal of valence charge from behind the Li nucleus, as indicated by the dashed contours, not present in the other molecules. There is also a large build up of charge, which can be considered localized on the hydrogen nucleus. Politzer and Brown (81) have recently given a similar  $\Delta\rho_{SA}$  map for LiH which employs the very elaborate wave function of Browne and Master (82). While the LiH wave function is far beyond the Hartree-Fock quality used here, for some reason Politzer and Brown chose to also use the Hartree-Fock wave function for the lithium atom in constructing  $\Delta\rho_{SA}$ . Thus their LiH and Li densities are of considerably different quality. However a comparison of Fig. XIV with their  $\Delta\rho_{SA}$  does show essential agreement of the qualitative features but unfortunately a quantitative comparison was not possible with the data given by Politzer and Brown. The depletion of charge on the non-bonded side of Li and the build-up of charge on



the hydrogen nucleus can be identified with a charge transfer from Li to H. Moreover the extreme localization of the density on the hydrogen nucleus, as shown by the total density map as well, places a restriction on the direction of polarization of the density localized on H and of the density remaining on Li. It is clear that the transfer of charge to a region which is localized on H and excludes the Li nucleus will lead to the creation of a net negative electric field at the Li nucleus. Furthermore, if the localized charge was symmetrically placed with respect to the H nucleus this nucleus would experience a net positive electric field originating from a partially descreened Li nucleus. For an ionic  $\text{Li}^+\text{H}^-$  description therefore there must be a polarization of the density surrounding the A and H nuclei in a direction counter to the electron transfer and hence counter to the direction of the bond dipole moment. The magnitude and direction of this atomic polarization at the Li and H nuclei is determined by the distribution of charge in the immediate vicinity of these nuclei. The inner contours on H are indeed polarized in the right sense as is the transfer of charge from the bonding side of Li to its non-bonding region.

In the remaining members of the series  $\text{BeH} \rightarrow \text{HF}$  an increasing amount of charge is removed from the non-bonded side of H, indicated by the magnitude and numbers of the dashed contours. The density difference maps for these hy-

hydrides all show the density increase on A to be polarized away from the positive end of the bond dipole  $A^{\delta-}H^{\delta+}$ . Moreover the polarization of the density on H is directed towards the A atom and hence the negative end of the dipole. Such polarizations were also found for the homonuclear diatomics and are thus suggestive of a covalent binding scheme. Here the charge transfer from H to A is not of sufficient magnitude nor sufficiently localized that the cations see a net negative field and the anion a net positive or repulsive field. In these molecules charge is also removed from a region that resembles a slightly inward polarized  $p_{\pi}$  atomic function centred on the heavy nucleus A;  $\pi$ -density, because of its location, has little effect in binding the nuclei. Compared to say the  $2p\sigma$  density which lies along the internuclear axis it exerts a minimum shielding of the A nucleus from the proton. In the formation of a molecule however this density is put to a more beneficial use where now it is partially transferred to the regions A and B (see Fig. XVI). The pattern of this charge increase can, in an orbital approximation, be associated with the presence of a  $2p\sigma$  atomic orbital<sup>a</sup>. The  $3\sigma$  molecular orbital singly occupied in BeH and doubly occupied in the other hydrides  $BH \rightarrow HF$ , will at large internuclear separations correlate with a  $2p\sigma$  on A and with a  $1s$  atomic orbital on H. According to the arguments of Blinder

<sup>a</sup> Although the  $2p$  atomic orbitals are unoccupied in the Be atom, it is the promotion of the valence electron into a  $2p\sigma$  atomic orbital, brought about by the formation of the molecule.

it is the relative energies of the atomic orbitals on A and H that, at the equilibrium bond length, will determine whether the molecular orbital has mono or bicentric character. Because of the close similarity in energy of the H1s, A2s and A2p atomic orbitals on B and C,  $\epsilon_{1s}(H)$ ,  $\epsilon_{2s}(A)$  and  $\epsilon_{2p}(A)$  respectively, one would expect the bonding orbital resulting from mixing these atomic orbitals to be delocalized over both nuclei in BH and CH. On the other hand one would expect as  $|\epsilon_{2s}(A)| \sim |\epsilon_{2p}(A)| \gg |\epsilon_{1s}(H)|$ , which is progressively the case in NH, OH and HF, this particular orbital ( $3\sigma$ ) should simulate the features of a distorted  $2p\sigma$  atomic orbital on A. The bonding in the hydrides, from these considerations, can therefore only be considered bicentric in as much as the proton lies within the compass of the  $2p\sigma$  atomic orbital. The common charge accumulation in the density-difference diagrams does support this view. As the energy difference between H1s and A2p increases, that is go from BeH  $\rightarrow$  HF, then the molecular orbital becomes increasingly localized on A as a  $2p\sigma$  atomic orbital. This being the case then the change in shape through this series of the two regions of charge increase, A and B, can be identified with an increasingly localized  $3\sigma$  molecular orbital on A with a proton embedded in its extremity.

The gradual and almost constant change between each member in the series BeH  $\rightarrow$  HF suggested in the  $\Delta\rho_{SA}$  maps is even more impressive when the valence state of the A atom is

substituted by its sphericalized density. For the Li, Be and N atoms the two approaches will, of course, be the same. However for B, C, O, and F each of the AP orbitals will now contain  $1/3$ ,  $2/3$ ,  $4/3$  and  $5/3$  electrons respectively instead of the valence state 1. The  $\Delta\rho_{SA}$  maps obtained are given in Fig. XVII. The unusual change in the shape of the OH and HF contour maps, although not being inconsistent with the new BeH  $\rightarrow$  HF  $\Delta\rho_{SA}$  series, is now due to the large increase in the atomic density along the internuclear axis brought about by the increased population of the  $2p\sigma$  atomic orbital. This same general pattern through the series BeH  $\rightarrow$  HF again persists with BeH and HF as the two extremes. Moreover the anomalous density shifts observed for LiH not present in BeH and the remaining members of the series is not a result of the method of calculation since both Li and Be have spherical atomic densities.

Whether one wishes to consider molecular formation from the sphericalized atomic densities or from the valence state approximation is dependent on which approach contains the most relevant information. In many cases the two methods can be used to supplement each other since features not immediately obvious by one treatment might stand out in a second. The valence bond idea of a two-electron two-centre bond, which would correspond in a  $\Delta\rho_{SA}$  map to placing one electron in a  $2p\sigma$  atomic orbital on A, is however more physically and chemically interpretable. For this reason all the ensuing results

will be quoted for the  $\Delta\rho_{SA}$  maps of Fig. XIV.

The identifying features of the  $\Delta\rho_{SA}$  maps are also borne out in the profile diagrams, all drawn to the same scale, of Fig. XV. These profiles represent the change in density that occurs along the internuclear axis on molecular formation. The density distribution along this axis is most important since it exerts a maximum effect on both the nuclei. Again the similarity in the profiles  $BH \rightarrow HF$  is striking. The increasing size of charge build-up on either side of A with a negative region at the A nucleus is characteristic. The maximum in the overlap density which is almost directly above the proton in BeH gradually broadens through the series and moves to the centre of the bond. This would suggest that the polarity of the latter members, as indicated by the position of this shared density, increases in the sense  $A^{\delta-} H^{\delta+}$ . The removal of negative charge from behind the proton is also evident and its magnitude increases with decreasing  $R_e$ . One further point to note is that the maximum appearing to the right of the A nucleus in  $BH \rightarrow HF$  is lacking in both LiH and BeH.

Despite the slightly different features in the density difference and profile maps for  $BeH \rightarrow HF$  there is really no strong evidence for a discontinuity in the bond type predicted by Fajans and Blinder. Rather a gradual change seems evident with BeH as one extreme and HF as the other.

Table X lists the total amount of negative charge

which is transferred to and contained in the two isolated regions of charge accumulation. These values were obtained by the numerical integration technique using a 0.02 a.u. grid. The letter A denotes the region defined by the zero contour on the non bonded side of the A nucleus (see Fig.XVI), and B the region enclosed by the contour which encompasses the proton. The zero contour which defines the B region also includes all of the density increase in the binding region and is thus of particular interest. The amount of charge contained and transferred to this region together with the shape of the defining contours and hence the position of the charge increase are of primary importance in determining the nature of the binding.

In LiH the contours of charge increase in the B region are spheroidal in shape and as such can be considered as a localized increase on the hydrogen. In fact this density simulates the case that an  $H^-$  ion might be present. Exactly the same state of affairs exists in the  $\Delta\rho_{SA}$  maps for LiF where now the contours of charge increase around the F atom can be considered localized. While the charge increase in this region is localized in both LiH and LiF there remains the problem of partitioning the total charge density. The value of  $0.55 e^-$  listed in Table IX is the amount of charge transferred to near the H nucleus, it does not represent the increase in charge from the free atomic value. This number represents the density increase of the molecule, in this region, over and above the sum of the atomic Li and H densities

since charge density from the Li atom is also placed in this region. To obtain the total charge contained on H and F in LiH and LiF, which should in an ionic  $\text{Li}^+\text{H}^-$  and  $\text{Li}^+\text{F}^-$  description be  $\sim 2e^-$  and  $\sim 10e^-$  respectively, then to a good approximation the total density distribution can be integrated over the volume bounded by the zero contour defining the B region in the  $\Delta\rho_{\text{SA}}$  maps. This integration yields a total of  $1.83e^-$  for LiH and  $9.84e^-$  for LiF. Both these values are  $< 0.2e^-$  below that expected for a charge increase of  $1e^-$ . The density distribution does however extend beyond the zero contour line of the B region and some discrepancy is expected. For the remaining members of the series the density increase in the B region is rather shared in increasing amounts by the two nuclei A and H there being a strong polarization towards A with once again BeH acting as an intermediate. The position of this density increase and especially its relation to the two nuclei is important in determining molecular properties. Consider, for example, the electric field gradient at the proton obtained by averaging the charge distribution over the operator  $r_{\text{H}}^{-3} (3\cos^2\theta_{\text{H}} - 1)^{\text{a}}$ . It is seen that the proton gradually shifts its relative position from near the centre of the  $\Delta\rho_{\text{SA}}$  map for LiH to a point on a steep gradient of the  $\Delta\rho_{\text{SA}}$  map for HF. This would suggest that the electric field gradient at the proton in the series LiH  $\rightarrow$  HF would change systematically through the series from a small, near-

<sup>a</sup>see page 57

zero value, at LiH to a much larger value at HF. This is actually the case found in the calculated values of the electric field gradients at the proton (82).

The density increase on the non-bonded side of the A nucleus, within the region defined by the zero contour, is almost completely contained in Berlins anti-binding region. Both the small positive value of this increase in LiH together with its localized nature is indicative of a redistribution of the inner  $1s^2$  density. Such a redistribution is completely consistent with an atomic polarization necessary for an ionic  $Li^+H^-$  description. In contrast the much larger and diffuse increase observed for BeH and the other hydride molecules seems to involve the redistribution of valence-shell density. The amount of charge contained in and transferred to the A region is however not easy to interpret. The fact, for example, that the charge increase  $\Delta A$  in the hydrides BH, CH and NH is the same rising slightly for OH and HF cannot readily be understood except perhaps suggesting a similarity in the binding mechanism.

In summary, on the basis of the total density distributions and the density difference maps, the binding in LiH is ionic, the binding in BH, CH, NH, OH and HF is covalent and the binding in BeH is intermediate between these two extremes. The common bond or overlap density in the covalent molecules is, however, unequally shared between A and H. This unequal sharing is a maximum for HF in the sense  $H^{\delta+} F^{\delta-}$



and a minimum for BH. From BH  $\rightarrow$  HF the majority of the charge increase occurs at A but it changes character from being delocalized over both nuclei to being centred principally near A. In BeH, which appears completely ambiguous referred to these two limiting classifications, the principal charge increase is near the proton.

The similarity of this hydride series to the appropriate united atom, centred on A, has led to a number of simplified models that approximate the nature of the binding. These models consider the electrostatic equilibrium of a proton embedded in the charge density of either  $A^-$  or the united atom with or without polarization. Hund (83), for example, has shown that the observed spectroscopic data for the first-row hydrides can be predicted on the single assumption that the hydride molecule (e.g. NH) is equivalent to the corresponding united-atom (e.g. O) in a strong electric field. Platt (84) has similarly made excellent predictions, for the interatomic distances and force constants of the diatomic hydrides, again assuming the density of these hydrides was not far removed from the united-atom. Another line of investigation has used wave-functions whose basis set is centred solely on the heavy nucleus (85).

In all of these treatments the departure of the united atom density from the molecular density is of prime importance. For this reason we have given in Fig. XVIII the  $\Delta\rho_{UA}$  contours resulting from subtracting the appropriate united-

atom densities from those of AH (at  $R = R_e$ ). The allowed spectroscopic states of the united atom can be obtained in the usual way. However, we are only interested in that atomic state which corresponds to the same spin multiplicity as the molecular state, lies lowest in energy and has the correct component of orbital angular momentum about a chosen axis. Thus for example  $BH(^1\Sigma^+)$  will, in the united atom approximation, correlate with the C atom which has a valence electron configuration  $p^2$ . This gives rise to the atomic states  $^3P$ ,  $^1D$  and  $^1S$ . The  $^1D$  and  $^1S$  have the correct spin multiplicity however the  $^1D$ , with the highest L value, lies lowest in energy and consequently we are required to find the charge density for the  $M_L = 0$  component of this state. Bingel (86) was able, using the results of Companion and Ellison (86a), to decompose the atomic charge distribution into terms of different angular symmetry and has listed for the  $M_L$  component of each term the appropriate orbital coefficients. By averaging the charge contained in the  $p_\pi$  atomic orbitals ( $p_+$  and  $p_-$  in Bingel's notation) the coefficients of the atomic orbitals in the correct united atom term can be obtained and these are given in Table XI. In two cases, BH and CH, the united atom is not the ground term. These ground terms would be respectively  $^3P$  and  $^4S$ , however, a correlation with their respective molecular states  $^1\Sigma^+$  and  $^2\pi$ , would correspond to a change in the spin multiplicity. For this reason the states of BH and CH correlate with the  $^1D$  state of C and the  $^2D$  state of N, respectively.

The negative contours in the immediate vicinity of the A nucleus in the  $\Delta\rho_{SA}$  density difference maps is the result of a decrease in nuclear charge obtained when a proton is removed from the united atom nucleus. The united atom having the larger  $(Z_A+1)$  nuclear charge will place more density in this region. In every case the symmetry of the united atom is distorted in the formation of the molecule. The charge increase in the region of the proton, almost symmetrically placed in the case of LiH and slightly polarized towards the F atom in HF shows that the united atom greatly underestimates the density at the proton. This itself is not surprising but the degree of difference is unexpected. The large removal of valence charge from the Li nucleus in LiH is again consistent with an ionic description  $\text{Li}^+\text{H}^-$ . The density increase in this molecule and BeH is confined primarily to only the region around the proton. In BH and CH the charge build up is both around the proton and on the non-bonded side of A. In NH, OH and HF these two regions of accumulation coalesce into a single region and the AH charge density is thus seen to exceed the united atom density in all regions except around the A nucleus. In the series BeH-HF the  $\Delta\rho_{UA}$  maps are in agreement with the previously concluded  $\text{A}^{\delta-}\text{H}^{\delta+}$  polarity, where an increasing amount of charge is transferred from the H atom to the A atom. In fact the pulling out of a proton from the Ne nucleus to form HF simulates, as did the total density distribution the presence of a polarized  $\text{F}^-$  ion.

Cade and Huo(87) have recently pointed out the more-or-less constant decrease in the correlation energy of AH at  $R_e$  relative to the correlation energy of the united atom for the first- and second-row hydrides. The correlation energy arises because of the electron-electron repulsion energy not taken into account in a Hartree-Fock treatment where here the position of each electron depends only on the average position of the others. It is usually defined as being the difference between the relativistically corrected experimental energy and the Hartree-Fock value. Because of the decrease in the molecular minus united atom correlation energies the  $\Delta\rho_{UA}$  diagrams should show some characteristic consistent with this. Consider first the increase in charge around the proton contained within the 0.02 a.u. contour. Both the shape and magnitude of the contours indicate the remarkable similarity of this region for the hydrides. Since this increase in charge is almost constant in the series  $LiH \rightarrow HF$  more charge will be left on the A nucleus. There will thus be a slight decrease in the importance of instantaneous repulsions or electron correlation in the hydrides.

Although a great deal of information is contained in the density and density difference charge distributions it is impossible to give a quantitative discussion of the bonding in terms of them. In the case of LiH, for example, it would seem that an ionic description is appropriate, however, just how close it approximates to an ideal separation

of equal and opposite charges is not answered. The information contained in these maps must somehow be related to a property of the molecule that enables a fuller and more definite discussion of the bonding. For such a direct relationship to be possible the physical property chosen must be dependent only on the coordinates of one electron at a time .

III      AN ANALYSIS OF THE BINDING IN TERMS OF THE  
FORCES EXERTED ON THE NUCLEI

a) INTRODUCTION

The very existence of a stable molecule demands that the nuclear forces of repulsion are balanced by the electrostatic forces of attraction. It is not sufficient for the vector sum of the forces on the nuclei to vanish, for this is true at all internuclear distances. Thus for a diatomic molecule at any R value

$$F_A(R) = - F_B(R)$$

and at  $R = R_e$

$$F_A(R_e) = - F_B(R_e) = 0$$

These equalities are also formally true (but in practice only approximately valid) when the forces acting are calculated using Hartree-Fock wave-functions (88,89). The well-known Hellmann-Feynman theorem (25,25A) indicates how to calculate these forces making use of the total molecular charge density determined by quantum mechanical calculations. However, the Hellmann-Feynman theorem is valid for only a restricted class of approximate wave functions, but this includes the Hartree-Fock wavefunctions for closed-shell cases and open-shell cases considered here (89)

According to previous arguments the net forces on the A and H nuclei,  $F_A(R_e)$  and  $F_H(R_e)$  respectively, in

the AH molecule will be given as

$$F_A(R_e) = \frac{Z_A}{R_e^2} (Z_H - Q'_H) \quad F_H(R_e) = \frac{Z_H}{R_e^2} (Z_A - Q'_A)$$

where  $Q'_A$  and  $Q'_H$  represent the number of virtual charges which when placed on the A and H nuclei respectively exert the same field at the H and A nuclei respectively as does the density distribution in the molecule. Because of the three basic electron populations  $\rho_A$ ,  $\rho_{AB}$  and  $\rho_B$  each  $Q$  will be the sum of three components - atomic, overlap and screening.

In an orbital approximation to the total wave function it is found more convenient to define a quantity  $f_{ix}$  for each molecular orbital as being the force exerted on nucleus x by the density contained in the  $i^{\text{th}}$  molecular orbital multiplied by  $R_e^2$ . If  $\phi_i$  represents the  $i^{\text{th}}$  molecular orbital with an occupation number  $n_i$  equal to 1 or 2 then in a diatomic molecule the total electronic force on A will be

$$- Z_A \sum_i n_i \int \phi_i^2 \frac{\cos\theta_A}{r_A^2} d\tau$$

and on H

$$- Z_H \sum_i n_i \int \phi_i^2 \frac{\cos\theta_H}{r_H^2} d\tau$$

Therefore

$$Q'_H = \sum_i f_{iA} = - R_e^2 \sum_i n_i \int \phi_i^2 \frac{\cos\theta_A}{r_A^2} d\tau$$

and

$$Q'_A = \sum_i f_{iH} = - R_e^2 \sum_i n_i \int \phi_i^2 \frac{\cos\theta_H}{r_H^2} d\tau$$

where now, for example, each  $f_{iA}$  is numerically equal to, in dimensions of electronic charge, the number of point charges which, when placed on the H nucleus, exerts the same field at the A nucleus as does the density distribution in the  $i^{\text{th}}$  molecular orbital. Each  $f_{iA}$  value can be either attractive or repulsive. They can thus be used as a quantitative gauge of the binding or antibinding characteristics of the  $i^{\text{th}}$  molecular orbital using a significant reference standard (65, 66). In these studies the reference standard is based on the contributions to the forces on A as  $R \rightarrow \infty$ . Clearly at large R the unperturbed atom A possesses a centre of symmetry and exerts a zero net force on nucleus A. One may interpret the vanishing of the force at large R as resulting from each electron on B screening one of the nuclear charges on B from nucleus A. Thus the limiting value at  $R \rightarrow \infty$  of the sum of the partial forces for nucleus A is the total electronic charge on atom H. Similarly the limiting value at  $R \rightarrow \infty$  of the sum of the partial forces for nucleus B is the total electronic charge on atom B. At the equilibrium bond length  $R = R_e$ , where once again the resultant forces on the A and H nuclei are zero

$$\sum_i f_{iA}(R_e) = Z_B \quad \sum_i f_{iH}(R_e) = Z_H$$



The electronic contribution to the force on the A nucleus at any value of  $R$  may thus be equated to an effective number of charges situated at the B nucleus, this number being the sum of the partial forces. At  $R_e$  the sum equals  $Z_H$ . At intermediate distances it exceeds  $Z_H$ , corresponding to a net force of attraction, and for large  $R$  the sum reduces to the number of electronic charges which correlate with the separated H atom. This suggests that the limiting value of each individual  $f_{iA}$  should be taken as the number of electrons in the  $i^{\text{th}}$  molecular orbital which correlate with the H atom for large values of  $R$ ,  $N_{iH}$ :

$$f_{iA} (R \rightarrow \infty) = N_{iH} \quad (= 0, 1 \text{ or } 2)$$

Similarly the limiting value of  $f_{iH}$  should be taken as the number of electrons in the  $i^{\text{th}}$  molecular orbital which correlate with the A atom for large values of  $R$ ,  $N_{iA}$ :

$$f_{iA} (R \rightarrow \infty) = N_{iA} \quad (= 0, 1 \text{ or } 2)$$

Unfortunately the correlation of the various molecular orbitals  $\phi_i$  into atomic orbitals centred on A and H is not rigorous. However, Mulliken (91) has pointed out that the electron configuration of any state of a diatomic hydride can usually be obtained by assuming that the electrons of the heavier atom are unchanged with respect to their quantum numbers (they do, of course, assume definite  $\lambda$  values) while the hydrogen electron is promoted to the lowest-energy  $\sigma$  orbital which has at least a single vacancy. The electronic con-

figuration of the first-row hydrides are  $1\sigma^2 2\sigma^2 3\sigma^n$ ,  $n = 0, 1, 2$  for LiH, BeH and BH respectively and  $1\sigma^2 2\sigma^2 3\sigma^2 1\pi^n$ ,  $n = 1, 2, 3, 4$  for CH, NH, OH and HF. Following Mulliken's arguments a correlation of the H1s orbital with the  $2\sigma$  molecular orbital in LiH and with the  $3\sigma$  molecular orbital in the remaining hydrides is anticipated. The  $1\sigma$ ,  $2\sigma$ ,  $3\sigma$  and  $1\pi$  molecular orbitals then correlate with the  $1s$ ,  $2s$ ,  $2p\sigma$  and  $2p\pi$  atomic orbitals respectively on the A nucleus. BeH does not however fit neatly into either of these correlation schemes since the  $1s$  orbital on H is considerably more stable than the  $2s$  orbital on Be.

At the equilibrium bond length the actual disposition of charge in a molecular orbital will determine the magnitude and sign of each  $f_{iA}(R_e)$ . Although by necessity at this bond length  $\sum_i f_{iA}(R_e)$  must equal the nuclear charge on H each  $f_{iA}(R_e)$  can in general be greater than, equal to or less than  $N_{iH}$  leading to the following definitions

$$f_{iA}(R_e) > N_{iH} \quad \text{binding}$$

$$f_{iA}(R_e) \sim N_{iH} \quad \text{nonbinding}$$

$$f_{iA}(R_e) < N_{iH} \quad \text{antibinding}$$

In a similar way the binding, nonbinding or antibinding character of the  $i^{\text{th}}$  molecular orbital with respect to the H nucleus can be determined by comparing the  $f_{iH}(R_e)$  value with  $N_{iA}$ . Furthermore a comparison of the partial forces on the A or H nuclei for a particular orbital in the series BeH  $\rightarrow$  HF

(which possess a common correlation scheme) will provide a quantitative comparison of the effectiveness of this orbital charge density in binding the nuclei.

Just as the total charge density can be broken down into the three basic electron populations - atomic, overlap and screening so can the constituent molecular orbitals. Each molecular orbital is approximated by a linear combination of atomic functions centred on A and H,  $\chi_i^A$  and  $\chi_k^H$  respectively

$$\phi_i = \sum_j c_{ij} \chi_j^A + \sum_k c_{ik} \chi_k^H$$

The atomic, overlap and screening populations -  $\chi_j^A \chi_j^A$ ,  $\chi_j^A \chi_k^H$  and  $\chi_k^H \chi_k^H$ , respectively will thus contribute an atomic, overlap and screening force to each  $f_{iA}$ . As a consequence of this  $f_{iA}$  can now be written as

$$f_{iA} = [f_{iA}^{(AA)} + f_{iA}^{(AH)} + f_{iA}^{(HH)}].$$

and similarly for  $f_{iH}$

$$f_{iH} = [f_{iH}^{(HH)} + f_{iH}^{(AH)} + f_{iH}^{(AA)}].$$

For example,  $f_{iA}^{(AA)}$  ( $\equiv$  atomic force) denotes the contribution to the partial force on nucleus A from the atomic population on A  $f_{iA}^{(AH)}$  ( $\equiv$  overlap force) denotes the overlap contribution to the partial force on A from the overlap population and  $f_{iA}^{(HH)}$  ( $\equiv$  screening force) denotes the contribution to the partial force on A from atomic density centred on H.

As important as the amount of charge in determining the binding in a molecule is the exact disposition of the

charge, whether it is polarized or whether it is diffuse or concentrated. The binding, nonbinding or antibinding nature of a particular molecular orbital can thus be described in terms of an atomic, overlap or screening contribution to its partial force. Moreover since the three components of each partial force are independent of both the nuclear charge and the equilibrium bond length it is possible to compare their values in a series of molecules for which A changes. This is particularly useful since it provides a quantitative assessment of the relative binding abilities of the orbital charge densities both for a given molecule or through a complete series of molecules.

As  $R \rightarrow \infty$  then because the charge distribution around the A and H nuclei is centrosymmetric  $f_{iA}$  and  $f_{iH}$  will simply reduce to the screening  $f_{iA}^{(HH)}$  and  $f_{iH}^{(AA)}$  contributions respectively which in turn are given by  $N_{iH}$  and  $N_{iA}$ . At  $R = R_e$ , however, the screening contribution will, in general, differ from the actual atomic population on A (or H) as the charge density on A (or H) may be diffuse and hence partially penetrated by the proton (or A atom) at  $R_e$  or it may be polarized either towards or away from the proton (or A atom). Similarly the magnitude of the overlap contribution is dependent upon whether the overlap charge density is diffuse in nature or concentrated along the inter-nuclear axis. Any inequality in the sharing of the overlap charge density by the nuclei in a heteronuclear molecule is made evident by the difference in

the partial forces.

b ) AN ANALYSIS OF THE BINDING IN TERMS OF THE PARTIAL FORCES

The partial forces for the  $1\sigma$  density together with their atomic, overlap and screening contributions are given in Table XII. The  $1\sigma$  molecular orbital correlates with , at large values of  $R$ , a doubly occupied  $1s$  atomic orbital on A. Because of the spherical symmetry of such an orbital the value of  $f_{1\sigma A}(\infty)$ , which is a measure of the force on the A nucleus due to the  $1s$  density on A, should be 0. The value of  $f_{1\sigma H}(\infty)$  on the other hand is expected to be 2 due to the  $f_{1\sigma H}^{(AA)}(\infty)$  screening contribution. Because the  $1s$  orbital energies of the first-row elements all lie well below that of the  $1s$  orbital (see Table XIII) the  $1\sigma$  molecular orbital should be essentially localized on A as  $1s^2$  in the molecule. This is borne out in the  $1\sigma$  density maps of Fig. XIX, which consists of spherical contours centred on the A nucleus. In every case the radius of the 0.0002 contour is considerably less than the bond length. One measure of the  $1s$  density rearrangement on molecular formation will be the values of  $f_{1\sigma H}$  and  $f_{1\sigma A}$  at  $R = R_e$ . Considering first the forces on the proton then the values of  $f_{1\sigma H}(R_e)$  are indeed very close to the predicted  $f_{1\sigma H}(\infty)$  value of 2. The fact that in LiH a value of 1.949 was obtained shows that there is a slight polarization of the  $1s$ -like density on the Li nucleus. As we go down the series,  $\text{LiH} \rightarrow \text{HF}$ , then this density on A is held tighter, due to the increased nuclear charge  $Z_A$ , such

that at BH it now effectively screens two units of positive charge from the proton. The  $1\sigma$  orbital can thus be considered nonbinding with respect to the proton. The forces that the  $1\sigma$  density exerts on the nuclei are also given in Table XII. In the case of LiH and BeH the negative value of  $f_{1\sigma A}(R_e)$  indicates that this orbital is antibinding, equivalent to placing 0.49 and 0.13 positive charges respectively on the proton. This is due to the large and negative atomic force caused by a polarization of the inner  $1s$ -like density in a direction removed from the hydrogen side of A. For the remaining molecules in the series BH  $\rightarrow$  HF the  $1\sigma$  orbital is binding for the A nucleus. Here there is a density shift rather to the bonding side of A, which results in a positive atomic force with a charge equivalent of approximately  $0.25\bar{e}$ . The size, sign and changeover of this atomic force on A is also evident in the profile maps of Fig. XV. In the series BH  $\rightarrow$  HF there is a spike-like increase in charge to the immediate left and right hand side of the A nucleus brought about by the rearrangement of the inner density on A. Both these regions of charge increase will produce an opposing atomic force, however in each molecule there is a net resultant force of approximately the same order of magnitude putting the A nucleus towards the hydrogen atom. In LiH and BeH however the charge increase is to the left hand side of the Li and Be nuclei tending to separate the A and H nuclei. The atomic polarization and hence the

resultant atomic force at the Li nucleus is, moreover, completely consistent with an ionic  $\text{Li}^+\text{H}^-$  description. Finally the reversal in sign of this atomic force at the B nucleus in BH is suggestive that there is a change in the binding type between BeH and BH.

Table XIV lists the partial forces with their atomic, overlap and screening contributions to the  $2\sigma$  density distribution. The  $2\sigma$  molecular orbital in the case of LiH correlates with, at large R, a singly occupied 2s function on Li and a singly occupied 1s function on H. For BeH and the remaining members of the hydride series it correlates with a doubly occupied 2s function on A. Because the energy difference between the A2s and H1s orbitals increases through the series, with the A2s function becoming lower in energy, at  $R = R_e$  the  $2\sigma$  molecular orbital should increasingly resemble a 2s orbital localized on A. The contour diagrams representative of the  $2\sigma$  orbital density are given in Fig. XX. In LiH and BeH the shape of these contours do indicate that the molecular orbital is primarily localized on the proton whereas from BH  $\rightarrow$  HF the  $2\sigma$  density gradually encompasses both nuclei becoming increasingly centred on A with spherical contours characteristic of a 2s atomic orbital. This change in localization of the  $2\sigma$  charge density from H to A should be reflected in the values of  $f_{2\sigma\text{H}}$  and  $f_{2\sigma\text{A}}$  given in Table XIV. In particular the change in the localized nature of the  $2\sigma$  molecular orbital from being primarily centred on H to being

primarily centred on A should be reflected in the screening contributions. Consider first the LiH molecule. The quantities  $f_{2\sigma H}$  and  $f_{2\sigma A}$  measure the force on the H and A nuclei respectively due to the density contained in the  $2\sigma$  molecular orbital. At large values of R since the  $2\sigma$  orbital correlates with a singly occupied A2s and H1s,  $f_{2\sigma H}(\infty)$  and  $f_{2\sigma A}(\infty)$  will simply be 1, in units of electronic charge, because of their respective  $f_{2\sigma H}^{(AA)}(\infty)$  and  $f_{2\sigma A}^{(HH)}(\infty)$  screening contributions. In the remaining members of the series,  $\text{BeH} \rightarrow \text{HF}$ ,  $f_{2\sigma H}^{(AA)}(\infty)$  and  $f_{2\sigma A}^{(HH)}(\infty)$  where now the  $2\sigma$  molecular orbital correlates with a doubly occupied 2s function on A are expected to be 2 and 0 respectively.

Comparing the values of  $f_{2\sigma H}(R_e)$  with those at infinite atomic separation then the  $2\sigma$  charge density can be seen to be non-binding for the proton in LiH, antibinding with respect to the proton in BeH and binding with respect to the proton in the hydrides  $\text{BH} \rightarrow \text{HF}$ . The binding is due both to an increase in the screening contribution and a relatively large overlap force. On going from  $\text{BH} \rightarrow \text{HF}$  the decrease in magnitude of the overlap force is paralleled by an increase in the screening force associated with the increasingly localized nature of the  $2\sigma$  molecular orbital. This is also borne out by the  $2\sigma$  density diagrams of Fig. XX which increasingly resembles an atomic 2s function on A. In fact for HF the components of the force exerted on the proton by the  $2\sigma$  density axis approach in value those expected for a  $2s^2$  atomic density



on F at large R; zero atomic and overlap contributions, and a screening contribution of two. In BeH, BH and to a slightly lesser extent in CH the A2s and H1s orbitals being of similar energies are predicted to mix strongly producing a bicentric  $2\sigma$  molecular orbital. The overlap forces are indeed the largest in the series and the screening of the Be, B and C nuclei is much less than the value of two required for an unperturbed 2s atomic orbital on A.

The  $f_{2\sigma A}(R_e)$  values in Table XIv all show that the  $2\sigma$  charge distribution is binding with respect to the A nuclei, being the greatest for Be in BeH and the least for F in HF. As the density becomes increasingly localized on A then both the screening and overlap forces drop and the binding is due mainly to a large inward polarization of the now almost localized density on A. In BH, for example, the atomic force is only 0.23 whereas in HF the value of 0.52 accounts for over 70% of its binding character. The atomic polarization in LiH and BeH is opposite to that for BH  $\rightarrow$  HF and tends to separate the A and H nuclei. In BH and CH the original spherical distribution of the separated atoms has been greatly distorted and the binding is caused primarily by an overlap charge density and to a lesser extent by a partial screening of the proton. The force contributions exerted on the N nucleus in NH are intermediate in character.

From a consideration of the  $1\sigma$  and  $2\sigma$  density maps and their respective force contributions there would seem to

be a great similarity in the binding for LiH and BeH not immediately obvious in either the total density or density difference charge distributions of Figs. XI and XIV. The  $1\sigma$  density is, for example, in both molecules non-binding with respect to the proton since on molecular formation it remains essentially as a doubly occupied  $1s$  orbital screening two units of positive charge. This same density is however strongly antibinding for the A nucleus (A=Li or Be) due to a large negative atomic force brought about by a back polarization of the  $1s$  density. The direction of the atomic force on A, due now to the  $2\sigma$  density, is also characteristic of the LiH and BeH molecules. One further identifying feature is that in both LiH and BeH the screening of the proton by the  $2\sigma$  density is greater than that of the A nucleus, while in BH and the remaining molecules this situation is reversed to an ever increasing extent through the series. Any screening of the A and H nuclei is a consequence of localized density and the above observation confirms the previous conclusion that the  $2\sigma$  charge distribution in LiH and BeH can be considered localized primarily on H whereas for BH  $\rightarrow$  HF it is localized primarily on A.

It is the presence of the  $3\sigma$  molecular orbital, singly occupied in BeH and unoccupied in LiH, which causes the abrupt observed change in the density distributions. The orbital density diagram (Fig. XXI) and the associated force contributions (Table XV) show that this orbital in BeH is

largely localized on the Be nucleus. In the case of an infinite separation of the Be and H nuclei the  $3\sigma$  molecular orbital will correlate with a singly occupied  $1s$  orbital on H, for which  $f_{3\sigma H}(\infty)$  and  $f_{3\sigma Be}(\infty)$  will equal 0 and 1 respectively. At the equilibrium bond length the  $3\sigma$  charge density is binding with respect to the proton and antibinding with respect to the Be nucleus. The values of  $f_{3\sigma H}(R_e)$  and  $f_{3\sigma A}(R_e)$  indicate that the only significant contributions are of the screening and atomic type respectively. This atomic force on Be is however in a direction that opposes bond formation while the screening force on H, because of the localized nature of the  $3\sigma$  charge, makes this orbital binding with respect to the proton. It is the large concentration of charge behind the Be nucleus, not present in LiH, that marks the difference between these two molecules. Furthermore, although BeH, because of near  $1s$  and  $2s$  degeneracy, is not adequately described by the correlation scheme relevant for LiH or to the correlation scheme relevant for the remaining members of the series its charge density and force contributions are clearly transitional between on the one hand LiH and on the other hand  $BH \rightarrow HF$ .

For this series  $BH \rightarrow HF$  the  $3\sigma$  molecular orbital correlates with, at large  $R$ , a singly occupied  $1s$  and a singly occupied  $A 2p\sigma$ . As the energy difference between these two orbitals increases then the  $3\sigma$  charge density should increasingly resemble a double occupied  $2p\sigma$  atomic orbital on A, which

is indeed reflected in the partial density diagrams of Fig. XXI

In the separated atoms  $f_{3\sigma H}(\infty)$  and  $f_{3\sigma A}(\infty)$ , or in particular  $f_{3\sigma H}^{(AA)}(\infty)$  and  $f_{3\sigma A}^{(HH)}(\infty)$ , will both equal 1 since the correlated H1s and A2p $\sigma$  atomic densities will screen one nuclear charge on each nucleus. The binding, antibinding and nonbinding nature of the 3 $\sigma$  density with respect to the proton and A nucleus for the molecules BH  $\rightarrow$  HF is dependant on the relative values of  $f_{3\sigma H}(R_e)$  and  $f_{3\sigma A}(R_e)$ . In the case of the proton it is the overlap and screening contributions,  $f_{3\sigma H}^{(AH)}$  and  $f_{3\sigma H}^{(AA)}(R_e)$  respectively, which are important. As we go through the series then there is an almost constant increase of 0.3 for  $f_{3\sigma H}(R_e)$  from its value in BH of 0.76, which makes the 3 $\sigma$  density antibinding with respect to the proton, to its value of 1.92 in HF, which makes the 3 $\sigma$  density binding with respect to the proton. Furthermore this increase in  $f_{3\sigma H}(R_e)$  is paralleled by an increase in the screening and overlap contributions explicable in terms of a charge transfer from the hydrogen atom to a localized 2p $\sigma$  orbital on A. If this is the case then because of the location of the charge increase on A, along the internuclear axis, density is placed in increasing amounts in the overlap region. If it is further remembered that the 1 $\sigma$  density, being centred on A as a doubly occupied 1s atomic orbital, is essentially nonbinding for the proton and the 2 $\sigma$  density is weakly binding then it is the 3 $\sigma$  charge distribution in HF and OH which is important in this respect. In HF, for example, the force on

the proton is equivalent to that exerted by 1.92 electronic charges situated at the F nucleus as opposed to the separated atom equivalent of one electronic charge. The  $3\sigma$  molecular orbital has thus almost doubled the number of charges which are effective in binding the proton. For the molecules, BH and CH, on the other hand it is the  $2\sigma$  density which is now more important in binding the proton while in NH the  $2\sigma$  and  $3\sigma$  molecular densities can be considered of equal importance.

The screening of the proton by the  $3\sigma$  charge density,  $f_{3\sigma A}^{(HH)}(R_e)$ , is uniformly low throughout the series reflecting the localized nature of the  $3\sigma$  charge density on A. In NH, OH and HF the partial  $3\sigma$  density diagrams closely resemble a  $2p\sigma$  on A whereas in BH and CH it is more bicentric in character. It is however the relative position of this charge with respect to the A nucleus that is important in determining the  $f_{3\sigma A}$  values. In BH, for example, the low overlap force contribution and large negative atomic force indicates that the transfer of charge accompanying bond formation is placed primarily behind the B nucleus whereas in HF these two same forces show that the charge transferred is roughly placed evenly on the bonding and non-bonding side of F. Moreover the force exerted on the A nucleus by the  $3\sigma$  overlap charge density is approximately twice as large as that exerted on the proton for each molecule. In contrast this same overlap force on the A and H nuclei due to the  $2\sigma$

charge density are of equal magnitude. Thus one anticipates a more polar type of bond in HF and OH where the binding of the proton is primarily by the  $3\sigma$  charge density than in BH and CH where the proton is bound primarily by the  $2\sigma$  charge density. This conclusion would also be consistent with the small and decreasing screening contribution  $f_{3\sigma A}^{(HH)}(R_e)$  associated with a large and negative atomic force.

In summary therefore the  $\sigma$  molecular orbitals show the different binding characteristics of the first-row hydrides. The  $1\sigma$  molecular orbital is primarily localized on the A nucleus as a doubly occupied  $1\sigma$  function screening two units of positive charge from the proton. This density is however unsymmetrically placed with respect to the A nucleus producing a negative atomic force (antibinding) on the Li and Be nuclei and a positive atomic force (binding) on the B, C, N, O and F nuclei. The  $2\sigma$  molecular density is binding with respect to both the H and A nuclei in the series BH  $\rightarrow$  HF whereas the  $3\sigma$  molecular density in this same series is antibinding with respect to A and goes from weakly antibinding to strongly binding with respect to the proton. The proton in BH and CH is primarily bound by the charge contained in the  $2\sigma$  molecular orbital whereas in OH and HF it is primarily bound by density contained in the  $3\sigma$  molecular orbital. For NH these two orbitals can be considered as being equally important in binding H. The relative magnitude of the force contributions in the series BH  $\rightarrow$  HF are suggestive of increa-

singly localized  $2\sigma$  and  $3\sigma$  molecular orbitals on A. There is still however an important overlap contribution. This overlap contribution for the  $2\sigma$  charge density is almost equally shared between the A and H nuclei whereas the overlap contribution due to the  $3\sigma$  charge density is unequally shared being greater for the A nucleus. Accordingly the molecules HF and OH are expected to have a more polar type of bond than the hydrides BH and CH. However, the charge transfer in HF and OH is not of sufficient magnitude nor localized sufficiently for the A and H nuclei to see a net positive and negative electric field respectively.

The molecules CH, NH, OH and HF contain 1, 2, 3 and  $4\pi$ -electrons respectively. At large internuclear distances the  $\pi$  molecular orbital correlates with a  $2p\pi$  atomic orbital centred on A, containing 1, 2, 3 and 4 electrons for A = C, N, O and F, and as such will shield an equivalent number of nuclear charges from H. This would mean that  $f_{1\pi A}^{(\infty)} = 0$  and  $f_{1\pi H}^{(\infty)} = f_{1\pi H}^{(AA)} = 1, 2, 3$  and 4 for A = C, N, O and F respectively. Both the orbital density diagrams of Fig. XXII and the overlap and screening force contributions (Table XV) suggest that this orbital is still essentially centred on A in the AH molecules. There is however a small overlap density which is almost equally shared by the A and H nuclei. Moreover a slight inward polarization of this  $\pi$  density makes this density binding with respect to A. An analysis of the  $\sigma$  force contributions showed that through the series CH  $\rightarrow$  HF an in-

creasing amount of charge was transferred from H to A. This, together with the results obtained for LiF (65), would suggest that it is a characteristic of the  $\pi$  density in heteronuclear molecules to be polarized in a direction counter to the direction of charge transfer and that one effect increases with the other. If this is the case then the almost constant increase of  $f_{1\pi A}^{(AA)}(R_e)$  of 0.07 is suggestive of a gradual change in the binding of the series CH  $\rightarrow$  HF with the charge transfer in HF being the greatest.

Although the  $\pi$  molecular orbital is primarily centred on A as a localized  $2p\pi$  atomic function with no significant  $\pi$ -bond formation it is the inefficiency of this density, at  $R = R_e$ , in screening the nuclear charges on A that results in this orbital being antibinding with respect to the proton.



### III A DISCUSSION OF THE BINDING IN THE AH MOLECULES

The relative values of the total atomic, overlap and screening forces can be used as a basis for the classification of the binding in molecules as being ionic or covalent (65,66). When comparing and contrasting the binding in a series of molecules, however, it is the changing role of a particular molecular orbital, as shown by both the partial forces and its three components, that reflects a change in the nature of the binding. By examining, for example, the  $f_{1\sigma A}(R_e)$ ,  $f_{2\sigma A}(R_e)$  etc. partial forces with particular reference to the magnitude and sign of the atomic, overlap and screening contributions, the relative importance of these orbitals in binding the A and H nuclei, which is after all the basic factor at issue, can be discussed. Just how close the charge density in these hydride molecules approximate to the ionic or covalent limiting cases are, however, questions of considerable interest and as such will also be considered.

The charge equivalents of the total atomic, overlap and screening forces for the first-row hydrides are listed in Table XVI and are obtained by summing the various orbital contributions. Also listed are the net forces  $F_A$  and  $F_H$  acting on the A and H nuclei respectively, where

$$F_A = \frac{Z_A}{R_e^2} (Z_H - Q_H') \quad F_H = \frac{Z_H}{R_e^2} (Z_A - Q_A')$$

$$Q_H' = \sum_i f_{iA}(R_e) = \sum_i f_{iA}^{(AA)} + f_{iA}^{(AH)} + f_{iA}^{(HH)}$$

$$Q_A' = \sum_i f_{iH}(R_e) = \sum_i f_{iH}^{(HH)} + f_{iH}^{(AH)} + f_{iH}^{(AA)}$$

These resultant forces can be seen in every case to be close to the expected value of zero. Since  $Z_A$  is the nuclear charge on A and  $\sum_i f_{iA}^{(AA)}$  is the number of charge equivalents on A in the molecule, then the quantity  $Z_A' = (Z_A - \sum_i f_{iA}^{(AA)})$  represents the amount by which the A nucleus has been descreened on molecular formation. Similarly defined for the proton is the quantity  $Z_H' = (Z_H - \sum_i f_{iA}^{(HH)})$ . Both  $Z_A'$  and  $Z_H'$  thus represent the effective nuclear charges on the A and H nuclei in the molecule. If the molecule is best described as being ionic in the sense  $A^+H^-$  then  $Z_A'$  and  $Z_H'$ , which represent the number of positive charges left unscreened on the A and H nuclei respectively, should take on the respective values of +1 and -1. In addition the overlap forces,  $\sum_i f_{iH}^{(AH)}$  and  $\sum_i f_{iA}^{(AH)}$ , should be zero and the atomic forces,  $\sum_i f_{iH}^{(HH)}$  and  $\sum_i f_{iA}^{(AA)}$ , should be directed in opposition to the dipole moment and hence counter to the electron transfer. None of the molecules in the hydride AH series, according to the calculations listed in Table XVI, simultaneously satisfies these conditions. Although in LiH the atomic forces on the Li and H nuclei are in the correct direction and the overlap forces take on their smallest value, still being far from zero, the values of  $Z_A'$  and  $Z_H'$  are very different from

those predicted by an  $\text{Li}^+\text{H}^-$  description. The ratio  $Z'_A/Z'_H$  does, however, take on its highest value for this molecule suggesting that it does come closest to the ionic limiting case.

While the force contributions based on a population analysis are not those predicted by the idealized model for ionic binding the density difference diagram for LiH and in particular a charge analysis of the different defined regions (see Table X) possesses all the necessary characteristics. The number of electrons on the non-bonded side of the Li nucleus together with the charge considered localized on the hydrogen, come close to their ideal values of 1 and 2 respectively. This discrepancy can best be understood in terms of the separate  $1\sigma$  and  $2\sigma$  density distributions and their associated forces. The  $1\sigma$  orbital according to the partial density diagram of Fig. XIX is predicted to be essentially localized at the Li nucleus as a doubly occupied  $1s$  atomic function. This is indeed reflected in the force analysis where in the molecule it simply screens two units of positive charge from the proton. Similarly, the  $2\sigma$  orbital, according to its density distribution, is predicted to be essentially localized on the hydrogen as a doubly occupied  $1s$  function. The forces however do not reflect this since there are now large overlap contributions to the orbital force,  $f_{2\sigma A}^{(AH)}$  and  $f_{2\sigma H}^{(AH)}$ . It would thus seem that there is not always a direct correspondence between an orbital population analysis and the appearance of the

final density distribution. Just as the one-electron densities are not sufficient by themselves to interpret the nature of the binding neither are the forces but one should rather be discussed in the light of the other. If this is the case then the density difference map,  $\Delta\rho_{SA}(\xi, \eta)$ , for LiH indicates that the charge transferred to the hydrogen is localized. Accordingly the charge equivalents of the force exerted by the overlap population can now be considered as localized atomic density on H. This would mean that  $\sum_i f_{iH}^{(HH)}$  and  $\sum_i f_{iA}^{(HH)}$  in Table XV should be replaced by  $(\sum_i f_{iH}^{(HH)} + f_{iH}^{(AH)})$  and  $(\sum_i f_{iA}^{(HH)} + \sum_i f_{iA}^{(AH)})$  respectively. A similar situation arises in the treatment of the LiF molecule where again there is no direct correspondence between the orbital population analysis and the total density distribution. By likewise assuming the overlap charge to be localized on the F nucleus the charge equivalent of the force as determined by the density difference maps can be obtained. Table XVII lists the results for LiH and LiF together with the values expected for ideal ionic binding. These molecules do indeed approach the ionic case. In LiF the transfer of one unit of charge is almost complete whereas in LiH it is not quite to the same extent, reflecting the difference in the electronegativities of the F and H atoms. The atomic force on the Li nucleus is however a little low. This force is due primarily to density that is close to the Li nucleus and hence a slight polarization can have a large effect. Such a shift in density close to the lithium nucleus

will not alter appreciably the outer or valence density distribution and hence the chemical nature of the bond.

In the remaining members of the series density is rather transferred in increasing amounts from the H to the A nucleus. The HF molecule of all the first-row hydrides approaches most nearly the limiting ionic structure  $F^-H^+$ . Although neither the electron population analysis nor the charge equivalents of the force, contained in Table XVI, suggest that this is the case it is interesting to partition these forces in a manner similar to that for LiH and LiF. This would imply, contrary to the information contained in the  $\Delta\rho_{SA}(\xi,\eta)$  map, that the overlap density can be considered localized on F. Even so the number of charge equivalents on the F atom is now only  $8.988e^-$ . Since this is less than the nuclear charge on F the proton will experience a net force of repulsion rather than the expected attractive force. Electrostatic equilibrium can only be attained by an inward polarization of the density remaining on the proton. In general it is impossible for an  $H^+$  ion to exist in a stable chemical bond outside the density sphere of an  $A^-$  anion; there would be an inward force on the proton equal to  $(Z_A - \sum_i f_{iH}^{(AA)})/R^2$  where  $\sum_i f_{iH} = (Z_A + 1)$ . Once it penetrates this sphere density contours will appear around the proton, simulating localized density and hence an  $H^{\delta+}$  cation, and it is the associated atomic force together with the decreased screening contribution,

$\sum_i f_{iH}^{(AA)}$ , that prevents bond closure.

The similarity and gradual change in the  $\Delta\rho_{SA}(\xi, \eta)$  maps for the series  $BH \rightarrow HF$  is also reflected in their charge equivalents of the total atomic, overlap and screening forces. Consider, for example, the expected transitions in the relative partial force contributions as the binding in a molecule changes from the predominantly covalent AH description to the partially ionic  $A^{\delta-}H^{\delta+}$  description. For AH the screening contribution to the forces on A and H are both expected to be less than  $Z_A$  and  $Z_H$  respectively and dependant on the magnitude of the overlap force contribution, which should roughly be the same for A and H, the atomic forces on A and H could conceivably be in any direction; although from experience in a covalent bond unlike the ionic case these are generally in the direction of the dipole moment. The formation of a polar molecule of  $A^{\delta-}H^{\delta+}$  on the other hand implies that charge is transferred from H to A. This would cause the screening contribution to the force on A to drop, as the number of charges on A left unscreened,  $Z_A^i$  decreases, and the screening contribution to the force on the proton to increase. That is to say as the bond becomes more polar, and hence closer to the ionic limiting case,  $Z_A^i$  should decrease and  $Z_H^i$  should increase. In a covalent bond it is shared or overlap density that simultaneously binds both the nuclei; in contrast the binding in an ionic molecule is due to localized density with the correct atomic polarizations. Thus on going from a predominantly covalent AH

description to a partially ionic description the overlap force contributions should decrease and in particular the position of the overlap density should shift towards the cationic nucleus and in the limit of a complete electron transfer should be localized on this nucleus. This would suggest that the ratio  $(\sum_i f_{iA}^{(AH)} / \sum_i f_{iH}^{(AH)})$  should increase with increasing bond polarity  $A\delta^-H\delta^+$ . Moreover the direction of the atomic forces should change in such a way that they approach that anticipated by the ionic model.

With this in mind it is interesting to re-examine the series  $BH \rightarrow HF$  with special regard to the behaviour of  $Z'_H$ ,  $Z'_A$  and the overlap and atomic partial forces on the A and H nuclei. For  $BH$ ,  $Z'_A$  takes on its highest value,  $Z'_H$  its lowest and the magnitude of the overlap force contribution on both the B and H nuclei suggests that this density is almost equally shared and hence close to the covalent bonding scheme. Progressing through the series a decrease in  $Z'_A$  is paralleled by an increase in both  $Z'_H$  and the ratio  $(\sum_i f_{iA}^{(AH)} / \sum_i f_{iH}^{(AH)})$ . In fact for the molecules  $NH$ ,  $OH$  and  $HF$  the overlap density exerts a force on the A nucleus of respectively 1.23, 1.27 and 1.36 times greater than that exerted on the proton. This shift in the overlap density for these hydrides is also evident in the  $\Delta\rho_{SA}(\xi, \eta)$  contour maps of Fig. XIV and in the appropriate profile diagrams of Fig. XV. Similarly the change in magnitude of the atomic forces at the position of the A and H nuclei is also suggestive of some gradual change in the

electronic structure. Although charge is transferred from the proton to the A atom in an increasing amount through the BH  $\rightarrow$  HF series this transfer is not of sufficient magnitude that the A and H nuclei experience a net positive and negative field respectively. If this were the case the atomic forces on the A and H nuclei would be expected to be negative and positive respectively. However, in HF, where the atomic force on the proton is almost zero, it comes closest to this extreme case.

In this way the binding in the molecules BH  $\rightarrow$  HF can be written in a series which represents an increasing divergence from the ideal covalent situation. This series is BH, CH, NH, OH and HF.

According to this study the binding in BeH can be considered as intermediate between ionic LiH and the remaining hydrides. Although the  $1\sigma$  and  $2\sigma$  density distributions for this molecule suggest a more ionic-type pattern than is observed in the total density and density difference maps it is, as mentioned previously, the presence of the  $3\sigma$  orbital, not occupied in LiH and doubly occupied in BH  $\rightarrow$  HF, that causes the abrupt change in the density distributions between LiH and BH. This orbital density is almost completely contained on the non-bonded side of the Be nucleus and as such replaces the valence density transferred to the hydrogen by the  $2\sigma$  molecular orbital.

There have, of course, been many other studies pertain-



ing to the bonding in the first-row hydrides. The predictions of Blinder (76) regarding this series are based on a consideration of the relative energies of the atomic orbitals centred on A and H. Atomic orbitals on different centres, he said, will overlap and result in the formation of two bicentric molecular orbitals, one bonding and one anti-bonding, if they are (a) of compatible symmetry and (b) have orbital energies that lie within  $\pm 0.2$  a.u. ( $\pm 5$  e.v) of one another (see Table XIII). When this matching of orbital energies is not found, the molecular orbital is essentially monocentric.

The  $1\sigma$  atomic orbital centred on the heavy nucleus A is in every case well outside the range predicted for a bicentric molecular orbital. The lowest occupied molecular orbital,  $1\sigma$ , will thus be expected to resemble a  $1s$  atomic orbital on A. The next lowest occupied molecular orbital will be the  $2\sigma$ . According to Blinder this orbital in LiH and BeH should be localized primarily on H as a doubly occupied  $1s$  orbital and the  $3\sigma$  orbital in BeH should be localized on Be as a singly occupied  $2s$  orbital. This would indicate that these two hydrides are best described as ionic,  $\text{Li}^+(\text{1s}^2)\text{H}^-(\text{1s}^2)$  and  $\text{Be}^+(\text{1s}^2\text{2s}^1)\text{H}^-(\text{1s}^2)$ . The near degeneracy of the  $2s$  energy level of B and the  $1s$  level of H results in strong mixing of the two orbitals and in the formation of a bicentric molecular orbital. The  $2\sigma$  orbital is thus primarily the bonding combination of  $B2s$  and  $H1s$  while the  $3\sigma$  orbital is primarily a mixture of the  $B2s$  and  $H1s$  antibonding combination with the non-bonding  $B2p\sigma$ .

The changeover from monocentric to bicentric character will occur, according to Blinder, between BeH and BH and this is indicative of a change in the bonding type. From carbon through the remaining members of the first-row hydrides the energy gap between the  $A2s$  and the  $H1s$  orbitals increases and now the bonding will be mainly due to the  $3\sigma$  molecular orbital. This orbital results from the overlap of an  $A2\sigma$  and  $H1s$ . That is to say as we go through the series LiH to HF the  $2\sigma$  molecular orbital will become increasingly localized on A as a doubly occupied  $2s$  function and the  $3\sigma$  molecular orbital resulting in the bonding. However, because of increasing stability of the  $2p\sigma$  orbital on A the  $3\sigma$  orbital will again resemble a  $2p\sigma$  on A. Even so this  $2p\sigma$  density encompasses the proton and can again be considered bicentric in nature.

The qualitative predictions of Blinder are borne out remarkably well by the  $1\sigma$ ,  $2\sigma$ ,  $3\sigma$  and  $1\pi$  orbital density diagrams shown in Figs. XIX, XX, XXI and XXII and in the orbital force analysis considered previously. The monocentric almost spherical  $1\sigma$  density is indeed characteristic of the  $1s$  atomic function on A. In going from LiH to HF this density becomes less diffuse due to an increased atomic number; however even in LiH the proton is well outside the outer 0.0002 contour. The  $2\sigma$  density for LiH and BeH on the other hand approximates a highly distorted  $1s$  density on H. The position of the nodal line, dashed contour in Fig. XX, indicates that the  $2\sigma$  density distribution for LiH is localized on the H nucleus. This to-

gether with the localized nature of the  $1\sigma$  density on Li bolsters an ionic description for LiH. The  $2\sigma$  density on BeH is also mainly localized on H whereas from BH on it encompasses both nuclei and becomes increasingly centred on the A nucleus with the spherical contours characteristic of a  $2s$  density distribution. The  $3\sigma$  molecular orbital according to Blinder's arguments is expected to be a singly occupied  $2s$  atomic orbital on Be. If this is the case, and assuming the  $2\sigma$  orbital to be mainly centred on H, a total of about  $1.5\bar{e}$  non-bonded charges on the Be atom is expected. The amount of charge actually present is  $2.0e^-$ , the free atomic value. The reason for this is the extreme back-polarization of the  $3\sigma$  density evident in both the partial force analysis and the density distribution diagram of Fig. XXI. It is the absence of this molecular orbital in LiH which accounts for its unusual short length  $L$  in contrast to the remaining hydrides.

From  $BH \rightarrow HF$  as the energy difference between the  $H1s$  and  $A2p$  atomic orbitals increases then the  $3\sigma$  molecular orbital resembles a doubly occupied  $2p\sigma$  function on A. Even so this density encompasses the proton and can again be considered bicentric in nature.

Fajans (74) unlike Blinder predicts a break in the bonding type of the hydride series to occur between BH and CH. His arguments are based on the quanticule theory of chemical binding. Here the word ionic and covalent are avoided and the bonding in a molecule is classified according to whether the

electrons are quantized with respect to the field of one nucleus or to the field of both nuclei. Accordingly the  $1\sigma$  and  $2\sigma$  orbitals in BeH, as in Blinder's treatment, correspond to two mononuclear quanticules localized on Be and H respectively. The  $3\sigma$  density on the other hand, although still predicted to be localized on Be, will now be strongly repelled by the quanticule  $H^-$ . The change from mononuclear to binuclear quantization occurs between BH and CH where here the  $3\sigma$  molecular orbital is predicted to be quantized with respect to the field of both the C and H nuclei.

In the present work an analysis of the binding based on the individual orbital contributions does not indicate a marked difference between the hydrides BeH and BH or between the hydrides BH and CH. The partial forces would rather suggest a gradual change with LiH and HF as the two extremes. Thus, for example, as the  $1\sigma$ ,  $2\sigma$  and  $3\sigma$  orbital densities become increasingly localized on the A nucleus as  $A1s$ ,  $A2s$  and  $A2\sigma$  respectively the atomic, overlap and screening contributions to the forces change accordingly.

While the orbital densities and their partial forces change uniformly throughout the series it is the absence of the  $3\sigma$  molecular orbital, as stated previously, that causes the abrupt change in both the total density and density difference charge distributions between LiH and BeH. If one wishes, therefore, to classify the binding in terms of the individual orbital contributions the binding in BeH can be

considered as being primarily ionic. If on the other hand the binding is classified in terms of the total density distribution BeH can be considered as being primarily covalent. One point is clear, however, BeH marks the transition between the examples of charge transfer (the ionic binding) and the sharing of charge (and covalent binding) regardless of the criteria which are employed. The BeH molecule indicates the necessarily arbitrary character of insisting that all systems be clearly associated with well-defined limiting cases, in this case with either the ionic or covalent bond.

In conclusion one further point that does seem significant concerns the density difference plot for the O-H bond. There is a marked similarity between this plot (Fig. XIV) and the one obtained for the water molecule (Fig. VIII). In the formation of the O-H bond, density is removed from a torus -like region surrounding the oxygen nucleus and perpendicular to the bond axis. This density is transferred along the bond axis, both to non-bonded side of the oxygen nucleus and to a region between the O and H nuclei that encompasses the proton. The formation of the water molecule from its separated atoms likewise removes density from a region that surrounds the oxygen nucleus but is now perpendicular to the symmetry axis of the molecule. Moreover the regions of charge build-up are similar being on the non-bonded side of the O nucleus and along the symmetry axis encompassing both the protons. Since in both cases the magnitude and shape of the density shifts are comparable it would suggest that the

binding between the oxygen atom and the two protons in  $H_2O$  can be likened to the binding between the oxygen atom and the hydrogen atom in  $OH$ , where the proton in the latter has been "split" into two equal parts. This result is very encouraging since it supports the previous calculation on the water molecule (and in particular the method used to calculate the wave function). Since this is the case it does suggest that approximate wave functions obtained by meeting the zero force requirement, and in particular their one-electron density distribution, can be used to examine the binding in larger molecules for which the more accurate Hartree-Fock functions are not available. It should be possible, for example, to examine the identifying features of the  $\Delta\rho_{SA}$  maps obtained from these approximate wave functions and to relate these features to the forces operative in binding the nuclei and hence the nature of the chemical bond.

FIGURES AND TABLES

FIG. IV

Graphical representation of the variation  
of the forces  $F_o$ ,  $F_{\parallel}$ ,  $F_{\perp}$  and DP with a  
change in the parameters  $\delta, \alpha$  or  $\epsilon b$



			$V_1$	$V_2$	$V_3$
—————	variation of	$\alpha$	$69^\circ$	$73^\circ$	$77^\circ$
- - - - -	variation of	$\epsilon b$	$115^\circ$	$123^\circ$	$131^\circ$
.....	variation of	$\delta$	0.3	0.4	0.5

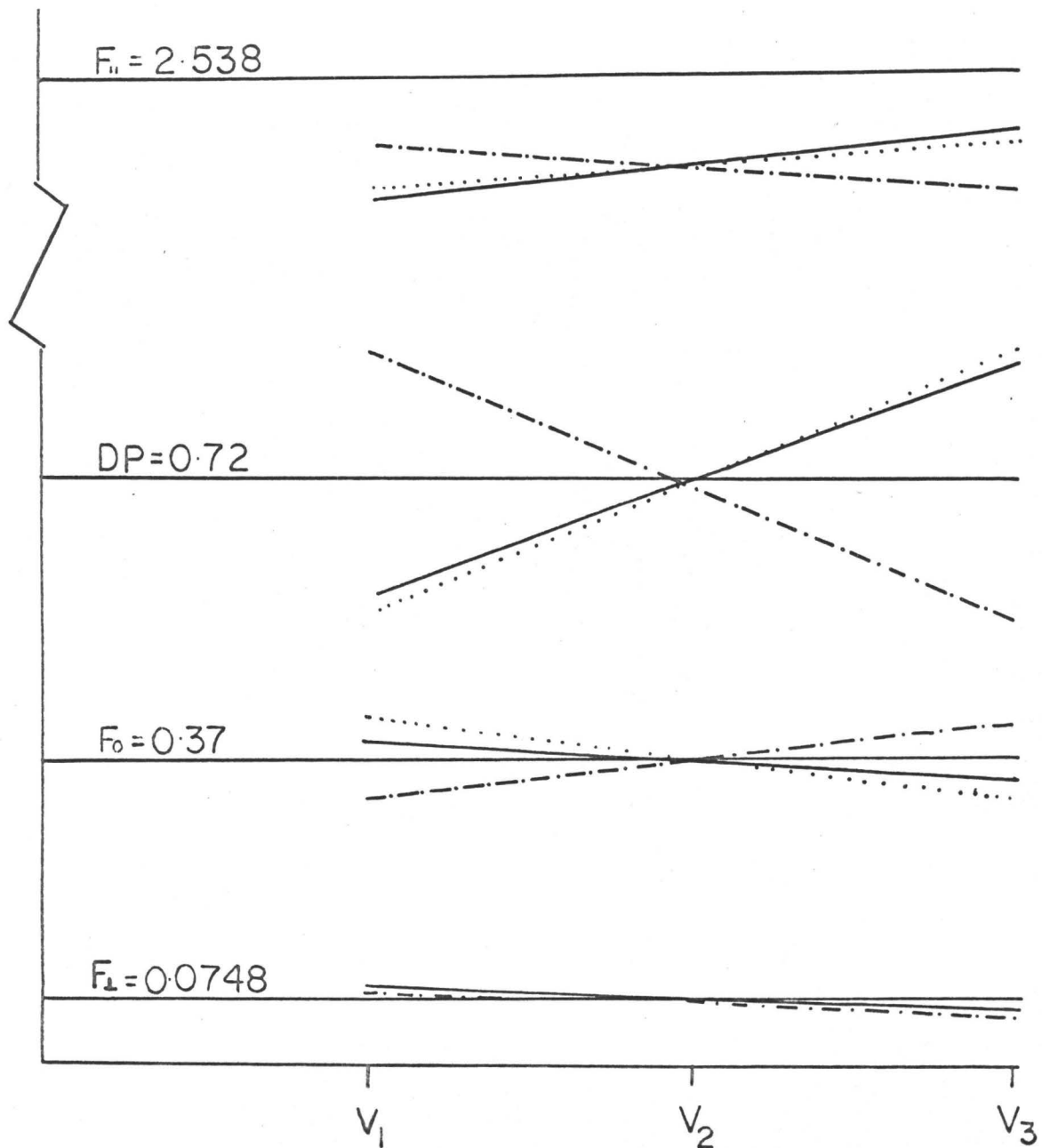


FIG. IV

FIG. VI

Electron density contour map in a.u. for the water molecule. The bottom map is in a plane containing the three nuclei. The top map is in a plane perpendicular to the above passing through the oxygen nucleus

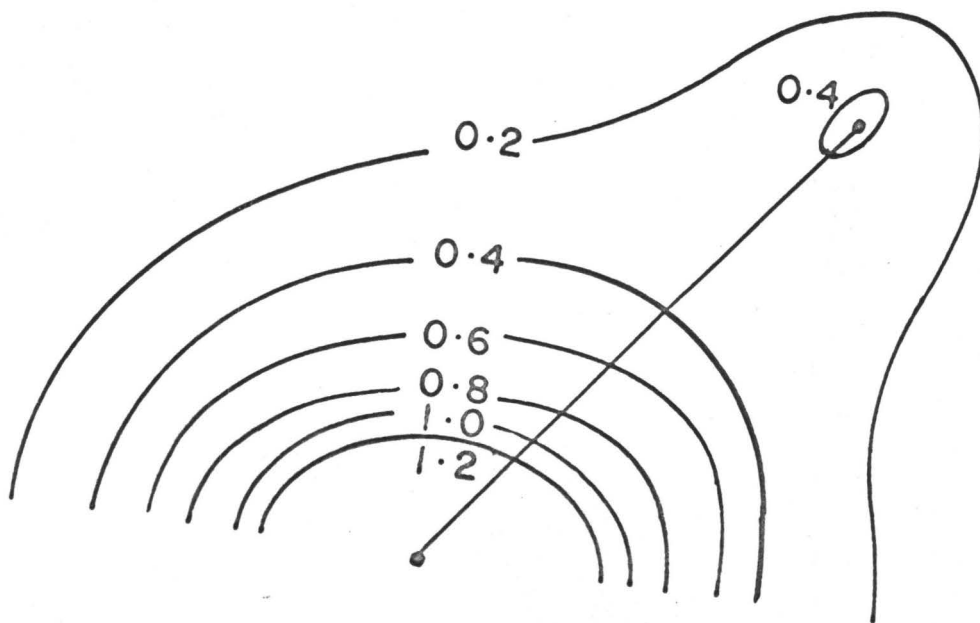
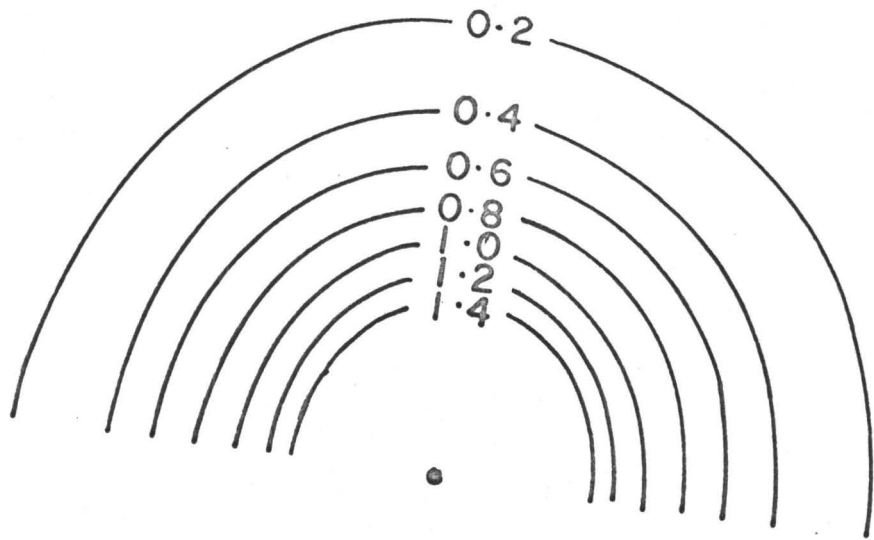
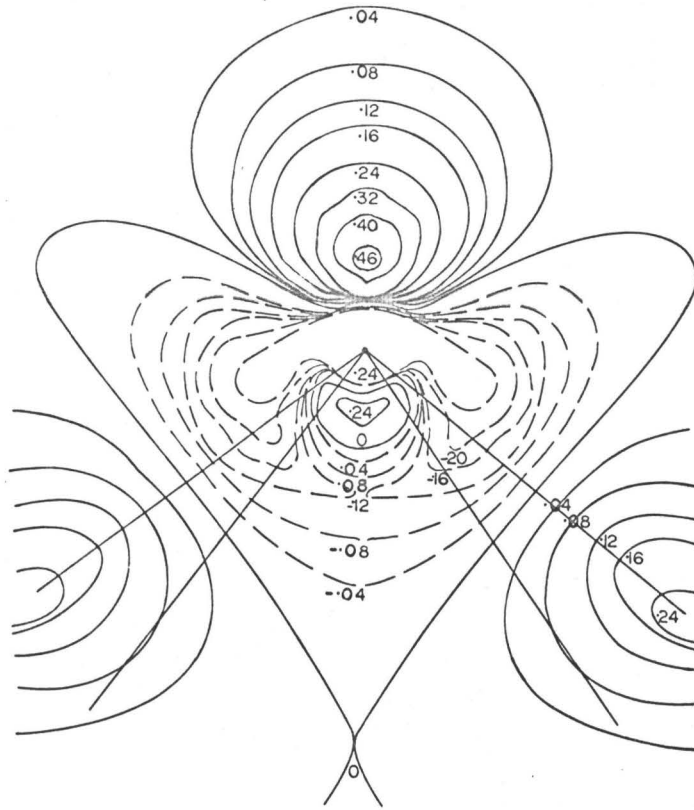


FIG. VI

FIG. VII

Plot of  $\Delta\rho_{SA}$  for  $H_2O$  corresponding to an approximately  $sp^3$  hybridisation of the oxygen atom. (a) the hydrogen nuclei are located at the ends of the two lines subtending the largest angle at the oxygen nucleus. The two inner lines are boundaries dividing the binding and antibinding regions. (b) plot of  $\Delta\rho_{SA}$  in a perpendicular plane. The nearly horizontal line divides the binding region from the antibinding region.

a



b

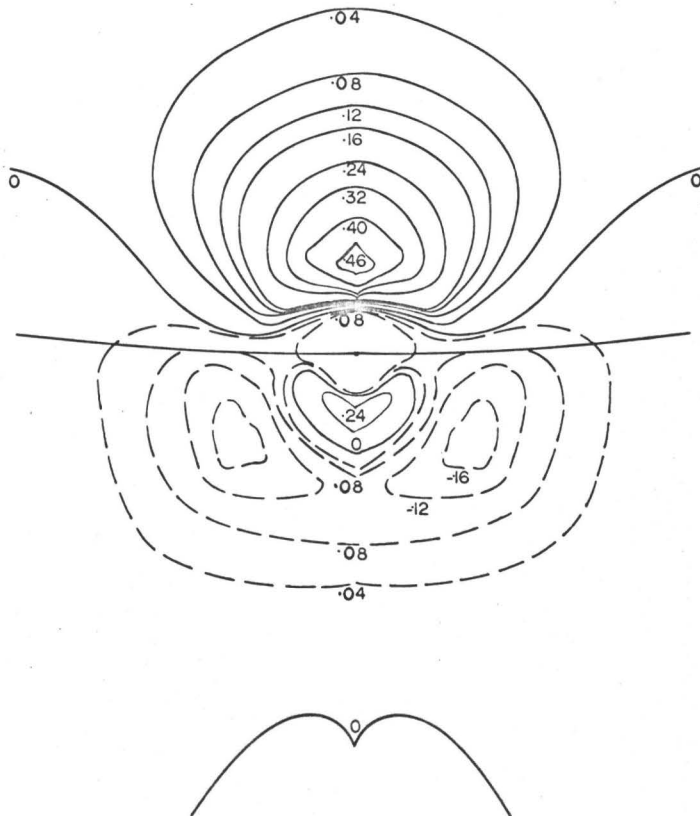


FIG. VII

FIGURE VIII

The in- and out-of-plane density difference maps ,(a) and (b) respectively ,for the water molecule

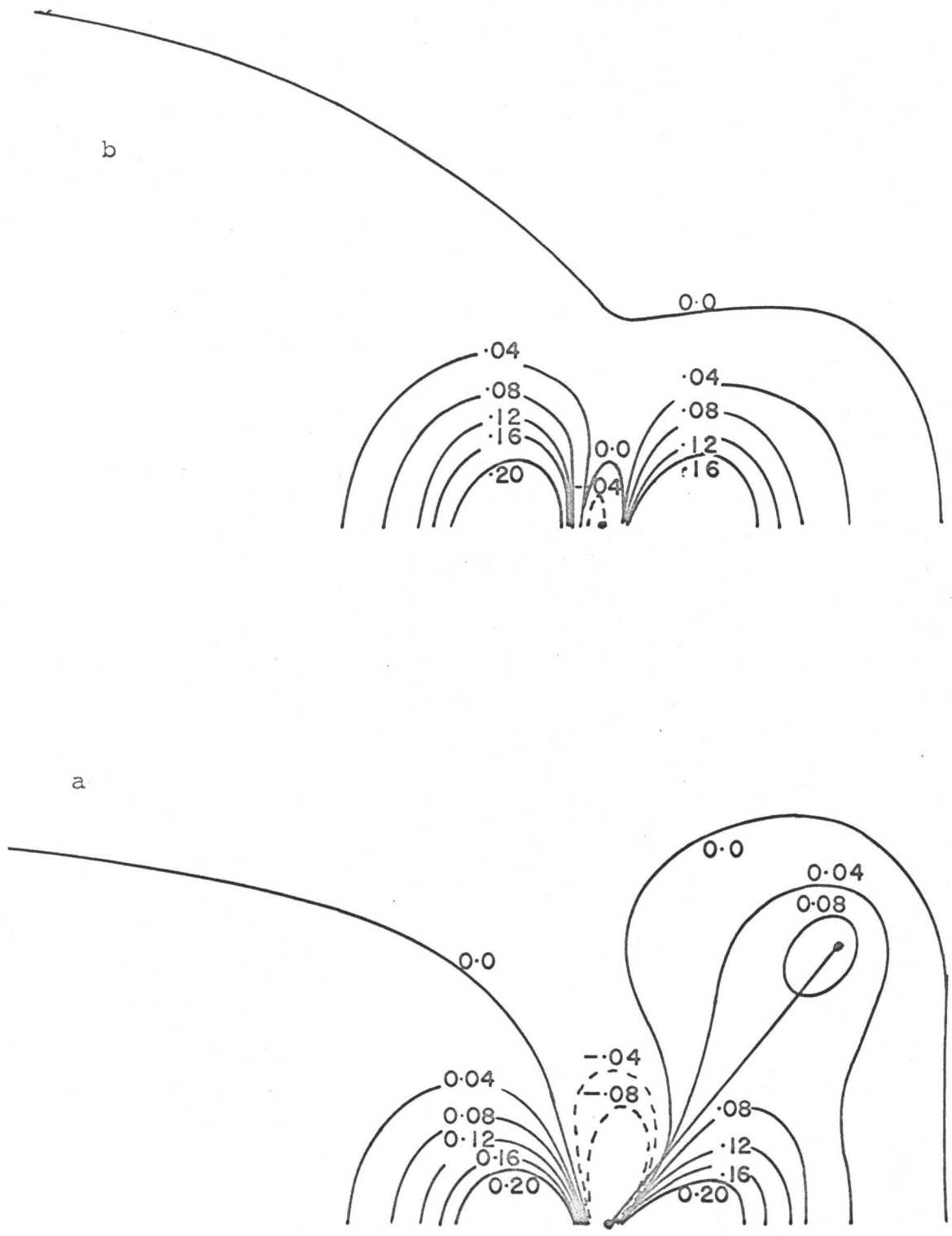


FIG. VIII

FIGURE IX

An electron density difference map between  
the LiF molecule and the Li and F atoms



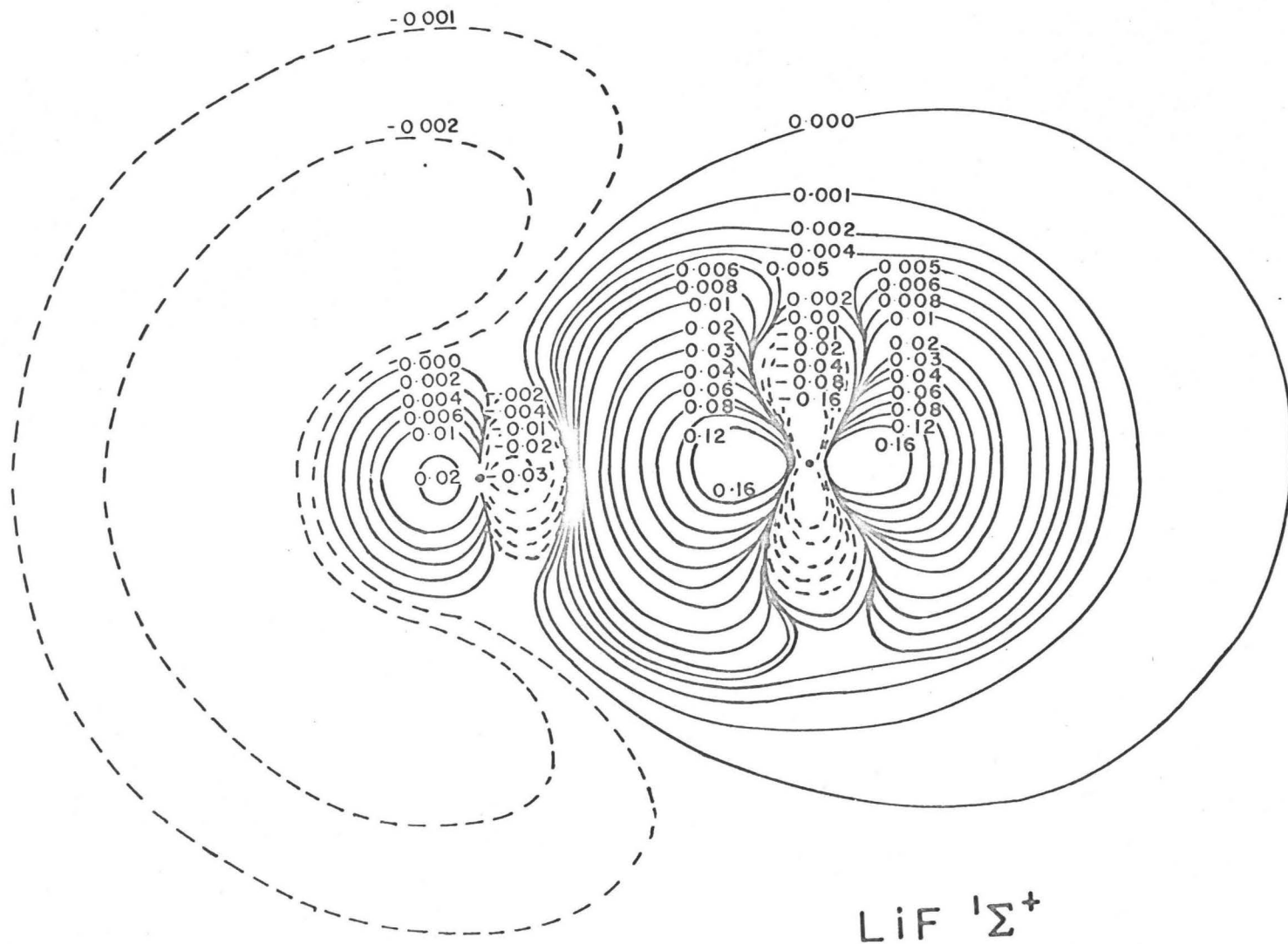


FIG. IX

FIGURE X

Density difference maps for the stable first-row homonuclear diatomic molecules. The same scale of length applies to all the maps. The dotted line (shown in full for  $N_2$ ) separate the binding from the antibinding regions.

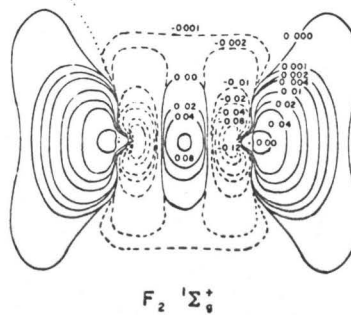
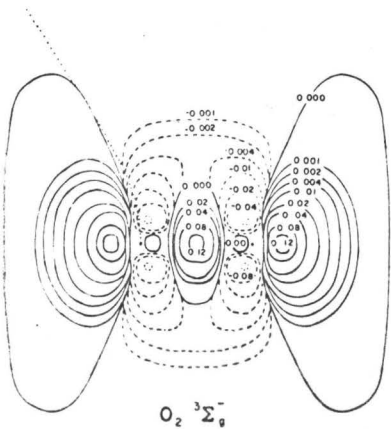
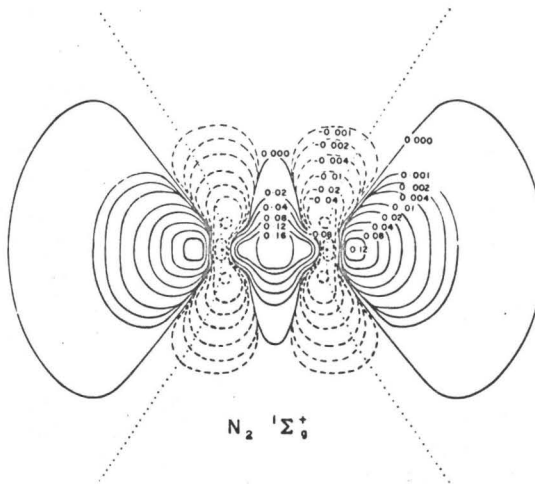
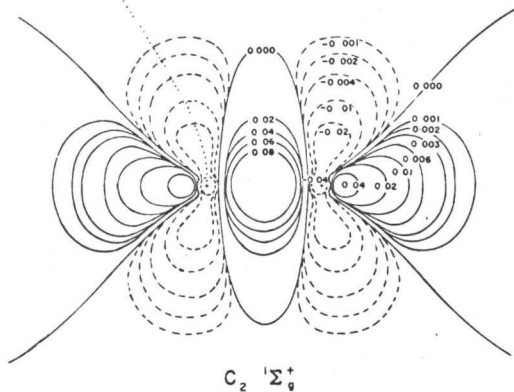
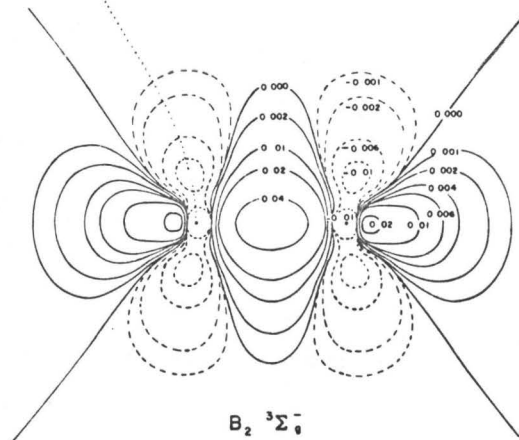
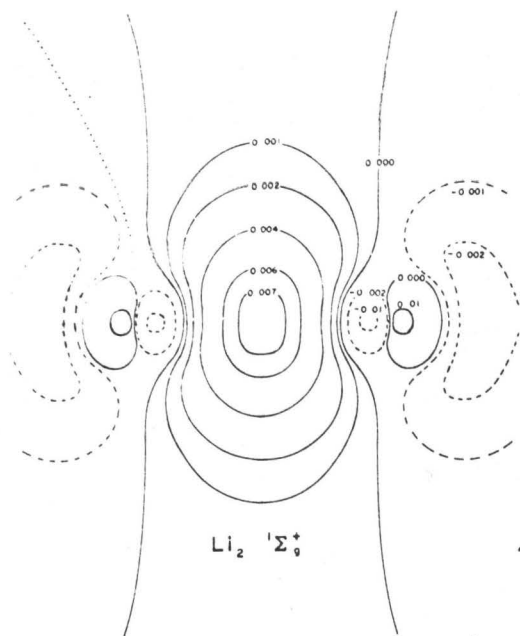
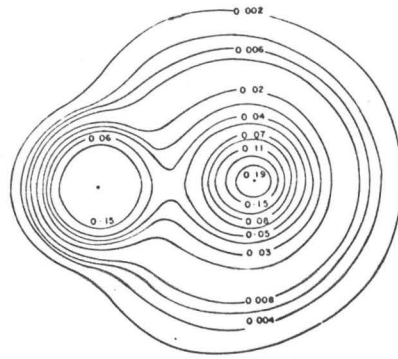


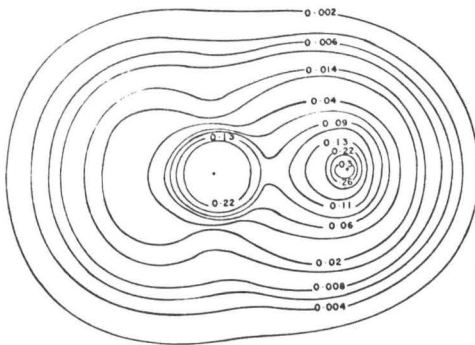
FIG. X

FIGURE XI

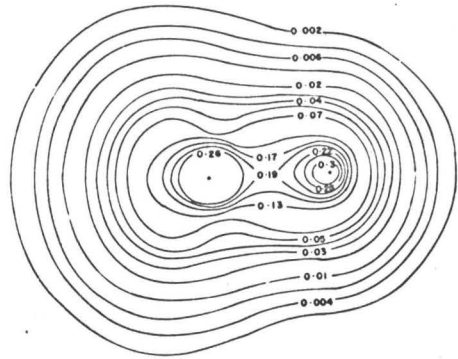
Total molecular charge density contours for the first-row diatomic hydrides in a.u. All maps are drawn to the same scale of length. The A nucleus is on the left in this and all succeeding figures. The innermost contours encircling the A nuclei have been omitted for the sake of clarity. The density at the A nucleus and at the proton is given in Table VIII.



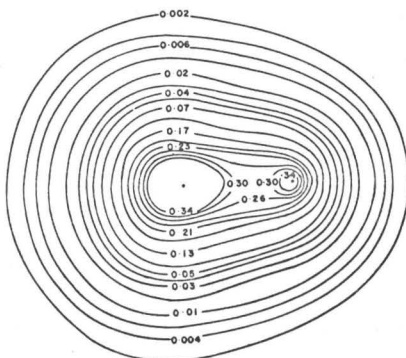
$\text{LiH } ^1\Sigma^+$



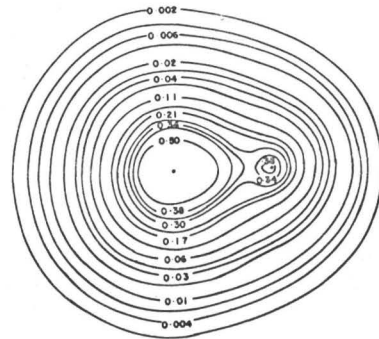
$\text{BeH } ^2\Sigma^+$



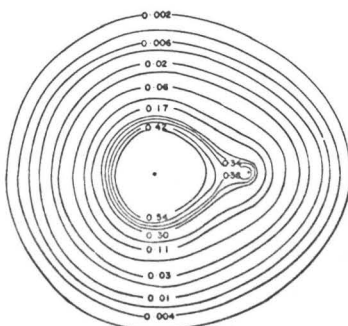
$\text{BH } ^1\Sigma^+$



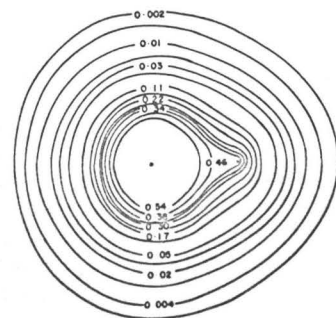
$\text{CH } ^2\Pi_1$



$\text{NH } ^2\Sigma^-$



$\text{OH } ^2\Pi_1$



$\text{HF } ^1\Sigma^+$

FIG. XI

FIG. XII

The definition of  $r_A$  and  $r_H$ . The outer line is to represent a typical 0.002 contour. The shaded areas indicate the non-bonded regions on A and H. The numerical integration used to obtain the non-bonded charges listed in Table IX was, however, extended beyond the 0.002 contour.

FIG. XVI

The definitions of the A and B regions

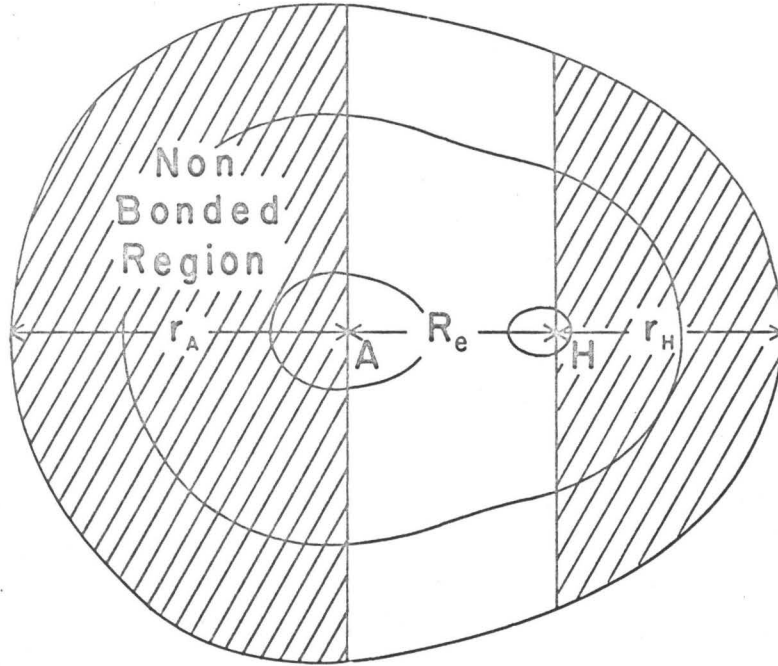


FIG. XII

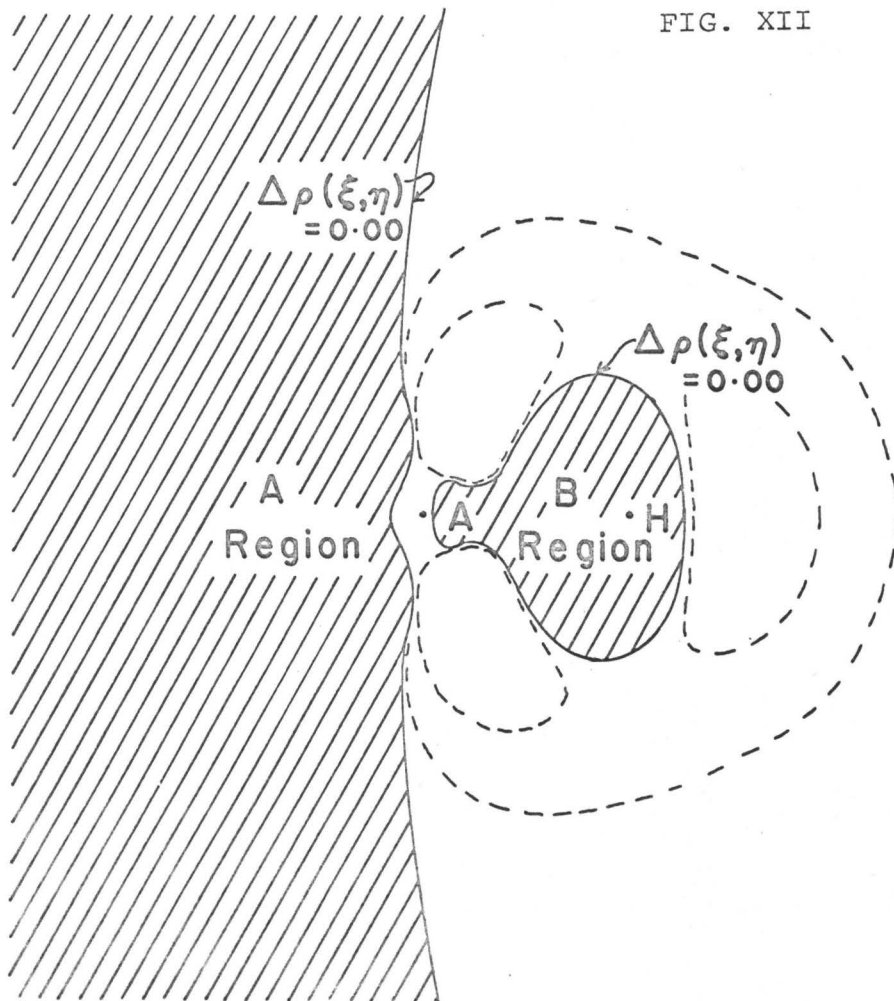


FIG. XVI

FIG. XIII

The binding and antibinding regions in  
the AH molecules with their respective  
electron populations



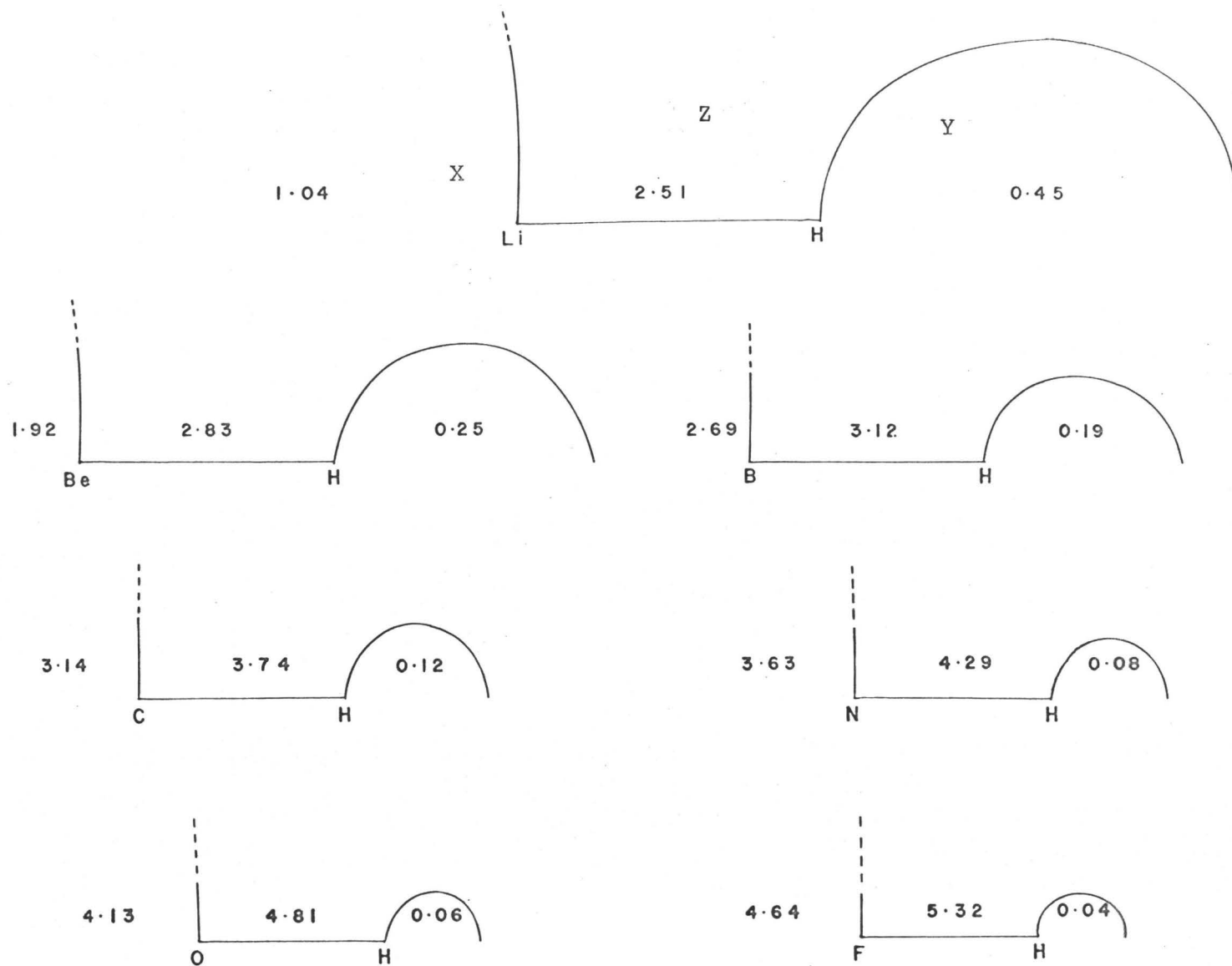


FIG. XIII

FIG. XIV

Contour maps of the density differences  
 $\Delta\rho_{SA}(\xi, \eta)$  (molecule-separated atoms) in  
a.u. for the first-row diatomic hydrides

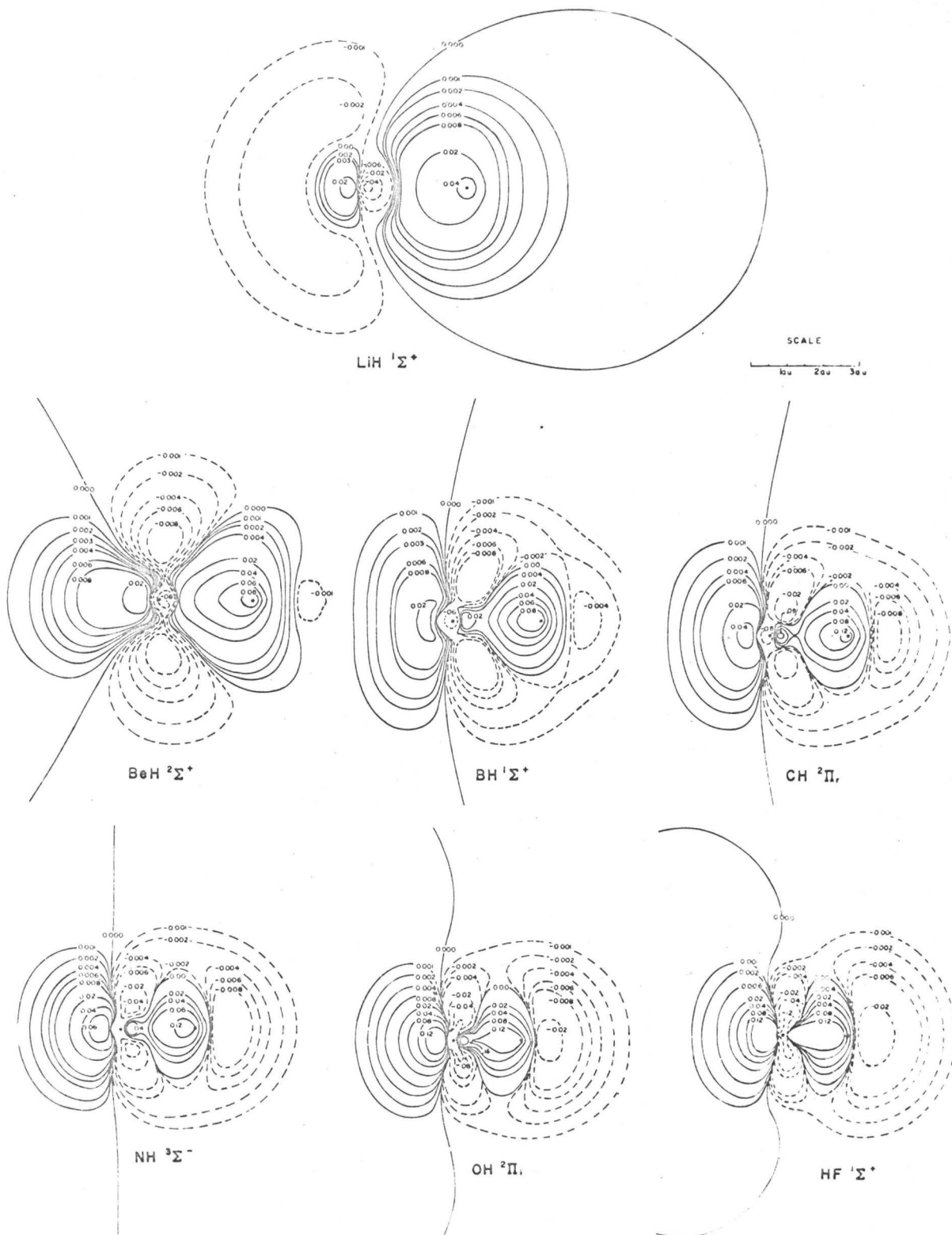


FIG. XIV

FIG. XV

Profiles of  $\Delta\rho_{SA}(\xi,\eta)$  in a.u. along the internuclear axis. The abscissa (distance along the internuclear axis) is in a.u. with the A nucleus as origin.

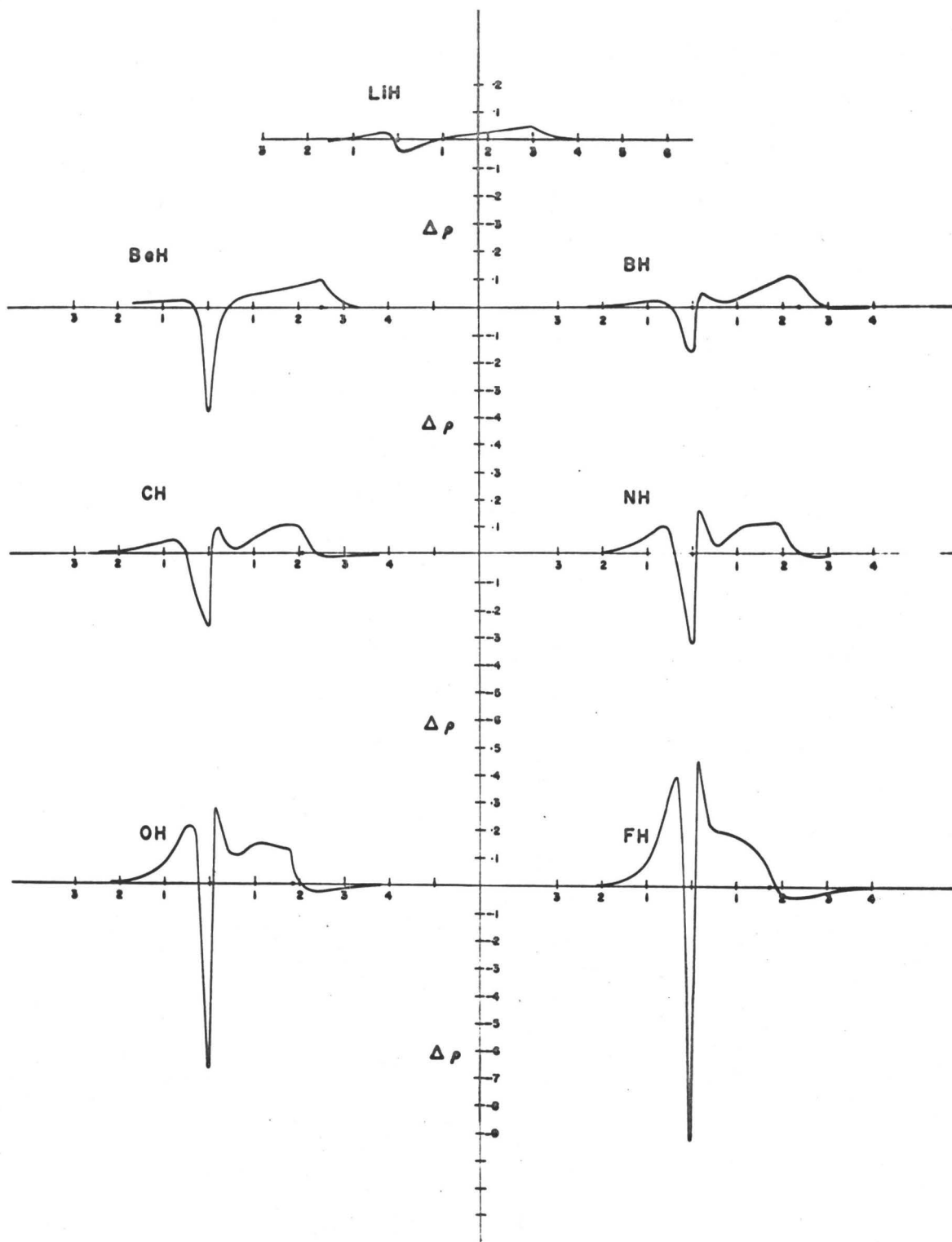


FIG. XV

FIG. XVII

Contour maps of the density differences  
 $\Delta\rho_{SA}(\xi,\eta)$  (molecule-separated atoms)  
employing the spherically atomic A  
density

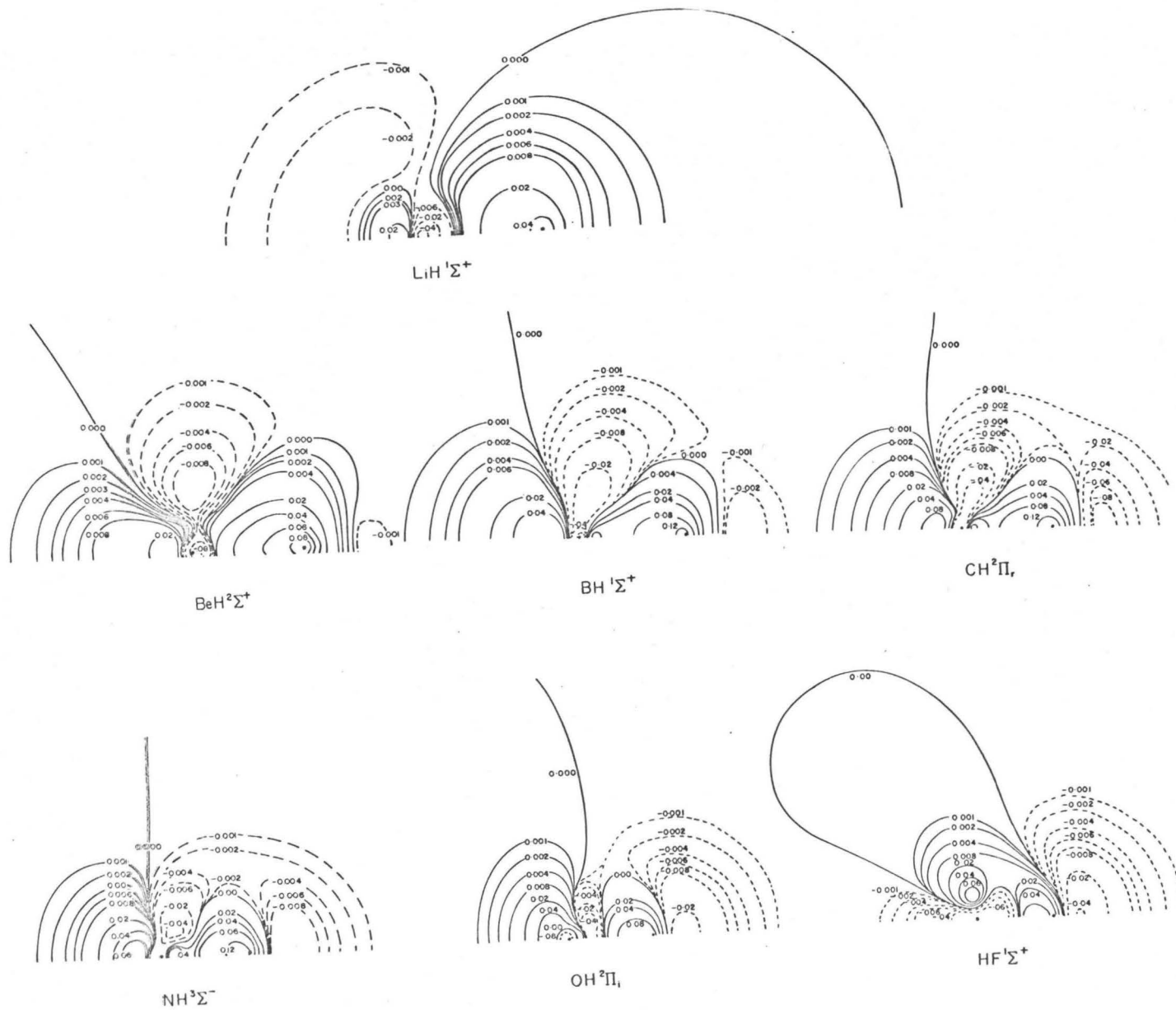


FIG. XVII

FIG. XVIII

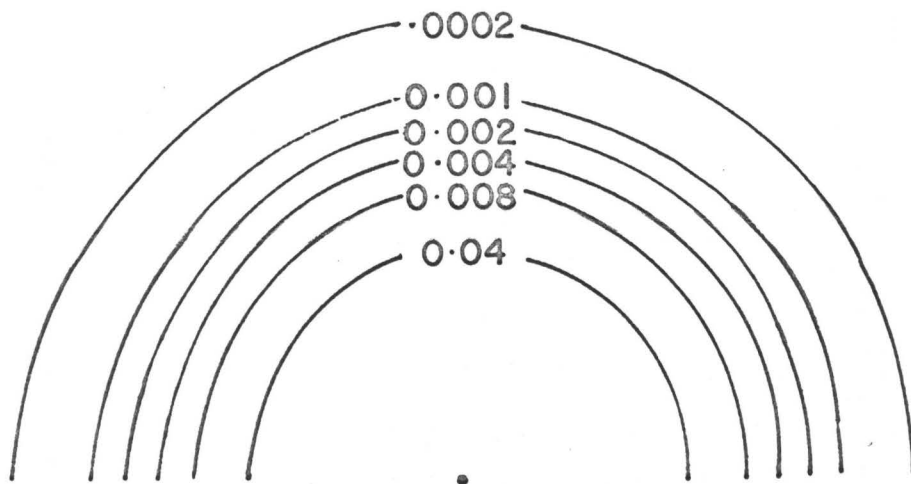
Contour maps of the density difference  
 $\Delta\rho_{\text{UA}}(\xi, \eta)$  (molecule-united atom) in a.u.  
for the first-row diatomic hydrides



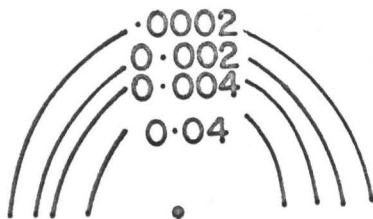


FIG. XIX

Contour maps of the  $1\sigma$  molecular orbital  
charge densities for LiH and HF



LiH  $1\sigma$



HF  $1\sigma$

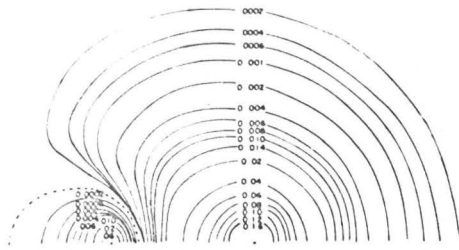
FIG. XIX

FIG. XX

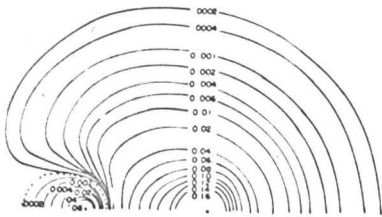
Contour maps of the  $2\sigma$  molecular orbital  
charge densities for the first-row hydrides

FIG. XXI

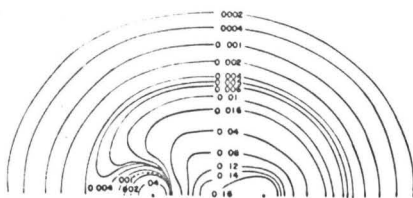
Contour maps of the  $3\sigma$  molecular orbital  
charge densities for the first-row hydrides



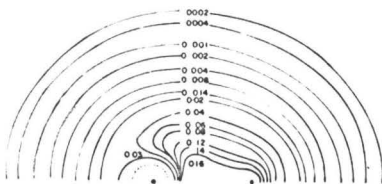
LIH  $2\sigma$



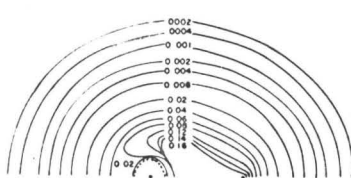
BeH  $2\sigma$



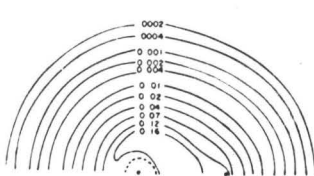
BH  $2\sigma$



CH  $2\sigma$



NH  $2\sigma$

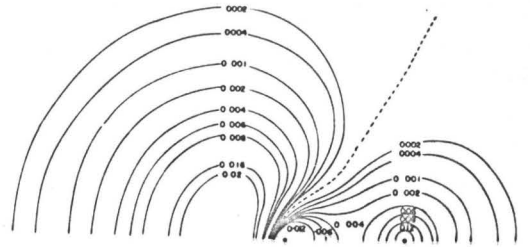


OH  $2\sigma$

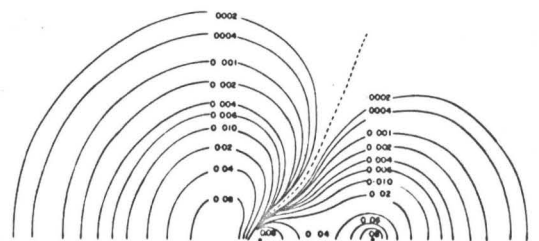


HF  $2\sigma$

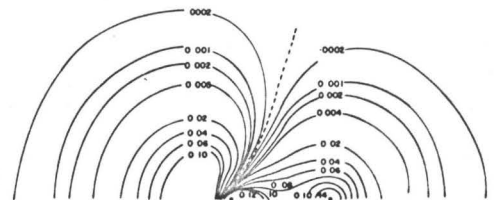
FIG. XX



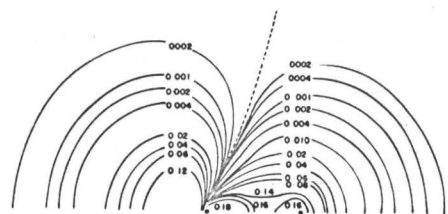
BeH  $3\sigma$



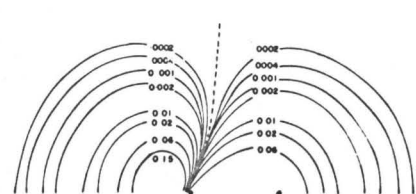
BH  $3\sigma$



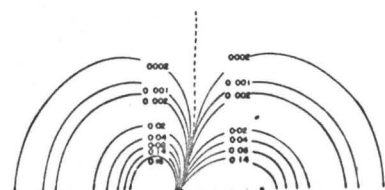
CH  $3\sigma$



NH  $3\sigma$



OH  $3\sigma$

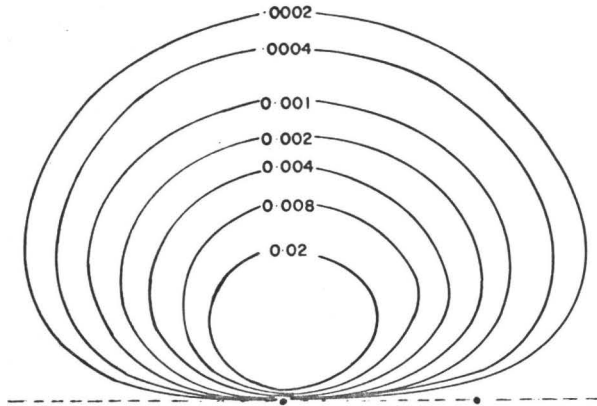


HF  $3\sigma$

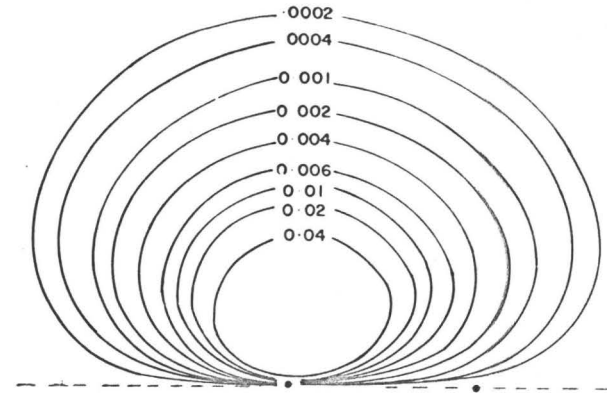
FIG. XXI

FIG. XXII

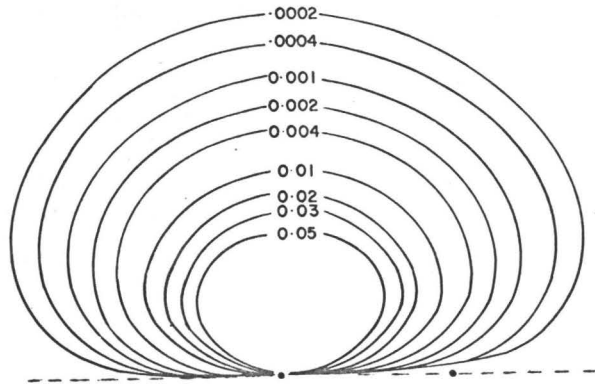
Contour maps of the  $1\pi$  molecular orbital  
charge densities for the first-row hydrides



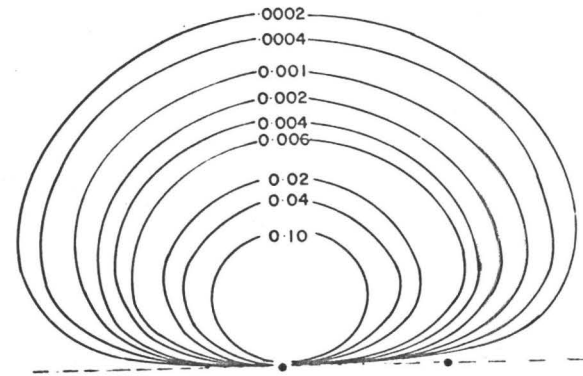
CH  $\pi$



NH  $\pi$



OH  $\pi$



HF  $\pi$

FIG. XXII

TABLE I

	$\phi_{b1}^2$	$\phi_{b2}^2$	$\phi_o^2$	$(\phi_{\ell 1}^2 + \phi_{\ell 2}^2)$	Total Value	True Value	% Error
$F_o$	-0.5752	-0.5752	1.0000	0.5190	0.3686	0.3739	0.5
$F_{\perp}$	0.0309	-0.1111	0.0026	0.1526	0.0750	0.0748	0.3
$F_{\parallel}$	0.3128	0.3745	0.6127	1.1103	2.4103	2.5383	4.7
$DP_E$	0.1085	0.2085	0.0113	1.0691	1.4974	1.4936	0



TABLE II

ranging  $\alpha$  about  $73^\circ$ 

	$\delta$	$\alpha$	$\epsilon b$	$\epsilon l$	$F_O$	$F_{\parallel}$	$F_{\perp}$	DP	$\beta$
1)	0.3882	$77^\circ$	$123.286^\circ$	$51.45^\circ$	0.345	2.441	0.067	0.856	$231^\circ$
2)	0.3882	$73^\circ$	$123.286^\circ$	$50.73^\circ$	0.369	2.410	0.075	0.715	$228^\circ$
3)	0.3882	$69^\circ$	$123.286^\circ$	$50.07^\circ$	0.390	2.370	0.084	0.579	$225^\circ$

contributions to the forces

1)	$\phi_{b1}^2$	$\phi_{b2}^2$	$\phi_{\ell 1}^2$	$\phi_{\ell 2}^2$	$\phi_0^2$	$\lambda$	$\mu$
$F_O$	-0.5990	-0.5990	0.5410	/	1.0025		
$F_{\perp}$	0.0264	-0.1232	0.1611	/	0.0026	0.8157	0.4283
$F_{\parallel}$	0.3224	0.2900	1.1158		0.6125		
DP <sub>E</sub>	0.1184	0.1184	1.1132	/	0.0105		
2) $F_O$	-0.5742	-0.5742	0.5181	/	0.9992		
$F_{\perp}$	0.0311	-0.1106	0.1522	/	0.0027	0.7970	0.4613
$F_{\parallel}$	0.3123	0.3738	1.1100		0.6127		
DP <sub>E</sub>	+0.2123	+0.2123	+1.0672	/	0.0113		
3) $F_O$	-0.5497	-0.5497	0.4948	/	0.9944		
$F_{\perp}$	0.0359	-0.0985	0.1435	/	0.0028	0.7790	0.4922
$F_{\parallel}$	0.3016	0.3586	1.1041		0.6128		
DP <sub>E</sub>	0.3038	0.3038	1.0193	/	0.0121		

TABLE III

ranging  $\delta$  around 0.3882

	$\delta$	$\alpha$	$\epsilon b$	$\epsilon l$	$F_O$	$F_{\perp}$	$F_{\parallel}$	DP	$\beta$
1)	0.3	73.165	123.286	49.418	0.425	0.084	2.379	0.545	223
2)	0.4	73.165	123.286	50.920	0.362	0.074	2.413	0.739	229
3)	0.5	73.165	123.286	52.201	0.318	0.066	2.435	0.872	233

contribution to the forces

	$\phi_{b1}^2$	$\phi_{b2}^2$	$\phi_{\lambda 1}^2$	$\phi_{\lambda 2}^2$	$\phi_0^2$	$\lambda$	$\mu$
1)							
$F_O$	-0.5327	-0.5327	0.4683	/	1.0220	0.7813	0.5012
$F_{\perp}$	0.0336	0.0870	0.1340	/	0.0030		
$F_{\parallel}$	0.3068	0.3619		1.0972	0.6129		
$DP_E$	0.3475	0.3475	0.9646	/	0.0129		
2)							
$F_O$	-0.5795	-0.5795	0.5245	/	0.9963	0.7994	0.4552
$F_{\perp}$	0.0306	-0.1139	0.1546	/	0.0027		
$F_{\parallel}$	0.3133	0.3758		1.1116	0.6126		
$DP_E$	0.1934	0.1934	1.0803	/	0.0111		
3)							
$F_O$	-0.6067	-0.6067	0.5614	/	0.9702	0.8091	0.4197
$F_{\perp}$	0.0284	-0.1343	0.1695	/	0.0025		
$F_{\parallel}$	0.3161	0.3852		1.1208	0.6124		
$DP_E$	0.0898	0.0898	1.1564	/	0.0098		

TABLE IV

ranging  $\epsilon b$  about  $123^\circ$ 

	$\delta$	$\alpha$	$\epsilon b$	$\epsilon l$	$F_O$	$F_\perp$	$F_\parallel$	DP	$\beta$
1)	0.3882	73.165	115.000	+47.88	0.324	0.063	2.440	.876	$215^\circ$
2)	0.3882	73.165	123.000	+50.65	0.366	0.075	2.411	.726	$228^\circ$
3)	0.3882	73.165	131.000	+53.94	0.415	0.089	2.375	.551	$238^\circ$

contribution to the forces

	$\phi_{b1}^2$	$\phi_{b2}^2$	$\phi_{\ell 1}^2$	$\phi_{\ell 2}^2$	$\phi_O^2$	$\lambda$	$\mu$
1)							
$F_O$	-0.5630	-0.5630	0.3904	/	1.0594	0.8000	0.4192
$F_\perp$	0.0397	-0.0883	0.1080	/	0.0033		
$F_\parallel$	0.3844	0.3654	1.076		0.6133		
DP <sub>E</sub>	0.2613	0.2613	0.8041	/	0.0152		
2)							
$F_O$	-0.5754	-0.5754	0.5154	/	1.0017	0.7979	0.4584
$F_\perp$	0.0312	-0.1105	0.1512	/	0.0027		
$F_\parallel$	0.3152	0.3742	1.1093		0.6127		
DP <sub>E</sub>	0.2093	0.2093	1.0615		0.0114		
3)							
$F_O$	-0.5579	-0.5579	0.5990	/	0.9314	0.7958	0.5041
$F_\perp$	0.0239	-0.1237	0.1865	/	0.0022		
$F_\parallel$	0.2496	0.3838	1.1298		0.6122		
DP <sub>E</sub>	0.2123	0.2123	1.2339	/	0.0082		

TABLE V

	$\delta$	$\alpha$	$\epsilon b$	$\epsilon l'$	$\lambda/\mu$	$S_o$	$C_o$	$C_1$	$C_2$	$C_3$	$F_o$	$F_{\perp}$	$F_{\parallel}$	DP	$\Delta E$
1	.1536	103°	63°	46°	1.19	0.056	1.0	0.0	0.0	0.0	.08	.03	2.30	.72	-20.22
2	.2031	97°	63°	44°	1.25	0.056	1.0	0.0	0.0	0.0	.10	.04	2.31	.72	-20.87
3	.2474	91°	64°	41.5°	1.29	0.056	1.0	0.0	0.0	0.0	.11	.04	2.33	.72	-21.75
4	.2037	97°	63°	44°	1.25	0.00	1.0	0.0	0.0	0.0	.28	.04	2.32	.72	-20.89
5	.2483	91°	64°	41.5°	1.29	0.00	1.0	0.0	0.0	0.0	.30	.041	2.33	.72	-21.77
*6	.3882	73° 10'	123°	26°	1.73	0.056	.995	-.044	-.088	-.085	.37	.075	2.41	.72	-27.01

TABLE VI

Calcn No.	$C^l(1s)$	$C^l(2s)$	$C^l(px')$	$C^{l1}(pz)$	$C^l(h_1^O+h_2^O)$	$g$	$C^b(1s)$	$C^b(2s)$	$C^b(px')$	$C^b(py)$	$C^{b1}h_1^O$	$C^{b1}h_2^O$
1	0.0000	0.6326	-0.3161	0.7070	0.0000	0.00	-0.0678	-0.4378	-0.5355	0.3975	0.4599	-.1785
2	0.0355	0.7682	0.0112	0.7070	-0.0737	0.08	-0.0578	-0.0416	-0.6218	0.3975	0.4391	-.1994
3	0.0505	0.7481	0.1884	0.7070	-0.1049	0.24	-0.0452	0.1796	-0.5926	0.3975	0.4130	-.2254
4	0.0598	0.6840	0.3237	0.7070	-0.1241	0.36	-0.0319	0.3521	-0.5309	0.3975	0.3854	-.2530
5	0.0657	0.5821	0.4395	0.7070	-0.1362	0.6	-0.0170	0.5030	-0.4400	0.3975	0.3544	-.2840
6	0.0678	0.4638	0.5219	0.7070	-0.1406	0.92	-0.0028	0.6318	-0.3382	0.3975	0.3251	-.3134

Note:  $C^{l1}_x$  = coefficient preceeding the atomic orbital  $x$  in the lone pair orbital  $\phi_{l1}^O$

$C^{b1}_x$  = coefficient preceeding the atomic orbital  $x$  in the bonding orbital  $\phi_{b1}$

Also,  $C^{b1}h_1^O = C^{b2}h_2^O$ ;  $C^{b1}h_2^O = C^{b2}h_1^O$ ;  $C^{l1}pz = -C^{l2}pz$ ;  $C^{b1}py' = -C^{b2}py'$

TABLE VII

N <sup>o</sup>	g	$\lambda$	$\mu$	$\delta$	$\alpha$	$\epsilon b$	c3	$\lambda'$	$\mu'$	$\epsilon l$	$\beta$	Lone Pair	Bonds
1	0.00	0.7978	0.4599	0.3882	73.1652 <sup>o</sup>	123.2862 <sup>o</sup>	-.0850	1.0000	0.0000	50.76 <sup>o</sup>	228.12	-SP <sup>1.5</sup>	-SP <sup>2.63</sup>
2	0.08	-.7391	0.4391	0.4541	65.1765 <sup>o</sup>	93.2301 <sup>o</sup>	-.0781	1.0043	-.0737	40.10	~178 <sup>o</sup>	SP <sup>0.84</sup>	~ P
3	0.24	0.7286	0.3043	0.5747	69.0265 <sup>o</sup>	71.7375 <sup>o</sup>	-.0563	1.0465	-.1049	44.37 <sup>o</sup>	150.17 <sup>o</sup>	SP <sup>0.94</sup>	~ P
4	0.36	0.7509	0.2854	0.6565	73.6352 <sup>o</sup>	62.0359 <sup>o</sup>	-.0425	1.0357	-.1241	48.67 <sup>o</sup>	130.80 <sup>o</sup>	SP <sup>1.42</sup>	SP <sup>2.5</sup>
5	0.60	0.7775	0.3544	0.8015	84.1867 <sup>o</sup>	49.6887 <sup>o</sup>	-.0218	1.0383	-.1362	55.90 <sup>o</sup>	118.50 <sup>o</sup>	SP <sup>2.02</sup>	SP <sup>1.4</sup>
6	0.92	0.8056	0.3251	0.9639	99.2146 <sup>o</sup>	40.3720 <sup>o</sup>	-.0035	0.9935	-.1406	62.17 <sup>o</sup>	107.11 <sup>o</sup>	SP <sup>3.66</sup>	SP <sup>.65</sup>

TABLE VIII  
PROPERTIES OF THE TOTAL DENSITY DISTRIBUTIONS<sup>a</sup>

AH	$\mu^b$	$R_e$	L	L/ $R_e$	UA	$r_A^c$ Molecule	A	$r_H^c$ Molecule	$\rho(H)^d$	$\rho(A)^d$
LiH	-6.002	3.015	7.7	2.6	3.6	1.7	3.2	2.9	0.3752	13.801
BeH	-0.282	2.538	9.2	3.6	3.4	4.1	3.6	2.6	0.4286	35.050
BH	1.733	2.336	8.7	3.7	3.2	3.8	3.4	2.5	0.4660	71.771
CH	1.570	2.124	7.9	3.7	3.0	3.5	3.2	2.3	0.4705	127.246
NH	1.627	1.961	7.2	3.7	2.9	3.2	3.0	2.1	0.4656	205.633
OH	1.780	1.834	6.7	3.7	2.8	2.9	2.9	2.0	0.4468	311.153
FH	1.942	1.733	6.3	3.6	2.7	2.7	2.8	1.9	0.4217	447.589

<sup>a</sup>Unless otherwise indicated, all quantities are expressed in a.u.; length, 1 a.u. = 0.52917 $\text{\AA}$ ; charge in units of one electronic charge, e; charge density 1 a.u. =  $e/a_0^3 = 67.49e/\text{\AA}^3$

<sup>b</sup> $\mu$  is in Debye units

<sup>c</sup> $r_A$  and  $r_H$  for the molecule are defined in Fig. XII. In the united atom (U.A.) and the free atom A  $r_A$  gives the radius of the 0.002 density contour.

<sup>d</sup>Charge density at the proton and the A nucleus. In the atom  $\rho(H) = 0.3183$  a.u.

TABLE IX

	<u>Non-Bonded Charge on A</u>		<u>Charge in the Overlap Region</u>		<u>Non-Bonded Charge on B</u>	
	<u>Mol.</u>	<u>Atom</u>	<u>Mol.</u>	<u>Atoms</u>	<u>Mol.</u>	<u>Atom</u>
LiH	1.09	1.50	2.20	1.95	0.71	0.55
BeH	1.96	2.00	2.42	2.43	0.62	0.57
BH	2.75	2.52	2.69	2.86	0.56	0.62
CH	3.21	3.02	3.30	3.40	0.49	0.58
NH	3.71	3.52	3.87	3.92	0.42	0.56
OH	4.22	4.04	4.41	4.41	0.36	0.55
FH	4.72	4.54	4.98	4.92	0.30	0.54



TABLE X

TOTAL CHARGE MIGRATION IN DIATOMIC HYDRIDES AS  
DETERMINED BY DENSITY DIFFERENCE MAPS<sup>a</sup>

AH	Charge increase	Charge increase
	in Region A	in Region B
	$\Delta A$	$\Delta B$
LiH	0.01	0.55
BeH	0.11	0.35
BH	0.20	0.16
CH	0.20	0.16
NH	0.20	0.16
OH	0.22	0.19
FH	0.24	0.22

<sup>a</sup>These figures were obtained by numerical integration using a grid of 0.02 a.u. Regions A and B are defined in Fig. XVI.

TABLE XI

Molecule	UA Coefficients					UA
	1s	2s	2p $\sigma$	2p $\pi$	2p $\pi$	
LiH( $^1\Sigma^+$ )	2	2	0	0	0	Be( $^1S$ )
BeH( $^2\Sigma^+$ )	2	2	1	0	0	B( $^2P$ )
BH( $^1\Sigma^+$ )	2	2	4/3	1/3	1/3	C( $^1D$ )
CH( $^2\Pi_r$ )	2	2	1	1	1	N( $^2D$ )
NH( $^3\Sigma^-$ )	2	2	2	1	1	O( $^3P$ )
OH( $^2\Pi_r$ )	2	2	2	3/2	3/2	F( $^2P$ )
FH( $^1\Sigma^+$ )	2	2	2	2	2	Ne( $^1S$ )

TABLE XII

PARTIAL FORCES AND THEIR CONTRIBUTIONS FOR THE  $1\sigma$  DENSITY

AH	Forces on the Proton					Forces on the A Nuclei				
	$f_{1\sigma H}(R_e)$	Atomic	Overlap	Screening	$f_{1\sigma H}(\infty)$	$f_{1\sigma A}(R_e)$	Atomic	Overlap	Screening	$f_{1\sigma A}(\infty)$
LiH	1.949	0.000	0.007	1.942	2	-0.489	-0.506	0.017	0.000	0
BeH	2.000	0.000	0.003	1.997	2	-0.127	-0.135	0.008	0.000	0
BH	2.002	0.000	0.002	2.000	2	0.244	0.238	0.006	0.000	0
CH	2.001	0.000	0.001	2.000	2	0.262	0.258	0.004	0.000	0
NH	2.001	0.000	0.001	2.000	2	0.256	0.254	0.002	0.000	0
OH	2.000	0.000	0.000	2.000	2	0.247	0.245	0.002	0.000	0
FH	2.000	0.000	0.000	2.000	2	0.227	0.226	0.001	0.000	0

TABLE XIII

A	<sup>a</sup> $\epsilon A1s$	$\epsilon A2s$	$\epsilon A2p$
Li	-2.48	-0.20	
Be	-4.73	-0.31	
B	-7.70	-0.49	-0.31
C	-11.33	-0.71	-0.43
N	-15.65	-0.95	-0.58
O	-20.67	-1.24	-0.63
F	-26.38	-1.57	-0.73

a All the energies are in atomic units, (1 a.u. = 28.2 eV);

$$\epsilon H1s = -0.50$$

TABLE XIV  
PARTIAL FORCES AND THEIR CONTRIBUTIONS  
FOR THE  $2\sigma$  DENSITY

AH	Forces on the Proton					Forces on the A Nuclei				
	$f_{2\sigma H}(R_e)$	Atomic	Overlap	Screening	$f_{2\sigma H}(\infty)$	$f_{2\sigma A}(R_e)$	Atomic	Overlap	Screening	$f_{2\sigma A}(\infty)$
LiH	1.075	0.225	0.566	0.284	1	1.495	-0.110	0.715	0.890	1
BeH	1.699	0.279	0.929	0.491	2	1.624	-0.022	0.971	0.675	0
BH	2.280	0.242	1.082	0.956	2	1.607	0.234	0.959	0.414	0
CH	2.397	0.119	0.780	1.498	2	1.367	0.564	0.654	0.149	0
NH	2.366	0.064	0.533	1.769	2	1.109	0.623	0.423	0.063	0
OH	2.315	0.040	0.381	1.894	2	0.904	0.581	0.292	0.031	0
FH	2.259	0.027	0.281	1.951	2	0.753	0.520	0.215	0.018	0

TABLE XV

PARTIAL FORCES AND THEIR CONTRIBUTIONS FOR THE3 $\sigma$  AND 1 $\pi$  DENSITIES

AH	Forces on the Proton					Forces on the A Nuclei				
	$f_{3\sigma H}(R_e)$	Atomic	Overlap	Screening	$f_{3\sigma H}(\infty)$	$f_{3\sigma A}(R_e)$	Atomic	Overlap	Screening	$f_{3\sigma A}(\infty)$
BeH	0.313	0.000	-0.007	0.320	0	-0.514	-0.605	0.065	0.026	1
BH	0.762	0.041	0.013	0.708	1	-0.817	-1.384	0.385	0.182	1
CH	1.058	0.058	0.207	0.793	1	-0.668	-1.465	0.606	0.191	1
NH	1.370	0.068	0.363	0.939	1	-0.485	-1.489	0.809	0.195	1
OH	1.681	0.068	0.472	1.141	1	-0.346	-1.430	0.915	0.169	1
FH	1.920	0.065	0.521	1.334	1	-0.250	-1.346	0.955	0.141	1
	$f_{1\pi H}(R_e)$	Atomic	Overlap	Screening	$f_{1\pi H}(\infty)$	$f_{1\pi A}(R_e)$	Atomic	Overlap	Screening	$f_{1\pi A}(\infty)$
CH	0.608	0.000	0.019	0.589	1.00	0.079	0.059	0.019	0.001	0
NH	1.335	0.001	0.043	1.291	1.00	0.158	0.116	0.041	0.001	0
OH	2.086	0.001	0.044	2.041	3.00	0.226	0.180	0.045	0.001	0
FH	2.902	0.001	0.062	2.839	4.00	0.295	0.231	0.062	0.002	0

TABLE XVI

TOTAL ATOMIC OVERLAP AND SCREENINGCONTRIBUTIONS FOR AH

Forces on the Proton

AH	$\Sigma_{i f_{iH}}^{(HH)}$	$\Sigma_{i f_{iH}}^{(AH)}$	$\Sigma_{i f_{iH}}^{(AA)}$	$Z_A - \Sigma_{i f_{iH}}^{(AA)}$	$F_H^a$
LiH	0.225	0.573	2.226	0.774	-0.003
BeH	0.279	0.925	2.808	1.192	-0.002
BH	0.283	1.097	3.664	1.336	-0.008
CH	0.177	1.007	4.880	1.120	-0.014
NH	0.133	0.940	5.999	1.001	-0.019
OH	0.109	0.897	7.076	0.924	-0.024
FH	0.093	0.864	8.124	0.876	-0.026

Forces on the A Nuclei

AH	$\Sigma_{i f_{iA}}^{(AA)}$	$\Sigma_{i f_{iA}}^{(AH)}$	$\Sigma_{i f_{iA}}^{(HH)}$	$Z_H - \Sigma_{i f_{iA}}^{(HH)}$	$F_A^a$
LiH	-0.616	0.732	0.890	0.110	-0.002
BeH	-0.762	1.044	0.701	0.299	0.010
BH	-0.912	1.350	0.596	0.404	-0.031
CH	-0.584	1.283	0.341	0.659	-0.053
NH	-0.496	1.275	0.259	0.741	-0.069
OH	-0.424	1.254	0.201	0.799	-0.074
FH	-0.369	1.233	0.161	0.839	-0.075

<sup>a</sup>Forces are expressed in a.u., 1a.u. =

$$e^2 / a_0^2 = 8.2378 \times 10^{-3} \text{ dyn.}$$

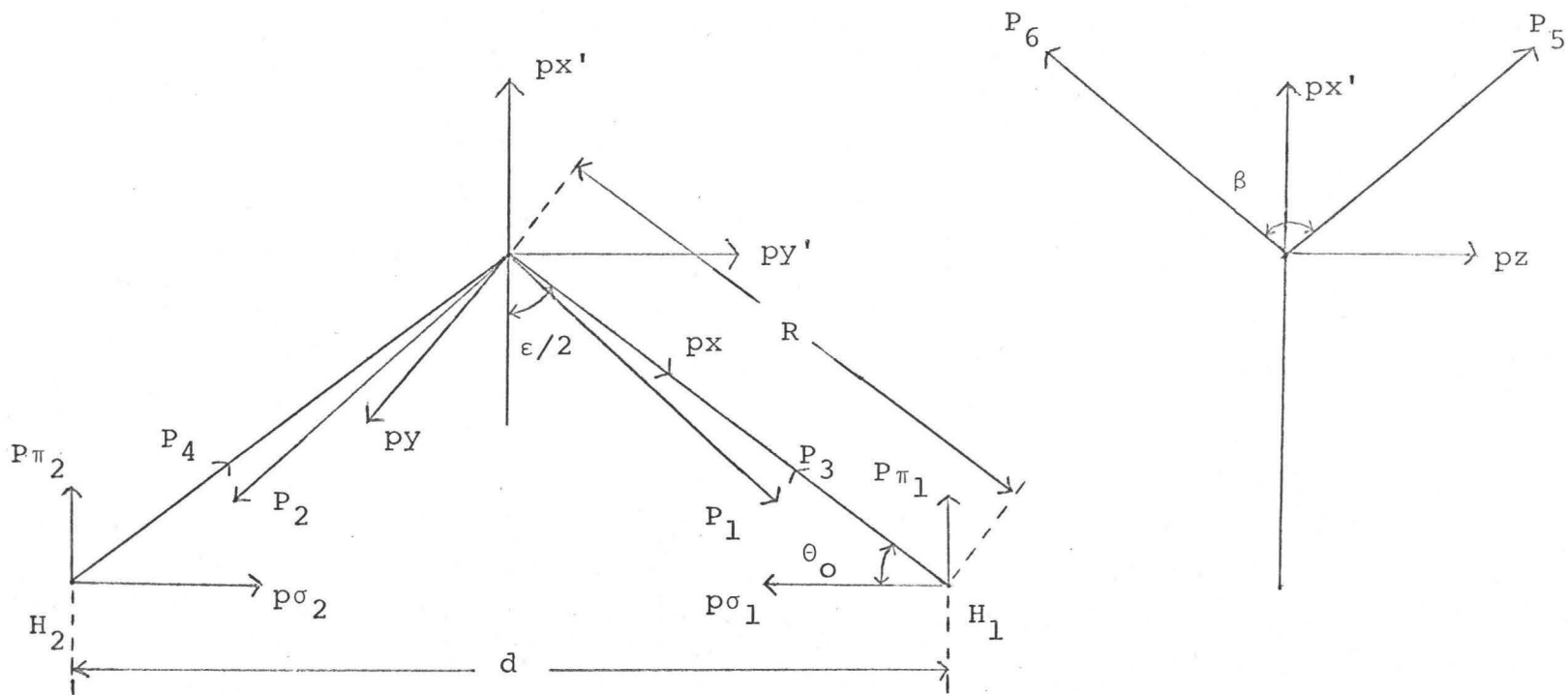
TABLE XVII  
FORCE CONTRIBUTIONS IN LiH AND LiF AS DETERMINED  
BY THE DENSITY DIFFERENCE MAPS

	Charge equivalents of the force exerted by <sup>a</sup>	
	density localized on H or F	density localized on Li
Force on H	0.80	2.23
Force on F	1.05	2.04
Ideal ionic binding	1.00	2.00 ( $=Z_{\text{Li}}-1$ )
Force on Li(LiH)	1.62	-0.62
Force on Li(LiF)	9.86	-0.71
Ideal ionic binding	LiH 2.00 ( $=Z_{\text{H}}+1$ )	-1.00
	LiF 10.00 ( $=Z_{\text{F}}+1$ )	

<sup>a</sup>The charge density localized on F or H exerts atomic force on F or H and a screening force on Li. Similarly the charge density localized on Li exerts an atomic force on Li and a screening force on F or H.



A P P E N D I X



$$R = 1.81 \text{ a.u.} \quad \theta_0 = 37.775^\circ$$

$$\epsilon = 104.45^\circ \quad d = 2.2179 \text{ a.u.}$$

Appendix 1Force equations

In these and the ensuing equations, it is found convenient to make the following identities

$$\begin{array}{lll}
 \cos(\epsilon b) & \equiv & \text{CEB} \\
 \sin(\epsilon b) & \equiv & \text{SEB} \\
 \cos(\alpha) & \equiv & \text{CA} \\
 \sin(\alpha) & \equiv & \text{SA} \\
 \sin(\epsilon/2) & \equiv & \text{SE2} \\
 \cos(\beta) & \equiv & \text{CB} \\
 \cos(\omega) & \equiv & \text{CW} \\
 \sin(\omega) & \equiv & \text{SW} \\
 \cos(\alpha/2) & \equiv & \text{CA2} \\
 \sin(\alpha/2) & \equiv & \text{SA2} \\
 \cos(\epsilon/2) & \equiv & \text{CE2} \\
 \cos(\beta/2) & \equiv & \text{CB2} \\
 \cos(t) & \equiv & \text{CT} \\
 \sin(t) & \equiv & \text{ST} \\
 \cos(\epsilon l') & \equiv & \text{CEL} \\
 \sin(\epsilon l') & \equiv & \text{SEL} \\
 \tan(\epsilon l') & \equiv & \text{TEL}
 \end{array}$$

and also

$$\langle \chi_A^{\hat{O}_A} \chi_A \rangle \equiv A(\chi_A \chi_A) \qquad \langle \chi_A^{\hat{O}_A} \chi_B \rangle \equiv O(\chi_A \chi_B)$$

$$\langle \chi_B^{\hat{O}_A} \chi_B \rangle \equiv P(\chi_B \chi_B) \qquad \langle \chi_B^{\hat{O}_A} \chi_C \rangle \equiv T(\chi_B \chi_C)$$

Where, for example,  $O(\chi_A \chi_B)$  is taken to represent the force on nucleus A due to the overlap density  $(\chi_A \chi_B)$ . Dependant on the nature of the operator  $\hat{O}_A$  this could be a force along the bond direction or perpendicular to the bond axis. For the forces F and F only  $H_1$  will be considered.

Force parallel

$$\begin{aligned}
 F(\phi_{D1}^2) = & \lambda^2 [\text{CEB}^2 P(2s2s) + \text{SEB}^2 \text{CW}^2 P(\text{pxpx}) + \text{SEB}^2 \text{SW}^2 P(\text{pypy}) + C_3^2 P(1s1s) \\
 & + 2\text{SEB} \cdot \text{CEB} \cdot \text{CW} \cdot P(2\text{spx}) + 2C_3 \text{CEB} \cdot P(1s2s) + 2C_3 \text{SEB} \cdot \text{CW} \cdot P(1\text{spx})] \\
 & + 2\lambda\mu [\text{CEB} \cdot o(h_1^o 2s) + \text{SEB} \cdot \text{CW} \cdot o(h_1^o \text{px}) + C_3 o(h_1^o s) + C_4 \text{CEB} \cdot o(p_3^o 2s) \\
 & + C_4 \text{SEB} \cdot o(p_3^o p_1) + C_3 C_4 o(p_3^o 2s) - \delta \{ \text{CEB} \cdot T(h_2^o 2s) + \text{SEB} \cdot \text{CW} \cdot T(h_2^o \text{px}) \\
 & + C_3 T(h_2^o 1s) + \text{SEB} \cdot \text{SW} \cdot T(h_2^o \text{py}) \}] + \mu^2 [\delta^2 P^a (h_2^o h_2^o) - 2\delta o^a (h_1^o h_2^o) \\
 & + A(h_1^o h_1^o) + 2C_4 A(h_1^o p_3^o) - 2C_4 \delta d (h_2^o p_3^o)
 \end{aligned}$$

---

<sup>a</sup>The prime signifies that the parallel component has been taken.

$$\begin{aligned}
F(\phi_{b2}^2) = & \lambda^2 [CEB^2P(2s2s) + SEB^2CT^2P(pxpx) + SEB^2ST^2P(pypy) + C_3^2P(1s1s) \\
& + 2SEB.CEB.CT.P(2spx) + 2C_3CEB.P(1s2s) + 2C_3SEB.CT.P(1s2s) \\
& + 2\lambda\mu [CEB.T(h_2^02s) + SEB.CT.T(h_2^0px) + SEB.ST.T(h_2^0py) + C_3T(h_2^01s) \\
& + C_4CEB.T(2sp_4^0) + C_4SEB.T(p_2p_4^0) + C_3C_4T(1sp_4^0) - \delta\{CEB.o(h_1^02s) \\
& + SEB.CT.o(h_1^0px) + C_3o(h_1^01s)\}] + \mu^2 [P'(h_2^0h_2^0) - 2\delta o'(h_1^0h_2^0) \\
& + \delta^2A(h_1^0h_1^0) + 2C_4A(h_1^0p_3^0) - 2C_4\delta o'(h_2^0p_3^0)]
\end{aligned}$$

$$\begin{aligned}
F(\phi'^2) = & CEL^2P(2s2s) + SEL^2SE2^2P(pypy) + SEL^2CE2^2P(pxpx) \\
& - 2CEL.SEL.CE2P(2spx)
\end{aligned}$$

$$F(\phi'^2) = P(pzpz)$$

$$\begin{aligned}
F(\phi_0^2) = & C_0^2P(1s1s) + C_1^2P(2s2s) + C_2^2CE2^2(pxpx) + C_2^2SE2^2P(pypy) \\
& + 2C_0C_1P(1s2s) - 2C_0C_2CE2^2P(1spx) - 2C_1C_2CE2^2P(2spx)
\end{aligned}$$

### Force Perpendicular

$$\begin{aligned}
F(\phi_{b1}^2) = & \lambda^2 [2SEB.SW.CEB.P(2spy) + 2SEB^2CW.SWP(pxpy) + 2C_3SEB.SW.P(1spy)] \\
& + 2\lambda\mu [SEB.SW.o(h_1^0py) + C_4SEB.o(p_1p_3^0) - \delta\{CEB.T(h_2^02s) + SEB.CW.T(h_2^0px) \\
& + SEB.SW.T(h_2^0py) + C_3T(h_2^01s)\}] + \mu^2 [\delta^2P''(h_2^0h_2^0)^a - 2\delta o''(h_1^0h_2^0) \\
& - 2C_4\delta o''(h_2^0p_3^0)]
\end{aligned}$$

$$\begin{aligned}
F(\phi_{b2}^2) = & \lambda^2 [2SEB.CEB.ST.P(2spy) + 2SEB^2ST.CT.P(pxpy) + 2C_3SEB.ST.P(1spy)] \\
& + 2\lambda\mu [CEB.T(h_2^02s) - SEB.CT.T(h_2^0px) + SEB.ST.T(h_2^0py) + C_3T(h_2^01s) \\
& + C_4CEB.T(2sp_4^0) + C_4SEB.T(p_2p_4^0) + C_3C_4T(1sp_4^0) - \delta\{CEB.T(h_2^02s) \\
& + SEB.CW.T(h_2^0px) + SEB.SW.T(h_2^0py) + C_3T(h_2^01s)\}] + \mu^2 [\delta^2P''(h_2^0h_2^0) \\
& - 2\delta o''(h_1^0h_2^0) + C_4^2P''(p_4^0p_4^0) + 2C_4P''(h_2^0p_4^0) - 2\delta C_4o''(h_1^0p_4^0)]
\end{aligned}$$

$$F(\phi'^2) = 2SEL^2SE2.CE2.P(pxpy) - 2CEL.SEL.SE2.P(2spy)$$

$$F(\phi_0^2) = 2C_2^2SE2.CE2.P(pxpy) - 2C_0C_2SE2.P(1spy) - 2C_1C_2SE2.P(2spy)$$

### Force on oxygen

$$F_O(\phi_{b1}^2) = F_O(\phi_{b2}^2) = \lambda^2 [2SEB.CEB.SW.A(2spx) + 2SEB.CEB.SW.A(2spy)]$$

<sup>a</sup>the double prime signifies the perpendicular component

$$\begin{aligned}
& +2C_3 \text{SEB.CW.A}(1\text{spx}) + 2C_3 \text{SEB.SW.A}(1\text{spx}) + 2\lambda\mu [\text{CEB.o}(2\text{sh}_1^\circ) \\
& + \text{SEB.CW.o}(p_x h_1^\circ) + \text{SEB.SW.o}(p_y h_1^\circ) + C_3 \text{o}(1\text{sh}_1^\circ) + C_4 \text{SEB.T}(2\text{sp}_4^\circ) \\
& + C_4 \text{SEB.T}(p_2 p_4^\circ) + C_3 C_4 \text{T}(1\text{sp}_4^\circ) - \delta \{ \text{CEB.o}(2\text{sh}_2^\circ) + \text{SEB.CW.o}(p_x h_2^\circ) \\
& + \text{SEB.SW.o}(p_y h_2^\circ) + C_3 \text{o}(1\text{sh}_2^\circ) \} ] + \mu^2 [ P(h_1^\circ h_1^\circ) + P(h_2^\circ h_2^\circ) \\
& - 2\delta T(h_1^\circ h_2^\circ) + C_4^2 P(p_3^\circ p_3^\circ) + 2C_4 P(h_1^\circ p_3^\circ) - 2C_4 \delta T(h_2^\circ p_3^\circ)
\end{aligned}$$

$$F_{\text{O}}(\phi_{\ell}^2) = -2\text{CEL.SEL.SE2.A}(2\text{spx}) - 2\text{SEL.CEL.CE2.A}(2\text{spx})$$

$$\begin{aligned}
F_{\text{O}}(\phi_{\text{O}}^2) = & -2C_{\text{O}}C_2 \text{CE A}(1\text{spx}) - 2C_{\text{O}}C_2 \text{SE2.A}(1\text{spx}) - 2C_1 C_2 \text{CE2.A}(2\text{spx}) \\
& - 2C_1 C_2 \text{SE2.A}(2\text{spx})
\end{aligned}$$

### Dipole moment

Here the integrals involved fall into one of two categories dependant on the nature of the dipole moment operator  $D_A$ , where A refers to the oxygen nucleus. For a dipole moment measured along the bond axis  $D_A = r_A \cos\theta_A$  and for one measured perpendicular to the bond axis  $D_A = r_A \sin\theta_A \sin\phi$ . If the symbol  $D(\chi_i \chi_j)$  is taken to represent the integral  $\langle \chi_i D_A \chi_j \rangle$  then

$$\begin{aligned}
\text{DP}_{\text{E}}(\phi_{b1}^2) = \text{DP}_{\text{E}}(\phi_{b2}^2) = & \lambda^2 [ 2\text{SEB.CEB.CW.D}(2\text{spx}) + 2\text{SEB.SW.CEB.o}(2\text{spx}) \\
& + 2C_3 \text{SEB.CW.D}(1\text{spx}) + 2C_3 \text{SEB.SW.D}(1\text{spx}) + 2\lambda\mu [ \text{EB.D}(2\text{sh}_1^\circ) \\
& + \text{SEB.CW.D}(p_x h_1^\circ) + \text{SEB.SW.D}(p_y h_1^\circ) + C_3 \text{D}(h_1^\circ 1\text{s}) + C_4 \text{CEB.D}(2\text{sp}_3^\circ) \\
& + C_4 \text{SEB.D}(p_1 p_3^\circ) + C_3 C_4 \text{D}(1\text{sp}_3^\circ) - \delta \{ \text{CEB.D}(2\text{sh}_2^\circ) + \text{SEB.CW.D}(p_x h_2^\circ) \\
& + \text{SEB.SW.D}(p_y h_2^\circ) + C_3 \text{D}(1\text{sh}_2^\circ) \} ] + \mu^2 [ \text{D}(h_1^\circ h_1^\circ) + \delta^2 \text{D}(h_2^\circ h_2^\circ) \\
& + 2\delta \text{D}(h_1^\circ h_2^\circ) + C_4^2 \text{D}(p_3^\circ p_3^\circ) + 2C_4 \text{D}(p_3^\circ h_1^\circ) - 2C_4 \delta \text{D}(h_2^\circ p_3^\circ) ]
\end{aligned}$$

$$\text{DP}_{\text{E}}(\phi_{\ell}^2) = -2\text{CEL.SEL.SE2.D}(2\text{spx}) - 2\text{SEL.CEL.CE2.D}(2\text{spx})$$

$$\begin{aligned}
\text{DP}_{\text{E}}(\phi_{\text{O}}^2) = & -2C_{\text{O}}C_2 \text{CE2.D}(1\text{spx}) - 2C_{\text{O}}C_2 \text{SE2.D}(1\text{spx}) - 2C_1 C_2 \text{CE2.D}(2\text{spx}) \\
& - 2C_1 C_2 \text{SE2.D}(2\text{spx})
\end{aligned}$$

## Appendix 2

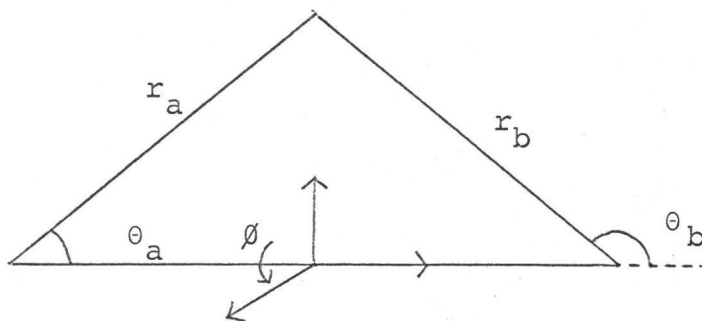
A number of one-, two- and three-centre integrals appear in both the force and dipole moment equations. The one-centre integrals, defined as being  $\langle \chi_A^0 \chi_A^1 \rangle^a$ , can readily be solved by ordinary calculus techniques. The two- and three-centre integrals are, however a little more complicated and were solved as follows.

### Two-centre integrals

These integrals,  $\langle \chi_B^0 \chi_C \rangle$ , can in general be written in the form

$$FKMN(AL, BE) = \int_{-1}^1 \int_{-1}^1 \frac{(\lambda^2 - 1)}{(\lambda + \mu)^{K+1}} \lambda^M \mu^N e^{-AL\lambda} e^{-BE\mu} d\lambda d\mu$$

Here AL and BE are respectively equal to  $(\alpha + \beta)R/2$  and  $(\alpha - \beta)R/2$  where  $\alpha$  and  $\beta$  refer to the two screening coefficients of the atomic orbitals  $\chi_A$  and  $\chi_B$  centred on the nuclei A and B respectively which are a distance R apart. In prolate spheroidal coordinates, namely



then

$$\begin{aligned} \lambda &= (r_a + r_b)/R \\ \mu &= (r_a - r_b)/R \\ \phi &= \phi \end{aligned}$$

---

<sup>a</sup> $\chi_A$  and  $\chi_A^1$  refer to atomic orbitals centred on A and  $\hat{o}_A$  is the operator on centre A.

thus

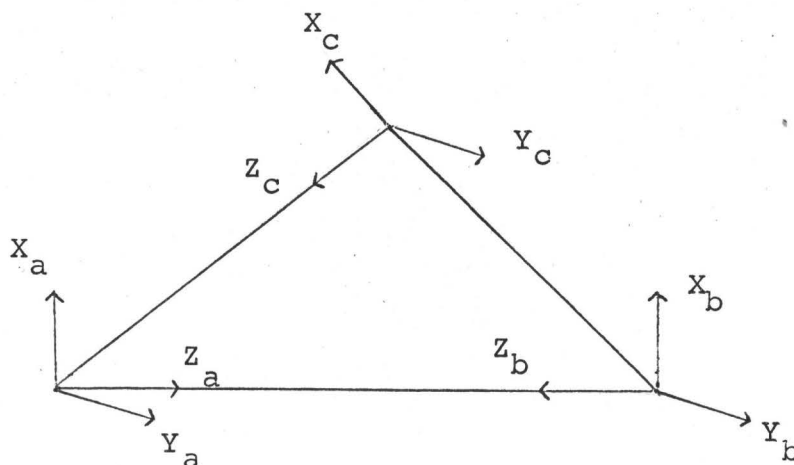
$$\begin{aligned}
 r_a &= (\lambda + \mu)R/2 & r_b &= (\lambda - \mu)R/2 \\
 \cos\theta_a &= (1 + \lambda\mu)/(\lambda + \mu) & \sin\theta_a &= \{(\lambda^2 - 1)(1 - \mu^2)\}^{1/2}/(\lambda + \mu) \\
 \cos\theta_b &= -(1 - \lambda\mu)/(\lambda - \mu) & \sin\theta_b &= \{(\lambda^2 - 1)(1 - \mu^2)\}^{1/2}/(\lambda - \mu) \\
 x &= r_a \sin\theta_a \cos\phi = R/2 \{(\lambda^2 - 1)(1 - \mu^2)\}^{1/2} \cos\phi \\
 y &= r_a \sin\theta_a \sin\phi = R/2 \{(\lambda^2 - 1)(1 - \mu^2)\}^{1/2} \sin\phi \\
 z &= r_a \cos\theta_a = \frac{R}{2} \lambda \mu
 \end{aligned}$$

The method of solving the integrals defined by  $FKMN/(AL, BE)$  has been given by Kotani (71) and it is his approach that will be used in the present work.

### Three-centre integrals

A program enabling such integrals to be calculated was made available to us by "Quantum Chemistry Exchange Programme (92)".

The coordinate system used in this program is



where all the three Y axes are at right angles to the plane of the paper. Thus, for example, the force on nucleus A in the  $X_a$  direction due to the overlap density  $(\chi_i^B \chi_j^C)$ , where  $\chi_i^B$  and  $\chi_j^C$  are atomic

orbitals centred on B and C respectively will be  $\langle x_j^C \frac{x_a}{r_a^3} x_i^B \rangle$ .



## APPENDIX 3

Atomic orbitals on the oxygen

The 1s, 2s and 2p atomic orbitals on the oxygen atom have been represented by accurate analytical self-consistent field atomic functions as calculated by Clementi et al (34). These are of the form

$$1s = C_1 1s_1 + C_2 1s_2 + C_3 2s_3 + C_4 2s_4 + C_5 2s_5 + C_6 2s_6$$

$$2s = C_{11} 1s_1 + C_{22} 1s_2 + C_{33} 2s_3 + C_{44} 2s_4 + C_{55} 2s_5 + C_{66} 2s_6$$

$$2p = C_7 2p_7 + C_8 2p_8 + C_9 2p_9 + C_{10} 2p_{10}$$

where

$$1s_i = \frac{\alpha_i^{3/2}}{\sqrt{\pi}} e^{-\alpha_i r}$$

$$i = 1, 2$$

$$2s_i = r \frac{\alpha_i^{5/2}}{\sqrt{3\pi}} e^{-\alpha_i r}$$

$$i = 3, 4, 5, 6$$

$$2p_{x_i} = r \cos\theta \frac{\alpha_i^{5/2}}{\sqrt{\pi}} e^{-\alpha_i r}$$

$$i = 7, 8, 9, 10$$

$$2p_{y_i} = r \sin\theta \sin\phi \frac{\alpha_i^{5/2}}{\sqrt{\pi}} e^{-\alpha_i r}$$

$$i = 7, 8, 9, 10$$

and

i	7.616	13.3243	1.7582	2.5627	4.2832	5.9445	1.1536	1.7960
$\alpha_i$	1	2	3	4	5	6	7	8

i	3.4379	7.907
$\alpha_i$	9	10

$C_1$	$C_2$	$C_3$	$C_4$	$C_5$	$C_6$
0.93850	0.03825	-0.00097	0.00439	-0.00829	0.04171

$C_{11}$	$C_{22}$	$C_{33}$	$C_{44}$	$C_{55}$	$C_{66}$
-0.21979	-0.00573	0.42123	0.54368	0.23061	-0.17856
$C_7$	$C_8$	$C_9$	$C_{10}$		
0.16371	0.57600	0.33920	0.01495		

### Atomic orbitals on the hydrogen

The 1s atomic orbital on the hydrogen has been given the symbol  $h_i$  ( $i = 1, 2$ ). When this orbital is made orthogonal to the 1s atomic function on oxygen there is a superscript zero such that  $h_i^0 = (1 - S_O^2)^{-1/2} (h_i - S_O(1s)) = N_O (h_i - S_O(1s))$

where

$$N_O = (1 - S_O^2)^{-1/2} \quad \text{and} \quad S_O = \langle h_i | 1s \rangle$$

Similarly for the  $p_i$  atomic orbital on hydrogen ( $i = 3, 4$ )

$$p_i = (1 - S_1^2)^{-1/2} (p_i - S_1(1s)) = N_1 (2p_i - S_1(1s))$$

where

$$N_1 = (1 - S_1^2)^{-1/2} \quad \text{and} \quad S_1 = \langle p_i | 1s \rangle$$

Appendix 4Overlap Integrals

An overlap integral is defined as being  $\langle \chi_i \chi_j \rangle$  and is given the symbol  $S(\chi_i \chi_j)$ . Assuming  $\chi_i$  to have a screening coefficient  $\alpha$  and  $\chi_j$  to have a screening coefficient  $\beta$  then

$$S(h_{1s}) = S_0 = R^{3\alpha} \frac{\beta^{3/2}}{4} (F030 - F012 + F021 - F003)$$

$$S(h_{12s}) = R^{4\alpha} \frac{\beta^{5/2}}{8\sqrt{3}} (F040 - 2F022 + F004)$$

$$S(h_{1px}) = R^{4\alpha} \frac{\beta^{5/2}}{8} (F030 - F012 + F021 - F003 - F041 + F023 - F032 + F014)$$

$$S(1sp_3) = R^{4\alpha} \frac{\beta^{5/2}}{8} \{F030 + F021 - F012 - F041 - F032 + F023 + F014\}$$

$$S(2sp_3) = R^{5\alpha} \frac{\beta^{5/2}}{16\sqrt{3}} (F040 - 2F031 - 2F013 - F004 - F051 - 2F042 + 2F024 + F015)$$

$$S(pxp_3) = R^{5\alpha} \frac{\beta^{5/2}}{16} (F030 + F021 - F012 - F003 - F052 - F043 + F034 - F025)$$

When  $\alpha$  equals  $\beta$  then it is found more convenient to solve the integrals by a method developed by Coulson. Thus if  $t = \alpha d$

$$S(P\pi_1 P\pi_2) = -(1+t+t^2/5 - 2t^3/15 - t^4/15)e^{-t}$$

$$S(P\sigma_1 P\sigma_2) = (1+t+2t^2/5 + t^3/15)e^{-t}$$

Force integrals

These integrals fall into one of four categories; atomic, screening, overlap and three-centre integrals. If  $\sigma_A$  is taken to represent the appropriate force operator on centre A and the following identities are made

$$A(\chi_i \chi_j) = \langle \sigma_A \chi_i^A(\alpha) \chi_j^A(\beta) \rangle$$

$$P(x_i x_j) \equiv \langle \phi_A x_i^B(\alpha) x_j^B(\beta) \rangle$$

$$O(x_i x_j) \equiv \langle \phi_A x_i^A(\alpha) x_j^B(\beta) \rangle$$

$$T(x_i x_j) \equiv \langle \phi_A x_i^B(\alpha) x_j^C(\beta) \rangle$$

where, for example,  $x_i^A(\alpha)$  refers to an atomic orbital centred on A with a screening coefficient  $\alpha$ . The force integrals appearing in  $F_{\parallel}$ ,  $F_{\perp}$  and  $F_0$  will thus be

Force parallel<sup>a</sup>

$$A(h_1 p_3) = 4 \frac{\alpha^{5/2} \beta^{3/2}}{3(\alpha + \beta)^2}$$

$$P(2s2s) = R^3 \frac{\alpha^{5/2} \beta^{5/2}}{12} (3F_{121} - F_{130} + F_{103} + 3F_{112} + F_{040} + 3F_{031} + 3F_{022} - F_{013})$$

$$P(pxpx) = R^3 \frac{\alpha^{5/2} \beta^{5/2}}{4} (F_{101} - F_{110} + F_{020} - F_{011} - 2F_{112} + 2F_{121} - 2F_{031} + 2F_{022} + F_{123} - F_{132} + F_{042} - F_{033})$$

$$P(pypy) = R^3 \frac{\alpha^{5/2} \beta^{5/2}}{8} (F_{110} + F_{121} - F_{101} - 2F_{112} - F_{123} + F_{103} + F_{114})$$

$$P(1s1s) = R^3 \frac{\alpha^{3/2} \beta^{3/2}}{1} (F_{101} - F_{110} + F_{020} - F_{011})$$

$$P(2sp_x) = R^3 \frac{\alpha^{5/2} \beta^{5/2}}{4\sqrt{3}} (2F_{111} - F_{030} - 2F_{021} - 2F_{122} + F_{131} - F_{041} - F_{120} + 2F_{032} - F_{102} + F_{012} + F_{113} - F_{023})$$

$$P(1s2s) = R^2 \frac{\alpha^{3/2} \beta^{5/2}}{2\sqrt{3}} (2F_{111} - F_{120} + F_{030} - 2F_{021} - F_{102} + F_{012})$$

$$P(1sp_x) = R^2 \frac{\alpha^{3/2} \beta^{5/2}}{1} (F_{101} - F_{110} + F_{020} - F_{011} - F_{112} + F_{121} - F_{031} + F_{022})$$

$$P'(h_2 h_2) = d \frac{\alpha^{3/2} \beta^{3/2}}{1} (F_{101} - F_{110} + F_{020} - F_{011}) \cos \theta_0$$

$$P(p\sigma_2 h_2) = d^2 \frac{\beta^{3/2} \alpha^{5/2}}{2} (F_{101} - F_{110} + F_{020} - F_{011} - F_{112} + F_{121} - F_{031} + F_{022})$$

$$P(h_2 p\pi_2) = d^2 \frac{\alpha^{3/2} \beta^{5/2}}{4} (F_{110} - F_{112} - F_{101} + F_{103})$$

$$O(h_1 1s) = R \frac{\alpha^{3/2} \beta^{3/2}}{1} (F_{101} - F_{110} + F_{020} - F_{011})$$

---

<sup>a</sup>all the forces are for  $H_1$  only.

$$O(h_1 2s) = R^2 \alpha^{3/2} \beta^{3/2} (2F_{111} - F_{120} + F_{030} - 2F_{021} - F_{102} + F_{012})$$

$$O(h_1 px) = R^2 \frac{\alpha^{3/2} \beta^{5/2}}{2} (F_{101} - F_{110} + F_{020} - F_{011} - F_{112} + F_{121} \\ - F_{031} + F_{022})$$

$$O'(h_1 h_2) = d \alpha^{3/2} \beta^{3/2} (F_{101} - F_{110} + F_{020} - F_{011}) \cos \theta_0$$

$$O(p\sigma_1 h_2) = d^2 \frac{\beta^{3/2} \alpha^{5/2}}{2} (F_{101} + F_{112} - F_{110} - F_{121} + F_{020} + F_{031} \\ - F_{011} - F_{022})$$

$$O(p\pi_1 h_2) = d^2 \frac{\alpha^{5/2} \beta^{3/2}}{4} (F_{110} - F_{101} - F_{112} + F_{103})$$

$$O(p_3 2s) = R^3 \frac{\alpha^{5/2} \beta^{5/2}}{4\sqrt{3}} (2F_{111} - F_{120} + F_{030} - 2F_{021} - F_{102} + F_{012} \\ + 2F_{122} - F_{131} + F_{041} - 2F_{032} - F_{113} + F_{023})$$

$$O(p_3 1s) = R^2 \frac{\alpha^{5/2} \beta^{3/2}}{2} (F_{101} - F_{110} + F_{020} - F_{011} + F_{112} - F_{121} \\ + F_{031} - F_{022})$$

$$O(p_3 px) = R^3 \frac{\alpha^{5/2} \beta^{5/2}}{4} (F_{101} - F_{110} + F_{020} - F_{011} - F_{123} + F_{132} \\ - F_{042} + F_{033})$$

$$O(h_1 p\sigma_2) = d^2 \frac{\beta^{3/2} \alpha^{5/2}}{2} (F_{101} - F_{110} + F_{020} - F_{011} - F_{112} + F_{121} \\ - F_{031} + F_{022})$$

$$O(h_1 p\pi_2) = d^2 \frac{\alpha^{3/2} \beta^{5/2}}{4} (F_{110} - F_{112} - F_{101} - F_{103})$$

For the three centre integrals the operator  $\hat{O}_a$  is taken to be

$$Za / r_a^3$$

Force perpendicular

$$P(1s py) = R^2 \frac{\alpha^{3/2} \beta^{5/2}}{4} (F_{110} - F_{101} - F_{112} + F_{103})$$

$$P(2s py) = R^3 \frac{\alpha^{5/2} \beta^{5/2}}{8\sqrt{3}} (F_{120} - F_{122} - 2F_{111} + 2F_{113} + F_{102} - F_{104})$$

$$P''(h_2 h_2) = d \alpha^{3/2} \beta^{3/2} (F_{101} - F_{110} + F_{020} - F_{011}) \sin \theta_0$$

$$P(\text{pxpy}) = R^3 \alpha^{5/2} \beta^{5/2} (F_{110} - F_{101} + F_{103} - F_{121} + F_{123} - F_{114})$$

$$O(h_1 p_y) = R^2 \frac{\alpha^{3/2} \beta^{5/2}}{4} (F_{110} - F_{101} - F_{112} + F_{103})$$

$$O''(h_1 h_2) = d \alpha^{3/2} \beta^{3/2} (F_{101} - F_{110} + F_{020} - F_{011}) \sin \theta_0$$

$$O(p_3 p_{\pi_2}) = d^3 \frac{\alpha^{5/2} \beta^{5/2}}{8} (F_{110} - F_{121} - F_{101} + F_{123} + F_{103} - F_{114})$$

For the three centre integrals the operator  $\hat{O}_a$  is taken to be

$$X_a / r_a^3 .$$

### Force on the oxygen

The force on the oxygen atom is taken to lie along the symmetry axis since by symmetry all the other components will be zero. The integrals however have been calculated along and perpendicular to the bond direction and therefore the correct components,  $\cos(\epsilon/2)$  and  $\sin(\epsilon/2)$  respectively, must be taken. In the integrals below the primed superscript signifies that the integral must be multiplied by  $\sin(\epsilon/2)$  otherwise the component is  $\cos(\epsilon/2)$ .

$$A(1sp) = 4 \frac{\alpha^{3/2} \beta^{5/2}}{3(\alpha+\beta)^3}$$

$$A(2sp) = 8 \frac{\alpha^{5/2} \beta^{5/2}}{3\sqrt{3} (\alpha+\beta)^3}$$

$$P(h_1 h_1) = R^3 \alpha^{3/2} \beta^{3/2} (F_{101} - F_{110} + F_{020} - F_{011})$$

$$P(h_1 p_3) = \frac{\alpha^{3/2} \beta^{5/2}}{2} (F_{101} - F_{110} + F_{020} - F_{011} - F_{112} + F_{121} - F_{031} + F_{022})$$

$$P(p_3 p_3) = \frac{R^3 \beta^5}{4} (F_{101} - F_{110} + F_{020} - F_{011} + F_{123} - F_{132} + F_{042} - F_{033})$$

$$O(lsh_1) = R \alpha^{3/2} \beta^{3/2} (F101 - F110 + F020 - F011)$$

$$O(2sh_1) = R^2 \frac{\alpha^{5/2} \beta^{3/2}}{2\sqrt{3}} (F030 - F120 + F102 - F012)$$

$$O(pxh_1) = R^2 \frac{\alpha^{5/2} \beta^{3/2}}{2} (F101 - F110 + F020 - F011 + F112 - F121 + F031 - F022)$$

$$O'(pyh_1) = R^2 \frac{\alpha^{5/2} \beta^{3/2}}{4} (F110 - F101 - F112 - F112 + F103)$$

$$O(lsp_3) = R^2 \frac{\alpha^{3/2} \beta^{5/2}}{2} (F101 - F110 + F020 - F011 - F112 + F121 - F031 + F022)$$

$$O(2sp_3) = R^3 \frac{\alpha^{5/2} \beta^{5/2}}{4\sqrt{3}} (F030 - F120 + F131 - F041 + F102 - F012 - F113 + F023)$$

$$O(pxp_3) = R^3 \frac{\alpha^{5/2} \beta^{5/2}}{4} (F101 - F110 + F020 - F011 - F123 + F132 - F042 + F033)$$

$$O'(pyp_3) = R^3 \frac{\alpha^{5/2} \beta^{5/2}}{8} (F101 - F112 - F101 + F103 - F121 + F123 + F112 - F114)$$

### Dipole moment

The dipole moment like  $F_o$  is measured along the symmetry axis and again the primed superscript signifies the perpendicular component must be taken.

$$D(lsp_x) = 32 \frac{\alpha^{3/2} \beta^{5/2}}{(\alpha+\beta)^5}$$

$$D(2sp_x) = \frac{170 \alpha^{5/2} \beta^{5/2}}{\sqrt{3} (\alpha+\beta)^6}$$

$$D(h_1h_1) = R^4 \frac{\alpha^{3/2} \beta^{3/2}}{8} (F030 - F012 + F031 - F031 + F041 - F023 + F032 - F014)$$

$$D(h_1p_3) = R^5 \frac{\alpha^{3/2} \beta^{5/2}}{16} (F030 + F021 - F012 - F003 - F052 - F043 + F034 + F025)$$

$$D(p_3p_3) = \frac{R^6 \beta^5}{32} (F030 + F021 - F012 - F003 - F052 - F043 + F034 \\ + F025 - F041 - F032 + F023 + F014 + F063 \\ + F054 - F045 - F036)$$

$$D(pxh_1) = R^5 \frac{\alpha^{5/2} \beta^{3/2}}{16} (F030 - F012 + F021 - F003 + 2F041 - 2F023 \\ + 2F032 - 2F014 + F052 - F034 + F043 - F025)$$

$$D'(pyh_1) = R^5 \frac{\alpha^{5/2} \beta^{3/2}}{32} (F050 + F041 - F030 - F003 + F012 - F021 \\ + F032 - F005 - F014 - F052 + F025 - F043)$$

$$D(1sh_1) = R^4 \frac{\alpha^{3/2} \beta^{3/2}}{8} (F030 - F012 + F031 - F013 + F041 - F023 \\ + F032 - F014)$$

$$D(2sh_1) = R^5 \frac{\alpha^{5/2} \beta^{3/2}}{16\sqrt{3}} (F040 + 2F031 - 2F013 - F004 - F051 + 2F042 \\ + 2F024 - F015)$$

$$D(1sp_3) = R^5 \frac{\alpha^{3/2} \beta^{5/2}}{16} (F030 + F021 - F012 - F003 - F052 - F043 \\ + F034 + F025)$$

$$D(2sp_3) = R^6 \frac{\alpha^{5/2} \beta^{5/2}}{32\sqrt{3}} (F040 + 2F031 - 2F013 - F004 - F062 - 2F053 \\ + 2F035 + F026)$$

$$D(pxp_3) = R^6 \frac{\alpha^{5/2} \beta^{5/2}}{32} (F030 - F012 + F021 - F003 - F052 + F034 \\ - F043 + F025 + F041 - F023 + F032 - F014 \\ - F063 + F045 - F054 + F036)$$

$$D'(pyp_3) = R^6 \frac{\alpha^{5/2} \beta^{5/2}}{64} (F050 - F030 + 2F041 - F021 + F012 - F023 \\ + F003 - F061 - 2F052 + F034 + F032 - F043 \\ - 2F014 + 2F025 - F005 + F063 + F054 - F045 \\ - F036 + F016)$$



NUMERICAL VALUES OF INTEGRALS

	A	B	C	D	E
$S(h_1 1s)$	0.056038	0.059961			0.052471
$S(h_1 2s)$	0.466114	0.489242			0.457449
$S(h_1 px)$	0.453394	0.444593			0.394475
$S(h_1 h_2)$	0.218211	0.269894			0.218210
$S(1sp_3)$			0.074363	0.112576	
$S(2sp_3)$			0.452010	0.576369	
$S(h_2 p\sigma_1)$			0.486487	0.492458	
$S(pxp_3)$			-.148234	-.041864	
$S(p\sigma_1 p\sigma_2)$			-.280792	0.119727	
$S(p\sigma_1 p\sigma_2)$			0.720805	0.497461	
$P(2s2s)$	0.273075	0.273075			0.271943
$P(pxp_x)$	0.336256	0.336256			0.380564
$P(pyp_y)$	0.211285	0.211285			0.227782
$P(1s1s)$	0.305242	0.305242			0.305241
$P(2sp_x)$	0.150608	0.150608			0.166433
$P(1s2s)$	-.000035	-.000035			-.000015
$P(1sp_x)$	0.020771	0.020771			0.018227
$P''(h_2 h_2)$	0.094668	0.093367			0.094668
$O(h_1 2s)$	0.176766	0.173968			0.184087
$O(h_1 px)$	0.194063	0.184211			0.234244
$O(h_1 1s)$	0.019417	0.020508			0.018532

	A	B	C	D	E
$O''(h_1 h_2)$	0.042311	0.046312			0.042318
$P(p_4 p_4)$			0.051587	0.097054	
$O(2sp_3)$			0.113242	0.188686	
$O(1sp_3)$			0.022778	0.035495	
$O(pxp_3)$			0.075178	0.170824	
$O(p_3 h_2)$			0.049365	0.068586	
$O(h_1 p_4)$			0.041656	0.073821	
$P(h_2 p_4)$			0.025082	0.038695	
$P(2spy)$	0.099272	0.099272			0.100790
$P(pxpy)$	0.070157	0.070157			0.068319
$P'(1spy)$	0.010416	0.010416			0.009114
$P(h_2 h_2)$	0.073382	0.072385			0.073365
$O(h_1 py)$	0.119798	0.118617			0.109553
$O''(h_1 h_2)$	0.032802	0.035904			0.032796
$P(p_4 p_4)$			0.001178	0.031072	
$P(h_2 p_4)$			0.003707	0.008172	
$O(p_3 py)$			0.413844	0.061883	
$O(h_1 p_4)$			-.008828	0.013433	
$O(p_3 h_2)$			0.020361	0.024640	

NUMERICAL VALUES OF INTEGRALS (continued)

	A	B	C	D	E
A(2sp)	0.324682	0.324682			0.487736
A(1sp)	2.867280	2.867280			2.235130
P(h <sub>1</sub> h <sub>1</sub> )	0.261103	0.246594			0.261103
O(pxh <sub>1</sub> )	0.348001	0.359243			0.336497
O(pyh <sub>1</sub> )	0.251696	0.271633			0.141007
O(1sh <sub>1</sub> )	0.089649	0.087622			0.089808
O(2sh <sub>1</sub> )	0.133526	0.128909			0.134039
A(h <sub>1</sub> p <sub>3</sub> )			0.182528	0.375685	
P(p <sub>3</sub> p <sub>3</sub> )			0.007552	0.093896	
P(h <sub>1</sub> p <sub>3</sub> )			0.032054	0.070541	
O(1sp <sub>3</sub> )			0.009325	0.062185	
O(2sp <sub>3</sub> )			-0.006660	0.042997	
O(pxp <sub>3</sub> )			0.330779	0.491263	
O(pyp <sub>3</sub> )			0.343415	0.495995	
D(2sp)	0.668776	0.668776			
D(1sp)	0.061803	0.061803			
D(pxh <sub>1</sub> )	0.758803	0.773900			
D(pyh <sub>1</sub> )	0.339436	0.380052			
D(2sh <sub>1</sub> )	0.400150	0.393311			
D(1sh <sub>1</sub> )	0.005793	0.005618			
D(h <sub>1</sub> h <sub>1</sub> )	1.81	1.81			

	A	B	C	D	E
D(1sp <sub>3</sub> )			0.000320	0.003193	
D(2sp <sub>3</sub> )			-.146745	-.067964	
D(h <sub>1</sub> p <sub>3</sub> )			-.564340	-.722056	
D(p <sub>3</sub> p <sub>3</sub> )			1.81	1.81	
D(pxp <sub>3</sub> )			0.259190	0.230810	
D(pyp <sub>3</sub> )			0.178496	0.285743	
T(2sh <sub>2</sub> )	0.082807	0.088204			0.085669
T(pxh <sub>2</sub> )	0.019978	0.025379			0.025084
T(pyh <sub>2</sub> )	0.056413	0.054973			0.055147
T(1sh <sub>2</sub> )	0.016487	0.017710			
T(2sh <sub>2</sub> )	0.031056	0.031021			0.030064
T(pxh <sub>2</sub> )	0.013183	0.014319			0.012473
T(pyh <sub>2</sub> )	0.053857	0.056300			0.049962
T(1sh <sub>2</sub> )	0.000830	0.000812			

A = Screening Coefficient on h<sub>i</sub> = 1.32 (i = 1,2).

B = Screening Coefficient on h<sub>i</sub> = 1.20 (i = 1,2).

C = Screening Coefficient on p<sub>i</sub> = 0.66 (i = 3,4).

D = Screening Coefficient on p<sub>i</sub> = 1.00 (i = 3,4).

E = Results obtained by Bader and Jones.

Appendix 5

Diamagnetic Susceptibility

The expectation value for the diamagnetic susceptibility is obtained by averaging the charge distribution over the operator  $r_0^2$

$$\langle \chi_d \rangle = - \frac{Ne^2}{6mc^2} \times 2 \times (\chi(\phi_0^2) + \chi(\phi_{b1}^2) + \chi(\phi_{b2}^2) + \chi(\phi_{\ell1}^2) + \chi(\phi_{\ell2}^2))$$

where

$$\chi(\phi_i^2) = \langle \phi_i r_0^2 \phi_i \rangle$$

thus

$$\begin{aligned} \chi(\phi_{b1}^2) = \chi(\phi_{b2}^2) = & \lambda^2 [CEB^2 \chi(2s2s)^a + 2C_3 CEB \cdot \chi(1s2s) + SEB^2 CW^2 \chi(pxp) \\ & + SEB^2 SW^2 \chi(pypy) + C_3^2 (1s1s)] + 2\lambda\mu [CEB \chi(h_1^0 2s) \\ & + SEB \cdot CW \cdot \chi(h_1^0 px) + C_3 \chi(h_1^0 1s) - \delta \{CEB \cdot \chi(h_2^0 2s) \\ & + SEB \cdot CW \cdot \chi(h_2^0 px) + SEB \cdot SW \cdot \chi(h_2^0 py) + C_3 \chi(h_2^0 1s)\}] \\ & + \mu^2 [\chi(h_1^0 h_1^0) - 2\delta \chi(h_1^0 h_1^0) + \delta^2 \chi(h_2^0 h_2^0)] \end{aligned}$$

$$\chi(\phi_{\ell1}^2) = CEL^2 \chi(2s2s) + SEL^2 CE2^2 \chi(pxp) + SEL^2 SE2^2 \chi(pypy)$$

$$\chi(\phi_{\ell2}^2) = \chi(pzpz)$$

$$\chi(\phi_0^2) = C_0^2 \chi(1s1s) + 2C_0 C_1 \chi(1s2s) + C_2^2 CE2^2 \chi(pxp) + C_2 SE2^2 \chi(pypy)$$

where

$$\chi(1s1s) = 96 \frac{\alpha^{3/2} \beta^{3/2}}{(\alpha+\beta)^5}$$

$$\chi(2s2s) = \chi(pxp) = \chi(pypy) = 960 \frac{\alpha^{5/2} \beta^{5/2}}{(\alpha+\beta)^7}$$

$$\chi(1s2s) = 480 \frac{\alpha^{3/2} \beta^{5/2}}{\sqrt{3} (\alpha+\beta)^6}$$

$$\chi(h_1 h_1) = R^2 (1 + \frac{3}{R\alpha\beta})$$

---

<sup>a</sup>  $\chi(x_i x_j) = \langle x_i(\alpha) r_0^2 x_j(\beta) \rangle$  where  $\alpha$  and  $\beta$  are the two screening coefficients of  $x_i$  and  $x_j$  respectively.

$$\chi(1sh_1) = J_{18}^a$$

$$\chi(2sh_1) = J_{27}$$

$$\chi(pxh_1) = -\frac{d}{d\alpha} J_{20}$$

$$\chi(h_1h_2) = R^2S(h_1h_2) + K_{27} - 2R\sin(\epsilon/2)K_7$$

Using these relationships the numerical values of the integrals involved can thus be calculated

$$\chi(1s1s) = 0.3308$$

$$\chi(1sh_1^\circ) = 0.0110$$

$$\chi(2s2s) = 1.5807$$

$$\chi(2sh_1^\circ) = 1.3095$$

$$\chi(1s2s) = 0.0441$$

$$\chi(pxh_1^\circ) = 1.7337$$

$$\chi(h_1^\circ h_1^\circ) = 5.0122$$

$$\chi(h_1^\circ h_2^\circ) = 0.8842$$

$$\chi(pxpx) = 1.9741$$

$$\chi(pxh_2^\circ) = -.4326$$

$$\chi(pyh_2^\circ) = 1.6789$$

and therefore

$$\chi(\phi_{b1}^2) = \chi(\phi_{b2}^2) = 2.9429$$

$$\chi(\phi_{l1}^2) = \chi(\phi_{l2}^2) = 1.8167$$

$$\chi(\phi_0^2) = 0.0675$$

---

<sup>a</sup>The analytical form of the J and K integrals are given by Barnett and Coulson (64).

Appendix 6

The expectation value for the diamagnetic contribution to the proton shielding constant is obtained by averaging the charge distribution over the operator  $1/r_H^a$ .

$$\langle \sigma_d \rangle = 2(\sigma(\phi_O^2) + \sigma(\phi_{b1}^2) + \sigma(\phi_{b2}^2) + \sigma(\phi^2) + \sigma(\phi_{l2}^2))$$

where

$$\sigma(\phi_i^2) = \langle \phi_i | 1/r_H | \phi_i \rangle$$

Since each  $\phi_i$  is a linear combination of atomic functions,  $\chi$ , the expression for  $\langle \sigma_d \rangle$  will contain a number of one, two and three-centre integrals;  $\sigma_1(\chi_i \chi_j)$ ,  $\sigma_2(\chi_i \chi_j)$  and  $\sigma_3(\chi_i \chi_j)$  respectively. Taking  $\chi_i$  to have a screening coefficient  $\alpha$  and  $\chi_j$  to have a screening coefficient  $\beta$  then

$$\sigma_1(h_1 h_1) = \alpha$$

$$\sigma_2(h_1 2s) = R^3 \frac{\alpha^{3/2} \beta^{5/2}}{4\sqrt{3}} \quad (F030 + F003 - F021 - F012)$$

$$\sigma_2(h_1 px) = R^3 \frac{\alpha^{3/2} \beta^{5/2}}{4} \quad (F020 - F031 - F002 + F013)$$

$$\sigma_2(h_1 h_2) = d^2 \frac{\alpha^{3/2} \beta^{3/2}}{2} \quad (F020 - F002)$$

$$\sigma_2(h_1 ls) = R^2 \frac{\alpha^{3/2} \beta^{3/2}}{2} \quad (F020 - F002)$$

$$\sigma_2(1s1s) = R^2 \frac{\alpha^{3/2} \beta^{3/2}}{2} \quad (F020 - F002)$$

$$\sigma_2(1s2s) = R^3 \frac{\alpha^{3/2} \beta^{5/2}}{4\sqrt{3}} (F030 - F021 - F012 + F003)$$

$$\sigma_2(2s2s) = R^4 \frac{\alpha^{5/2} \beta^{5/2}}{24} (F040 - 2F031 + 2F013 - F004)$$

$$\sigma_2(\text{pxpx}) = R^4 \frac{\alpha^{5/2} \beta^{5/2}}{8} (F020 - 2F031 + F042 - F002 + 2F013 - F024)$$

$$\sigma_2(1\text{spx}) = R^3 \frac{\alpha^{3/2} \beta^{5/2}}{4} (F020 - F031 - F002 + F013)$$

$$\sigma_2(2\text{spx}) = R \frac{\alpha^{5/2} \beta^{5/2}}{8\sqrt{3}} (F030 - F013 - F021 + F003 - F041 + F023 + F032 - F014)$$

$$\sigma_2(\text{pypy}) = R^4 \frac{\alpha^{5/2} \beta^{5/2}}{16} (F130 - F112 + F121 - F103 - F132 + F114 - F123 + F105)$$

$$\sigma_2(h_2h_2) = d^2 \frac{\alpha^{3/2} \beta^{3/2}}{2} (F020 - F002)$$

$$\sigma_1(p_3p_3) = R^4 \frac{\alpha^{5/2} \beta^{5/2}}{8} (F020 + 2F031 + F042 - F002 - 2F013 - F024)$$

$$\sigma_1(p_3h_1) = R^3 \frac{\alpha^{5/2} \beta^{3/2}}{4} (F021 + F031 - F002 - F013)$$

$$\sigma_2(p_3h_2) = d^3 \frac{\alpha^{5/2} \beta^{3/2}}{4} (F020 + F031 - F002 - F013) \cos\theta_0$$

$$\sigma_2(p_4h_2) = d^3 \frac{\alpha^{5/2} \beta^{3/2}}{4} (F020 - F031 + F002 - F013) \cos\theta_0$$



$$\begin{aligned}
\sigma_2(p_4 p_4) = & \left[ d^4 \frac{\alpha^{5/2} \beta^{5/2}}{8} (F020 - 2F031 + F042 - F002 + 2F013 \right. \\
& \left. - F024) \cos^2 \theta_o \right] + \left[ \frac{\alpha^{5/2} \beta^{5/2}}{16} d^4 (F040 - F020 \right. \\
& \left. - F022 + F002 - F042 + F022 + F024 - F004) \right. \\
& \left. \sin^2 \theta_o \right]
\end{aligned}$$

NUMERICAL VALUES FOR THE PROTON SHIELDING  
CONSTANT INTEGRALS

---

	A	B		C	D
$\sigma_2(h_1 1s)$	0.03303	0.03511	$\sigma_2(1sp_3)$	0.04115	0.10434
$\sigma_2(h_1 2s)$	0.40199	0.40183	$\sigma_2(2sp_3)$	0.21229	0.51478
$\sigma_2(h_1 px)$	0.52700	0.50700	$\sigma_2(p_3 px)$	0.05420	0.71648
$\sigma_2(1s1s)$	0.55249	0.55249	$\sigma_1(p_3 p_3)$	0.33	0.5
$\sigma_2(1s2s)$	-.00001	-.00001	$\sigma_1(h_1 p_3)$	0.0	0.0
$\sigma_2(2s2s)$	0.54294	0.54294	$\sigma_2(h_2 p_3)$	0.10693	0.10913
$\sigma_2(pxp_x)$	0.61741	0.61741	$\sigma_2(h_2 p_4)$	0.03390	0.03776
$\sigma_2(1spx)$	0.01885	0.01885	$\sigma_2(h_1 p_4)$	0.78730	0.67674
$\sigma_2(2spx)$	0.17968	0.17968	$\sigma_2(p_4 p_4)$	0.03931	0.14298
$\sigma_2(pyp_y)$	0.49046	0.49046	$\sigma_3(2sp_4)$	0.19956	0.23913
$\sigma_1(h_1 h_1)$	1.32	1.2	$\sigma_3(pyp_4)$	0.03590	0.07330
$\sigma_3(h_1 2s)$	0.21015	0.22284	$\sigma_3(1sp_4)$	0.01114	0.01678
$\sigma_3(h_2 px)$	0.17541	0.17191	$\sigma_3(2sp_4)$	0.10957	0.15284
$\sigma_3(h_2 1s)$	0.03037	0.03263			
$\sigma_2(h_1 h_2)$	0.14435	0.17169			
$\sigma_2(h_2 h_2)$	0.34861	0.34787			
$\sigma_3(h_2 px)$	0.01252	0.02056			

A = Screening Coefficient on  $h_i = 1.32$  ( $i = 1,2$ ).

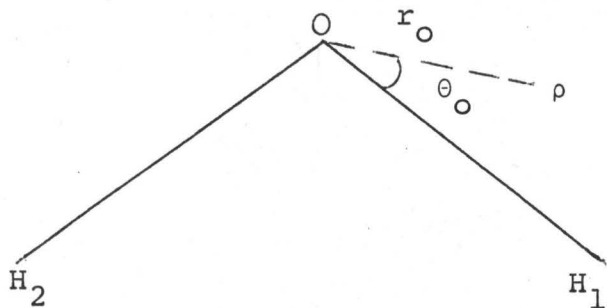
B = Screening Coefficient on  $h_i = 1.20$  ( $i = 1,2$ ).

C = Screening Coefficient on  $p_i = 0.66$  ( $i = 3,4$ ).

D = Screening Coefficient on  $p_i = 1.00$  ( $i = 3,4$ ).

Appendix 7

The expectation value for the electronic contribution to the field gradient at the position of the proton, along the bond direction, is obtained by averaging the one-electron charge density over the operator  $\frac{(3\cos^2\theta_o - 1)}{r_o^3}$  where



Thus

$$\langle q_e \rangle = \frac{\langle \rho (3\cos^2\theta_o - 1) \rangle}{r_o^3}$$

$$\langle q_e \rangle = q(\phi_o^2) + q(\phi_{b1}^2) + q(\phi_{b2}^2) + q(\phi_{l1}^2) + q(\phi_{l2}^2)$$

Because of the complicated nature of the operator, the two- and three-centre integrals are rather more difficult to solve. In the present work the method proposed by Barnett and Coulson (64) has been employed.

In general a two-centre integral of the type

$$\langle \chi_i^a(\alpha) \frac{(3\cos^2\theta_a - 1)}{r_a^3} \chi_j^b(\beta) \rangle, \text{ where } \chi_i^a \text{ and } \chi_j^b \text{ are atomic orbitals}$$

centred on the nuclei A and B respectively with the respective

screening coefficients  $\alpha$  and  $\beta$ , can be written in the form

$$J(k, \ell, m) = \int e^{-\alpha r_a} e^{-\beta r_b} \cos^k \theta_a r_a^{\ell-1} r_b^{m-1} dv$$

If  $r_b^{m-1} e^{-\beta r_b}$  is expanded in terms of  $r_a$  and  $\cos \theta_a$ , then dependant

on whether  $m=0, 1$  or  $2$  functions denoted by  $\gamma_n(\beta, r_a; \rho)$ ,  $p_n(\beta, r_a; \rho)$

and  $q_n(\beta, r_a; \rho)$  are obtained (Coulson 1937). In this way the integrals can be reduced to the form

$$G_{n, \ell + 1/2}(\kappa, T) = \int e^{-\kappa t} \gamma_n(1, t; T) t^{\ell + 1/2} dt \quad \text{for } m=0$$

or

$$|P_{n, \ell + 1/2}(\kappa, T) = \int e^{-\kappa t} p_n(1, t; T) t^{\ell + 1/2} dt \quad \text{for } m=1$$

where

$$\kappa = \alpha/\beta$$

$$t = \beta r_a$$

$$T = \beta R$$

If the symbols  $q_1(x_i x_j)$ ,  $q_2(x_i x_j)$  and  $q_3(x_i x_j)$  are taken to represent the one-, two- and three-centre integrals respectively in the expression for  $\langle q_e \rangle$ , where for example

$$q_2(x_i x_j) = \langle x_i(\alpha) \cdot \frac{(3\cos^2 \theta_o - 1)}{r_o^3} x_j^{H1}(\beta) \rangle,$$

then

$$q_1(pxp) = 16 \frac{\alpha^{5/2} \beta^{5/2}}{15} \left( \frac{1}{(\alpha + \beta)^2} \right)$$

$$q_1(\text{pyp}_y) = - \frac{8\alpha^{5/2}\beta^{5/2}}{15} \left( \frac{1}{(\alpha+\beta)^2} \right)$$

$$q_2(\text{lsh}_1) = \frac{\alpha^{3/2}\beta^{3/2}}{5} 8\sqrt{\tau} (G_1, -1 + 1/2 - G_3, -1 + 1/2)$$

$$q_2(\text{2sh}_1) = \frac{\alpha^{5/2}\beta^{3/2}}{\sqrt{3}\beta} \frac{8\sqrt{\tau}}{5} (G_1, 0 + 1/2 - G_3, 0 + 1/2)$$

$$q_2(\text{pxh}_1) = \frac{\alpha^{5/2}\beta^{3/2}}{\beta\sqrt{\tau}} \frac{8}{5} (2|P_{1,-1+1/2} + 3|P_{3,-1+1/2})$$

$$q_2(\text{h}_1\text{h}_1) = -\frac{8}{3} \alpha^3 e^{-2\alpha r} + \frac{2}{R} P(\text{h}_1\text{h}_1)$$

The operator  $\frac{(3\cos^2\theta_0 - 1)}{r_0^3}$  was chosen such that the above field

gradient integrals are measured with respect to the O-H bond.

In order that this gradient lie along the symmetry axis, a component must be taken  $(\cos^2(\epsilon/2) - (1/2)\sin^2(\epsilon/2))$  where  $\epsilon/2$  is the angle between the O-H bond and the symmetry axis. Furthermore,  $q^s(\text{h}_1\text{p}_y)^a$  and  $q^s(\text{p}_x\text{p}_y)$ , which have a zero component along the bond, are now given as

$$q^s(\text{p}_y\text{h}_1) = \cos(\epsilon/2)\sin(\epsilon/2) \alpha^{5/2}\beta^{3/2} 6 \left\{ \frac{e^{-\alpha r_a} \cos\theta_a}{r_a^2} e^{-\beta r_b} \right\} - J\left(3, -1, 1\right) \frac{1}{2\pi}$$

$$q^s(\text{p}_x\text{p}_y) = \frac{\cos(\epsilon/2)\sin(\epsilon/2)}{15(\alpha+\beta)^2} \alpha^{5/2}\beta^{5/2} .24$$

---

<sup>a</sup>the superscript s signifies that the integral is calculated with respect to the symmetry axis.

Appendix 8

TOT corresponds to the expansion of a 5x5 determinant of overlap integrals. If  $S_{ij}$  ( $s_{ij}$ ) is taken to represent  $\langle \phi_i | \phi_j \rangle$  where  $i=1, 2, 3, 4$  and 5 correspond to the five occupied molecular orbitals of the water molecule and  $j = 6, 7, 8, 9$  and 10 correspond to the five occupied atomic orbitals of the neon atom, then TOT will be equal to

$$\begin{aligned}
 & (s_{49}s_{510} - s_{410}s_{59}) (s_{16}s_{27}s_{38} - s_{16}s_{28}s_{37} - s_{17}s_{26}s_{38} + s_{17}s_{28}s_{36} - s_{18}s_{27}s_{36} \\
 & \hspace{20em} + s_{18}s_{26}s_{37}) \\
 & + (s_{27}s_{510} - s_{210}s_{57}) (s_{16}s_{38}s_{49} - s_{16}s_{39}s_{48} - s_{18}s_{36}s_{49} + s_{18}s_{39}s_{46} - s_{19}s_{38}s_{46} \\
 & \hspace{20em} + s_{19}s_{36}s_{48}) \\
 & + (s_{27}s_{38} - s_{28}s_{37}) (s_{16}s_{49}s_{510} - s_{16}s_{410}s_{59} - s_{19}s_{46}s_{510} + s_{19}s_{410}s_{56} \\
 & \hspace{10em} - s_{110}s_{49}s_{56} + s_{110}s_{46}s_{59}) \\
 & + (s_{16}s_{510} - s_{110}s_{56}) (s_{27}s_{38}s_{49} - s_{27}s_{39}s_{48} - s_{28}s_{37}s_{49} + s_{28}s_{39}s_{47} - s_{29}s_{38}s_{47} \\
 & \hspace{20em} + s_{29}s_{37}s_{48}) \\
 & + (s_{16}s_{38} - s_{18}s_{36}) (s_{27}s_{49}s_{510} - s_{27}s_{410}s_{59} - s_{29}s_{47}s_{510} + s_{29}s_{410}s_{57} \\
 & \hspace{10em} - s_{210}s_{49}s_{57} + s_{210}s_{47}s_{59}) \\
 & + (s_{27}s_{49} - s_{29}s_{47}) (s_{16}s_{38}s_{510} - s_{16}s_{310}s_{58} - s_{18}s_{36}s_{510} + s_{18}s_{310}s_{56} \\
 & \hspace{10em} - s_{110}s_{38}s_{56} + s_{110}s_{36}s_{58}) \\
 & + (s_{16}s_{27} - s_{17}s_{26}) (s_{38}s_{49}s_{510} - s_{38}s_{410}s_{59} - s_{39}s_{48}s_{510} + s_{39}s_{410}s_{58} \\
 & \hspace{10em} - s_{310}s_{49}s_{58} + s_{310}s_{48}s_{59}) \\
 & + (s_{16}s_{49} - s_{19}s_{46}) (s_{27}s_{38}s_{510} - s_{27}s_{310}s_{58} - s_{28}s_{37}s_{510} + s_{28}s_{310}s_{57} \\
 & \hspace{10em} - s_{210}s_{38}s_{57} + s_{210}s_{37}s_{58}) \\
 & + (s_{38}s_{49} - s_{39}s_{48}) (s_{16}s_{27}s_{510} - s_{16}s_{210}s_{57} - s_{17}s_{26}s_{510} - s_{17}s_{210}s_{56} \\
 & \hspace{10em} - s_{110}s_{27}s_{56} + s_{110}s_{26}s_{57}) \\
 & + (s_{38}s_{510} - s_{310}s_{58}) (s_{16}s_{27}s_{49} - s_{16}s_{29}s_{47} - s_{17}s_{26}s_{49} + s_{17}s_{29}s_{46} \\
 & \hspace{10em} - s_{19}s_{27}s_{46} + s_{19}s_{26}s_{47})
 \end{aligned}$$

Appendix 9

Associated with each  $H_{ij}$  integral in the equation that determines  $\Delta E$  there is a product of overlap integrals given the symbol  $SUM(I)$  and defined as being the co-factor of the  $ij$  element in the  $5 \times 5$  determinant TOT. Listed below for each  $H_{ij}$  are the diagonal elements of this co-factor. Again the symbol  $s_{ij}$  is taken to mean the integral  $\langle \phi_i \phi_j \rangle$  where  $i = 1, 2, 3, 4$  and 5 define the five occupied molecular orbitals of water molecule and  $j = 6, 7, 8, 9$  and 10 define the five occupied atomic orbitals of the neon atom.

<u><math>H_{ij}</math></u>	<u>I</u>	<u>SUM (I)</u>
H16	1	s27 s38 s49 s510
H17	2	s26 s38 s49 s510
H18	3	s26 s37 s49 s510
H19	4	s26 s37 s48 s510
H110	5	s26 s37 s48 s59
H26	6	s17 s38 s49 s510
H27	7	s16 s38 s49 s510
H28	8	s16 s37 s49 s510
H29	9	s16 s37 s48 s510
H210	10	s16 s37 s48 s59
H36	11	s17 s28 s49 s510
H37	12	s16 s28 s49 s510
H38	13	s16 s27 s49 s510
H39	14	s16 s27 s48 s510
H310	15	s16 s27 s48 s59
H46	16	s17 s28 s39 s510

<u>H<sub>ij</sub></u>	<u>I</u>	<u>SUM (I)</u>
H47	17	s16 s28 s39 s510
H48	18	s16 s27 s39 s510
H49	19	s16 s27 s38 s510
H410	20	s16 s27 s38 s59
H56	21	s17 s28 s39 s410
H57	22	s16 s28 s39 s410
H58	23	s16 s27 s39 s410
H59	24	s16 s27 s38 s410
H510	25	s16 s27 s38 s410

Each SUM(I) is, of course, a sum of 4! or 24 terms, each term being a product of four overlap integrals. For example, SUM (1) is given as

$$\begin{aligned}
 & (+s_{27} s_{38} s_{49} s_{510} - s_{29} s_{38} s_{47} s_{510} - s_{28} s_{37} s_{49} s_{510} \\
 & -s_{27} s_{38} s_{410} s_{59} + s_{29} s_{38} s_{410} s_{57} + s_{28} s_{37} s_{410} s_{59} \\
 & -s_{27} s_{39} s_{48} s_{510} + s_{29} s_{310} s_{47} s_{58} + s_{28} s_{39} s_{47} s_{510} \\
 & +s_{27} s_{39} s_{410} s_{58} - s_{29} s_{310} s_{48} s_{57} - s_{28} s_{39} s_{410} s_{57} \\
 & +s_{27} s_{310} s_{48} s_{59} + s_{29} s_{37} s_{48} s_{510} - s_{28} s_{310} s_{47} s_{59} \\
 & -s_{27} s_{310} s_{49} s_{58} - s_{29} s_{37} s_{410} s_{58} + s_{28} s_{310} s_{49} s_{57} \\
 & -s_{210} s_{37} s_{48} s_{59} + s_{210} s_{37} s_{49} s_{58} + s_{210} s_{38} s_{47} s_{59} \\
 & -s_{210} s_{38} s_{49} s_{57} - s_{210} s_{39} s_{47} s_{58} + s_{210} s_{39} s_{48} s_{57})
 \end{aligned}$$



Appendix 10Integrals required for the  $\Delta E$  calculation(a) overlap integrals

These integrals are written in the form  $S(\chi_i \chi_j) = \langle \chi_i \chi_j \rangle$

where  $\chi_i$  refers to an atomic orbital on the oxygen or hydrogen nuclei and  $\chi_j$  refers to an atomic orbital on the neon.

$$S16 = C_0 S(1s1s) + C_1 S(2s1s) - C_2 (CE2.S(\underline{px1s}) + SE2.S(\underline{py1s}))$$

$$S26 = C_0 S(1s2s) + C_1 S(2s2s) - C_2 (CE2.S(\underline{px2s}) + SE2.S(\underline{py2s}))$$

$$S36 = C_0 S(\underline{1spx}) + C_1 S(\underline{2spx}) - C_2 (CE2.S(\underline{pxpx}) + SE2.S(\underline{pypx}))$$

$$S46 = C_0 S(\underline{1spx}) + C_1 S(\underline{2spx}) - C_2 (CE2.S(\underline{pxpx}) + SE2.S(\underline{pypx}))$$

$$S56 = C_0 S(\underline{1spx}) + C_1 S(\underline{2spx}) - C_2 (CE2.S(\underline{pxpx}) + SE2.S(\underline{pypx}))$$

$$S17 = \lambda (CEB.S(2s1s) + SEB(CW.S(\underline{px1s}) + SW.S(\underline{py1s})) + C_3 S(1s1s)) \\ + \mu (S(h_1^0 1s) - \delta S(h_2^0 1s))$$

$$S27 = \lambda (CEB.S(2s2s) + SEB(CW.S(\underline{px2s}) + SW.S(\underline{py2s})) + C_3 S(1s2s)) \\ + \mu (S(h_1^0 2s) - \delta S(h_2^0 2s))$$

$$S37 = \lambda (CEB.S(\underline{2spx}) + SEB(CW.S(\underline{pxpx}) + SW.S(\underline{pypx})) + C_3 S(\underline{1spx})) \\ + \mu (S(h_1^0 px) - \delta S(h_2^0 px))$$

$$S47 = \lambda (CEB.S(\underline{2spx}) + SEB(CW.S(\underline{pxpx}) + SW.S(\underline{pypx})) + C_3 S(\underline{1spx})) \\ + \mu (S(h_1^0 px) - \delta S(h_2^0 px))$$

$$S57 = \lambda (CEB.S(\underline{2spx}) + SEB(CW.S(\underline{pxpx}) + SW.S(\underline{pypx})) + C_3 S(\underline{1spx})) \\ + \mu (S(h_1^0 px) - \delta S(h_2^0 px))$$

$$S18 = \lambda (CEB.S(2s1s) + SEB(CT.S(\underline{px1s}) + ST.S(\underline{py1s})) + C_3 S(1s1s)) \\ + \mu (S(h_2^0 1s) - \delta S(h_1^0 1s))$$

$$S28 = \lambda (CEB.S(2s2s) + SEB(CT.S(\underline{px2s}) + ST.S(\underline{py2s})) + C_3 S(1s2s)) \\ + \mu (S(h_2^0 2s) - \delta S(h_1^0 2s))$$

$$S38 = (\text{CEB.S}(\underline{2\text{spx}}) + \text{SEB}(\text{CT.S}(\underline{\text{pxpx}}) + \text{ST.S}(\underline{\text{pypx}})) + C_3\text{S}(\underline{\text{lspx}})) \\ + \mu(\text{S}(\underline{h_2^{\circ}\text{px}}) - \delta\text{S}(\underline{h_1^{\circ}\text{px}}))$$

$$S48 = (\text{CEB.S}(\underline{2\text{spy}}) + \text{SEB}(\text{CT.S}(\underline{\text{pxpy}}) + \text{ST.S}(\underline{\text{pypy}})) + C_3\text{S}(\underline{\text{lspy}})) \\ + \mu(\text{S}(\underline{h_2^{\circ}\text{py}}) - \delta\text{S}(\underline{h_1^{\circ}\text{py}}))$$

$$S58 = (\text{CEB.S}(\underline{2\text{spz}}) + \text{SEB}(\text{CT.S}(\underline{\text{pxpz}}) + \text{ST.S}(\underline{\text{pypz}})) + C_3\text{S}(\underline{\text{lspz}})) \\ + \mu(\text{S}(\underline{h_2^{\circ}\text{pz}}) - \delta\text{S}(\underline{h_1^{\circ}\text{pz}}))$$

$$S19 = \text{CEL.S}(\underline{2\text{s1s}}) - \text{SEL}(\text{CE2.S}(\underline{\text{px1s}}) + \text{SE2.S}(\underline{\text{py1s}}))$$

$$S29 = \text{CEL.S}(\underline{2\text{s2s}}) - \text{SEL}(\text{CE2.S}(\underline{\text{px2s}}) + \text{SE2.S}(\underline{\text{py2s}}))$$

$$S39 = \text{CEL.S}(\underline{2\text{spx}}) - \text{SEL}(\text{CE2.S}(\underline{\text{pxpx}}) + \text{SE2.S}(\underline{\text{pypx}}))$$

$$S49 = \text{CEL.S}(\underline{2\text{spy}}) - \text{SEL}(\text{CE2.S}(\underline{\text{pxpy}}) + \text{SE2.S}(\underline{\text{pypy}}))$$

$$S59 = \text{CEL.S}(\underline{2\text{spz}}) - \text{SEL}(\text{CE2.S}(\underline{\text{pxpz}}) + \text{SE2.S}(\underline{\text{pypz}}))$$

$$S110 = \text{S}(\underline{\text{pz1s}})$$

$$S210 = \text{S}(\underline{\text{pz2s}})$$

$$S310 = \text{S}(\underline{\text{pzpx}})$$

$$S410 = \text{S}(\underline{\text{pzpy}})$$

$$S510 = \text{S}(\underline{\text{pzpz}})$$

All the integrals underlined are numerically equal to zero.

If  $\alpha$  refers to the screening coefficient of the oxygen atomic orbital and  $\beta$  refers to the screening coefficient of the neon atomic orbital, then the non-zero integrals in the above equations are given in appendix 4.

Integrals involving the operators  $1/r_a$ ,  $1/r_b$  and  $1/r_c$

For simplicity the following identities will be made:

$$\langle \chi_i^a(\alpha) \frac{1}{r_a} \chi_j^b(\beta) \rangle \equiv A(\chi_i^a \chi_j^b)$$

$$\langle \chi_i^a(\alpha) \frac{1}{r_b} \chi_j^b(\beta) \rangle \equiv B(\chi_i^a \chi_j^b)$$

$$\langle \chi_i^a(\alpha) \frac{1}{r_c} \chi_j^b(\beta) \rangle \equiv C(\chi_i^a \chi_j^b)$$

Where, for example,  $\chi_i^a(\alpha)$  is an atomic orbital centred on the oxygen or neon atom with a screening coefficient  $\alpha$  (the symbols  $b$  and  $c$  refer to  $H_1$  and  $H_2$  respectively)

$$A(1s^a 1s^a) = \frac{\alpha^{3/2} \beta^{3/2}}{(\alpha+\beta)^2} \cdot 4$$

$$A(1s^a 2s^a) = \frac{\alpha^{3/2} \beta^{5/2}}{\sqrt{3} (\alpha+\beta)^3} \cdot 8$$

$$A(2s^a 2s^a) = \frac{\alpha^{5/2} \beta^{5/2}}{(\alpha+\beta)^4} \cdot 8$$

$$A(px^a px^a) = \frac{\alpha^{5/2} \beta^{5/2}}{(\alpha+\beta)^4} \cdot 8$$

$$A(1s^a h_1^b) = R^2 \frac{\alpha^{3/2} \beta^{3/2}}{2} (F020 - F002)$$

$$A(2s^a h_1^b) = R^3 \frac{\alpha^{5/2} \beta^{3/2}}{4\sqrt{3}} (F030 - F012 + F021 - F003)$$

$$A(px^a h_1^b) = R^3 \frac{\alpha^{5/2} \beta^{3/2}}{4} (F020 - F002 + F031 - F013)$$

$$A(px^a h_2^c) = \cos \epsilon \quad A(px^a h_1^b)$$

$$B(1s^a 1s^a) = R^2 \frac{\alpha^{3/2} \beta^{3/2}}{2} (F020 - F002)$$

$$B(1s^a 2s^a) = R^3 \frac{\alpha^{3/2} \beta^{5/2}}{4\sqrt{3}} (F030 + F003 - F021 - F012)$$

$$B(2\bar{s}^a 2\bar{s}^a) = R^4 \frac{\alpha^{5/2} \beta^{5/2}}{24} (F040 - 2F031 + 2F013 - F004)$$

$$B(p_x^a p_x^a) = R^4 \frac{\alpha^{5/2} \beta^{5/2}}{8} (F020 - 2F031 + F042 - F002 + 2F013 - F024)$$

$$B(p_y^a p_y^a) = R^4 \frac{\alpha^{5/2} \beta^{5/2}}{16} (F040 - F042 - F020 + F024 + F002 - F004)$$

$$B(h_1^b l_s^a) = R^2 \frac{\alpha^{3/2} \beta^{3/2}}{2} (F020 + 2F011 + F002)$$

$$B(h_1^b 2\bar{s}^a) = R^3 \alpha$$

$$B(2\bar{s}^a p_x^a) = R^4 \frac{\alpha^{5/2} \beta^{5/2}}{8\sqrt{3}} (F030 - F012 - F021 + F003 - F041 + F023 - F032 + F014)$$

$$B(l_s^a p_x^a) = R^3 \frac{\alpha^{3/2} \beta^{5/2}}{4} (F020 - F002 - F031 + F013)$$

$$C(l_s^a l_s^a) = B(l_s^a l_s^a)$$

$$C(l_s^a 2s^a) = B(l_s^a 2s^a)$$

$$C(2s^a 2s^a) = B(2s^a 2s^a)$$

$$C(p_x^a p_x^a) = CE^2 \cdot B(p_x^a p_x^a) + SE^2 \cdot B(p_y^a p_y^a)$$

$$C(p_y^a p_y^a) = SE^2 B(p_x^a p_x^a) - CE^2 \cdot B(p_y^a p_y^a)$$

$$C(h_2^c l_s^a) = B(h_2^b l_s^a)$$

$$C(h_2^c 2s^a) = B(h_1^b 2s^a)$$

$$C(h_2^c p_x^a) = B(h_1^b p_x^a)$$

Numerical values of the integrals

$$S(1s^a 1s^{a'})^a = 0.9810$$

$$S(2s^a 2s^{a'}) = 0.9562$$

$$S(1s^a 2s^{a'}) = 0.1090$$

$$S(2s^a 1s^{a'}) = -0.0739$$

$$A(1s^a 1s^{a'}) = 8.4647$$

$$A(2s^a 2s^{a'}) = 1.3573$$

$$A(1s^a 2s^{a'}) = -0.8379$$

$$A(2s^a 1s^{a'}) = -1.4206$$

$$B(1s^a 1s^{a'}) = 0.5420$$

$$B(2s^a 2s^{a'}) = 0.5229$$

$$B(2s^a 1s^{a'}) = -0.0408$$

$$B(1s^a 2s^{a'}) = 0.0643$$

$$B(px^a px^{a'}) = 0.5999$$

$$B(py^a py^{a'}) = 0.4900$$

$$B(h_1^b p_x^{a'}) = 0.4244$$

$$S(p_x^a p_x^{a'}) = S(p_y^a p_y^{a'}) = 0.9751$$

$$S(h_1^b p_x^{a'}) = 0.3625$$

$$S(h_1^b 1s^{a'}) = 0.0396$$

$$S(h_1^b 2s^{a'}) = 0.3742$$

$$A(1s^{a'} h_1^b) = 0.1829$$

$$A(2s^{a'} h_1^b) = 0.3390$$

$$A(px^{a'} p_x^a) = 1.2343$$

$$A(px^{a'} h_1^b) = 0.2691$$

$$B(h_1^b 1s^{a'}) = 0.2310$$

$$B(h_1^b 2s^{a'}) = 0.8623$$

$$B(1s^{a'} p_x^a) = 0.5364$$

$$B(2s^{a'} p_x^a) = 2.1662$$

$$B(1s^{a'} p_x^a) = 0.4248$$

$$B(2s^{a'} p_x^a) = 2.4584$$

$$\langle \frac{1}{r_b} 1s^{a'} h_2^c \rangle = 0.2166$$

$$\langle \frac{1}{r_b} 2s^{a'} h_2^c \rangle = 0.1771$$

$$\langle \frac{1}{r_b} p_x^{a'} h_2^c \rangle = 0.0123$$

$$\langle \frac{1}{r_c} p_x^{a'} h_1^b \rangle = 0.1373$$

---

<sup>a</sup>The superscript *a* signifies an atomic orbital on oxygen whereas the superscript *a'* signifies an atomic orbital on neon.

APPENDIX 11

$$\begin{aligned} \phi_{\ell 1}^0 &= (1 + g)^{-1} \{ (\text{CEL}(1 - g) - 2g^{1/2} \lambda \text{CEB}) 2s + (\text{SEL.SB2}(1 + g)) pz \\ &+ (-2g^{1/2} \lambda C_3) 1s + (\text{SEL.CB2}(1 - g) + 2\lambda g^{1/2} \text{SEB.CA2}) px' \\ &+ (-g^{1/2} \mu(1 - \delta)) (h_1^0 + h_2^0) \} \end{aligned}$$

$$\begin{aligned} \phi_{\ell 2} &= (1 + g)^{-1} \{ (\text{CEL}(1 - g) - 2g^{1/2} \text{CEB}) 2s - (\text{SEL.SB2}(1 + g)) pz \\ &+ (-2g^{1/2} C_3(1s + (\text{SEL.CB2}(1 - g) + 2g^{1/2} \text{SEB.CA2}) px' \\ &+ (-g^{1/2} \mu(1 - \delta)) (h_1^0 h_2^0) \} \end{aligned}$$

$$\begin{aligned} \phi_{b1} &= (1 + g)^{-1} \{ (\lambda \cdot \text{CEB}(1 - g) + 2g^{1/2} \text{CEL}) 2s + (\text{SEB.SA2}(1 + g)) py' \\ &+ (\lambda \text{SEB.CA2}(g - 1) + 2g^{1/2} \text{SEL.CB2}) px' + (\lambda C_3(1 - g)) 1s \\ &+ (\mu(1 + g\delta)) h_1^0 + (-\mu(\delta + g)) h_2^0 \} \end{aligned}$$

$$\begin{aligned} \phi_{b2} &= (1 + g)^{-1} \{ (\lambda \text{CEB}(1 - g) + 2g^{1/2} \text{CEL}) 2s - (\lambda \text{SEB.SA2}(1 + g)) py' \\ &+ (\lambda \text{SEB.CA2}(g - 1) + 2g^{1/2} \text{SEL.CB2}) px' + (\lambda C_3(1 - g)) 1s \\ &+ (-\mu(\delta + g)) h_1^0 + (\mu(1 + g\delta)) h_2^0 \} \end{aligned}$$

APPENDIX 12CALCULATION OF THE DENSITIES

In order to calculate the one-electron charge distribution in a molecule all the orbitals were expressed in terms of one central polar coordinate system  $(r, \theta, \phi)$ . For the water molecule this coordinate system was centred on the oxygen nucleus with the z-axis coincident with the symmetry axis. If this is the case then the two proton coordinates will be given as

$$r_{H1} = (r^2 + R_e^2 - 2R_e r(\cos \epsilon/2 \cos \theta/2 + \sin \epsilon/2 \sin \theta/2 \cos \phi))^{1/2}$$

$$r_{H2} = (r^2 + R_e^2 - 2R_e r(\cos \epsilon/2 \cos \theta/2 - \sin \epsilon/2 \sin \theta/2 \cos \phi))^{1/2}$$

where  $\phi$  is measured from the plane passing through H1, H2 and O nuclei. For the hydride molecules AH the coordinate system was centred on A, in which case

$$r_H = (r^2 + R_e^2 - 2rR_e \cos \theta)^{1/2}$$

The procedure is therefore to read in the orbital coefficients, bond parameters and orbital exponents and some chosen range of  $r, \theta$  and  $\phi$  values. Lines of constant density are observed by interpolation between the computed values and are plotted.

Any desired plane can be examined by a suitable choice of  $r, \theta$  and  $\phi$ . Thus, for example, the In-and Out-of-Plane plots of Fig. VIII for the water molecule are obtained by setting  $\phi$  equal to  $0^\circ$  and  $90^\circ$  respectively and ranging  $r$  and  $\theta$ .

The atomic densities used in Parts I and II were taken from Clementi et al (34). However, a check using later, equivalent wave functions of Bagus and Gilbert (90) showed no

significant changes. Atomic densities based on wave functions worse than Hartree-Fock wavefunctions would, however, begin to show significant changes.



BIBLIOGRAPHY

1. W. Heitler, Z. Physik, 46, 47 (1960).
2. F. London, Z. Physik, 46, 455 (1928).
3. L. Pauling, J. Am. Chem. Soc., 53, 1367 (1931).
4. C. Beevers and H. Lipson, Zeits. f. Kryst., 82, 297 (1932)  
83, 123 (1932).
5. R. Meche and W. Baumann, Phys. Zeits. 33, 833 (1932).
6. J. H. Van Vleck and P. C. Cross, J. Chem. Phys., 1, 357  
(1933); 1, 350 (1933).
7. J. D. Bernal and R. H. Fowler, J. Chem. Phys. 1, 515  
(1933).
8. R. S. Mulliken, Phys. Rev., 41, 756 (1932).
9. E. J. W. Verwey, Rec. Trav. Chim., 60, 887 (1941).
10. W. H. Barnes, Proc. Roy. Soc., A125, 670 (1929).
11. N. V. Sidgwick and H. M. Powell, Proc. Roy. Soc., A176,  
153 (1940).
12. D. F. Heath and J. W. Linnett, Nature, 161, 243 (1948).
13. J. C. Slater, Phys. Rev., 37, 481 (1931).
14. J. A. Pople, Proc. Roy. Soc., A202, 323 (1950).
15. Sir Lennard-Jones and J. A. Pople, Proc. Roy. Soc.,  
A202, 166 (1950).
16. J. A. Pople, Quart. Revs., XI, 273 (1957).
17. R. J. Gillespie and R. S. Nyholm, Quart. Revs., XI, 339  
(1957).
18. R.F.W. Bader and H. Preston, Can. J. Chem., 43, 1131 (1966).
19. R. G. Parr, in Molecular Orbitals in Chemistry, Physics  
and Biology, Edited by P.-O Lowdin and B. Pullman  
(Academic Press, N. Y., 1964), pp 21-35.
20. V. Fock, Z. Physik, 61, 126 (1930).

21. P. R. Hartree, Proc. Cam. Phil. Soc., 24, 89 (1928).
22. C. C. J. Roothaan, Rev. of Mod. Phys., 23, 69 (1951).
23. W. Koros and C. C. J. Roothaan, Revs. Mod. Phys., 32, 219 (1960).
24. A. Mukherji and M. Karplus, J. Chem. Phys. 38, 44 (1963).
25. H. Hellmann, Einführung in die Quantenchemie Franz Deuticke Leipzig, 1937.
- 25a. R. P. Feynman, Phys. Rev., 56, 340 (1939).
26. T. Berlin, J. Chem. Phys., 19, 208 (1951).
27. Sir Lennard-Jones, Proc. Roy. Soc., A198 (1949).
28. D. Peters, J. Chem. Soc. 4017 (1963).
29. K. Edmiston and C. Ruedenberg, Rev. Mod. Phys., 35, 457 (1963); J. Chem. Phys., 43, 597 (1965).
- 29a. Sir Lennard-Jones and J. A. Pople, Proc. Roy. Soc., A210, 190 (1951).
30. J. N. Murrell, J. G. Stamper and N. Trinajstić, J. Chem. Soc., A11, 1624 (1966).
31. R. F. W. Bader and G. Jones, Can. J. Chem., 41, 586 (1963).
32. L. Burnelle and C. A. Coulson, Trans. Faraday Soc., 53, 403 (1957).
33. L. Salem and M. Alexander, J. Chem. Phys., 39, 2994 (1963).
34. E. Clementi, C. C. J. Roothaan, M. Yoshimine, Phys. Rev., 127, 1618 (1962).
35. A. C. Hurley, Proc. Roy. Soc., A226, 170, 179, 193 (1954).
36. J. W. Richardson and A. K. Pack, J. Chem. Phys., 41, 897 (1964).
37. R. G. Parr, J. Chem. Phys., 40, 3726 (1964).
38. R. McWeeney and K. A. Ohno, Proc. Roy. Soc., A255, 367 (1960).

39. P. Debye, Polar Molecules (Dover Publications, Inc.), pp 63-76 (1928).
40. R. Moccia, J. Chem. Phys., 40, 2164, 2176 (1964).
41. R. F. W. Bader, Can. J. Chem., 38, 2117 (1960).
42. S. L. Kahalas and R. K. Nesbet, J. Chem. Phys., 39, 529 (1963).
43. J. H. Van Vleck, The Theory of Electric and Magnetic Susceptibilities (Oxford Univ. Press, N.Y. 1932), pg. 275 ff.
44. W. Weltner Jr., J. Chem. Phys., 28, 477 (1958).
45. P. W. Selwood, Magnetochemistry (Interscience Publishers, N.Y. 1956), Pg. 86 ff.
46. R. B. Hake and K. E. Baynyard, J. Chem. Phys. 43, 657 (1965).
47. R. Moccia, J. Chem. Phys., 40, 2186 (1964).
48. F. O. Ellison and H. Shull, J. Chem. Phys., 23, 2348 (1955).
49. K. A. Venkatachalam and M. B. Kabadi, J. Chem. Phys., 59, 740 (1955).
50. S. I. Chan and T. P. Das, J. Chem. Phys., 37, 1527 (1962).
51. N. F. Ramsey, Molecular Beams. (Oxford University Press, N. Y., 1956) pp 163-207.
52. T. P. Das and T. Ghose, J. Chem. Phys., 31, 42 (1959).
53. H. S. Gutowsky and C. J. Hoffman, J. Chem. Phys., 19, 1259 (1951).
54. C. H. Townes and B. P. Dailey, J. Chem. Phys., 17, 782 (1949).
55. R. F. W. Bader and G. Jones, J. Chem. Phys., 38, 2791 (1963).
56. N. Bessis, H. Lefebvre-Brion and C. M. Moser, Phys. Rev., 124, 1124 (1961).

57. N. Bessis, H. Lefebvre-Brion and C. M. Moser, *Phys. Rev.*, 128, 213 (1962).
58. P. O. Lowdin, *Phys. Rev.*, 97, 1474 (1955).
59. B. L. Moiseiwitsch in *Quantum Theory*, Edited by D. R. Bates (Academic Press, N.Y., 1961), pp 211-228.
60. J. I. Musher, *J. Chem. Phys.* 43, 2145 (1965).
61. H. J. Kim and R. G. Parr, *J. Chem. Phys.*, 41, 2892 (1964); R. G. Parr, *J. Chem. Phys.*, 40, 3726 (1964). R. E. Wyatt and R. G. Parr, *J. Chem. Phys.*, 41, 3262 (1964).
62. S. L. Kahalas and R. K. Nesbet, *J. Chem. Phys.*, 39, 529 (1963).
63. R.F.W. Bader, *J. Am. Chem. Soc.*, 86, 5070 (1964).
64. M. P. Barnett and C. A. Coulson, *Phil. Trans. Roy. Soc. London*, A243, 221 (1951).
65. R. F. W. Bader and W. Henneker, *J. Am. Chem. Soc.*, 87, 3063 (1965).
66. R. F. W. Bader, W. Henneker and P. E. Cade, *J. Chem. Phys.* (to be published).
67. L. Pauling, "The Nature of the Chemical Bond" (Cornell University Press, Ithaca, N. Y., 1960).
68. P. O. Lowdin and H. Shull, *Phys. Rev.* 101, 1730 (1956); *J. Chem. Phys.*, 30, 617 (1959).
69. H. Shull, *J. App. Phys.*, 33, 290 (1962).
70. L. Wharton, W. Klemperer, L. P. Gold, R. Strauch, J. J. Gallagher and V. E. Derr, *J. Chem. Phys.*, 38, 1203 (1963).
71. M. Kotani, A. Amemiya, E. Ishiguro, T. Kimura, "Table of Molecular Integrals" (Manizen Co., Ltd., Tokyo 1963).
72. S. L. Kahalas and R. K. Nesbet, *J. Chem. Phys.*, 39, 529 (1963).
73. R. K. Nesbet, *J. Chem. Phys.*, 36, 1518 (1962).
74. K. Fajans, *J. Chem. Phys.*, 40, 1773 (1964); 41, 4005 (1964); 43, 2159 (1965).
75. K. Fajans and T. Berlin, *Phys. Rev.* 63, 309, 399 (1943).

76. S. M. Blinder, *J. Chem. Phys.*, 41, 4004 (1964).
77. R. S. Mulliken, *Phys. Rev.*, 33, 730 (1929).
78. R. F. W. Bader and W. Henneker, *J. Am. Soc.*, 88, 280 (1966).
79. P. E. Cade and W. M. Huo, "The Electronic Structure of Diatomic Molecules VI. A. Hartree-Fock Wave Functions and Energy Quantities for the Ground State of the First-Row Hydrides, AH", *J. Chem. Phys.* (to be published).
80. M. McCarty, Jr. and G. W. Robinson, *J. Am. Chem. Soc.*, 81, 4772 (1959); *Mol. Phys.*, 2, 415 (1959).
81. P. Politzer and R. E. Brown, *J. Chem. Phys.*, 45, 451 (1966).
82. J. C. Browne and F. A. Matsen, *Phys. Rev.*, 135, A1227 (1964).
83. For an annotated bibliography, see Technical Report-1966 (Laboratory of Molecular Structure and Spectra, University of Chicago, Chicago, Illinois).
84. J. R. Platt, *J. Chem. Phys.*, 18, 932 (1950); in *Handbuch der Physik*, edited by S. Flügge (Springer-Verlag, Berlin, 1961), Volume XXXVII/2, Moleküle, pp. 240-249.
85. See ref. 83, also D. M. Bishop and J. R. Hoyland, *Mol. Phys.*, 7, 161 (1963).
86. W. A. Bingel, *J. Chem. Phys.*, 32, 1522 (1960).
- 86a. A. L. Companion and F. O. Ellison, *J. Chem. Phys.* 28, 1 (1958).
87. See ref. 79, also P. E. Cade and W. M. Huo, "The Electronic Structure of Diatomic Molecules. VI.B. Certain Expectation Values and Molecular Properties for the Ground States of the First-Row Hydrides AH", *J. Chem. Phys.* (to be published).
88. C. W. Kern and M. Karplus, *J. Chem. Phys.* 40, 1374 (1964).
89. A. C. Hurley, in *Molecular Orbitals in Chemistry, Physics and Biology*, Edited by P. O. Löwdin and B. Pullman (Academic Press, N. Y., 1964), pp 161-191).

90. P. Bagus and T. L. Gilbert (private communications).
91. R. S. Mulliken, Rev. Mod. Phys., 4, 3 (1932).
92. R. M. Pitzer, J. P. Wright and M. P. Barnett, "Some Programmes to Evaluate Multicenter Integrals by the Zeta Function Method" (Massachusetts Institute of Technology) QCPE 22-25 (1963).